Characterisation of Novel Evasins



James R. O. Eaton
Magdalen College
University of Oxford

A thesis submitted for the degree of
Doctor of Philosophy
Michaelmas 2018

DECLARATION

I hereby confirm that the work submitted is my own excepting figures:

2.6 Chemokine EC80 determination in THP-1 cells – Data for parts A, D, E and F were obtained by Mr Graham Davies

3.1 Yeast surface display screen to identify P672 – This data was obtained by Ms Yara Alenazi

4.2 Analysis of the CCL8-P672 complex using non-denaturing mass spectrometry – This data was obtained by Dr Lucia Geis-Asteggiante

5.1 Sequence coverage of HDX-MS peptides for A. P672 and B. CCL8 - This data was obtained by Dr Lucia Geis-Asteggiante

5.2 Percentage of hydrogen/deuterium exchange measured at four incubation time points (5s, 30s, 5 min, 60min) for the P672/CCL8 complex - This data was obtained by Dr Lucia Geis-Asteggiante

5.8 Characterisation of P672_PEP binding to CCL8 by non-denaturing mass spectrometry - This data was obtained by Dr Lucia Geis-Asteggiante

I confirm that appropriate credit has been given within the thesis where reference has been made to the work of others.

This copy has been supplied on the understanding that it is copyright material and that no quotation from the thesis may be published without proper acknowledgement.

ACKNOWLEDGMENTS

Firstly, I thank Professor Shoumo Bhattacharya and Dr Akane Kawamura for supervising me over the past three years. Their guidance, advice, patience and support has had no limit during my time in their labs.

Yara Alenazi and Graham Davies have provided unrivalled support and guidance during my time in lab and I thank them for that. I also thank Dr Tom McAllister for productive discussions and answering my seemingly endless questions.

I must also thank my collaborators, Professor Dame Carol Robinson and her post-doc Dr Lucia Geis-Asteggiante for their help with mass spectrometry studies and providing vital data that helped keep this project moving forward.

I need to thank all my friends from Magdalen College Middle Common Room, in particular Sam Griffiths and Hamish Lemmey, who have made my time at Oxford so memorable.

I also thank my family for their unwavering support not only at Oxford but throughout my life as without their belief in me I would not be writing this today.

Finally, I thank my girlfriend Sophia Epstein. She has supported me in ways that I cannot explain and, although she didn't have much choice in the matter, she always seemed interested in my work despite having heard about it more times than I care to mention.

ABSTRACT

Chemokines are a family of chemotactic cytokines that recruit innate and adaptive immune cells to sites of inflammation. Whilst these signalling proteins are vital for ensuring an effective immune response, several chemokines have been shown to be associated with the pathophysiology of a number of inflammatory diseases. Despite their relevance to disease there remain no treatments that target chemokines for inflammatory disorders. This may be due, in part, to the chemokines signalling through a robust network, driven through “one-to-many” interactions between the chemokine ligands and their receptors. This renders the “one-drug-one-target” mechanism of action that is associated with most drugs ineffective in this context. Evasins are the family of proteins found in tick saliva that bind to chemokines with a “one-to many” binding mechanism, possibly to neutralise the chemokine network to allow the tick to feed on the host for several days without eliciting an immune response. As a consequence of this novel mechanism, evasins present a possible route to a new anti-chemokine therapeutic. This thesis describes the identification and characterisation of a new evasin, P672, which can bind to and neutralise multiple CC-class chemokines. P672 was found to possess a chemokine binding domain where this domain and its functional properties can be transferred to another evasin. This domain can also be synthesized as a peptide that possesses the “one-to-many” binding mechanism observed in the P672 protein. This work has identified a novel evasin and provides proof of concept that peptides with the “one-to-many” binding mechanism that has evolved in the tick evasins can be rationally designed through the study of an evasin/chemokine interaction.

PUBLICATIONS

The assays developed in chapter 2 were used in the following papers:

Singh K, Davies G, Alenazi Y, **Eaton J.R.O**., Kawamura A, & Bhattacharya S. “Yeast surface display identifies a family of evasins from ticks with novel polyvalent CC chemokine-binding activities.” Sci. Rep. 2017 Jun 27; 7, 4267.

Alenazi Y, Singh K, Davies G, **Eaton J.R.O**., Elders P, Kawamura A and Bhattacharya S. “Genetically engineered two-warhead evasins provide a method to achieve precision targeting of disease-relevant chemokine subsets.” Sci. Rep. 2018 April 20; 8, 6333

The results from chapters 3 and 4 formed the basis of the following paper:

Eaton, J. R. O., Alenazi Y, Singh K, Davies G, Geis-Asteggiante L, Kessler B, Robinson C.V., Kawamura A and Bhattacharya S. “The N-terminal domain of a tick evasin is critical for chemokine binding and neutralization and confers specific binding activity to other evasins.” J. Biol. Chem. 2018 April 20, 293, 6134-6146

TABLE OF CONTENTS

Declaration ..... *i*

Acknowledgments ..... *ii*

Abstract ..... *iii*

Publications ..... *iv*

List of figures ..... *viii*

List of tables ..... *xi*

List of abbreviations ..... *xii*

1 Introduction *1*

1.1 Cardiovascular disease **1**

1.1.1 Atherosclerosis 2

1.1.2 Myocardial Fibrosis 3

1.1.3 Myocarditis 3

1.1.4 The immune system as a target for cardiovascular disease 4

1.2 Chemokines **6**

1.2.1 Chemokine structure 8

1.2.2 Chemokine dimerization 9

1.2.3 Chemokine ligand/receptor interaction 12

1.2.4 Chemokine oligomerisation and GAG binding 16

1.2.5 Atypical chemokine receptors 18

1.3 Chemokines and cardiovascular disease **19**

1.4 Clinical and pre-clinal studies of compounds that target chemokines **23**

1.5 Challenges in targeting the chemokine system **25**

1.5.1 Animal models 25

1.5.2 The chemokine network 26

1.6 Evasins **29**

1.7 Further evidence of the "one-to-many" mechanism **37**

1.8 Nature and therapeutics **38**

1.9 Aims of this work **40**

2 Assay development *41*

2.1 Introduction **41**

2.2 Biolayer interferometry binding assay **41**

2.3 Fluorescent ligand/receptor blocking assay **48**

2.4 Cell migration assay **50**

2.5 Summary **53**

3 Characterisation of P672 ..... *55*

3.1 Introduction **55**

3.2 Aims **61**

3.3 Results **61**

3.3.1 Sequence analysis of P672 61
3.3.2 Expression of P672 62
3.3.3 Tandem mass spectrometry identification of glycosylation sites in P672 64
3.3.4 Binding of P672 to chemokines 65
3.3.5 Binding of deglycosylated P672 to CCL8 67
3.3.6 Neutralisation of chemokine migration by N-tagged P672 68
3.3.7 Comparison of N- and C- terminally tagged P672 in a cell migration assay 70
3.3.8 Expression of CCL8 71

3.4 Discussion **72**

3.5 Conclusions **79**

4 Engineering of hybrid evasins ***81***

4.1 Introduction **81**

4.2 Aims **86**

4.3 Results **87**

4.3.1 Homology modelling of the P672/CCL8 complex 87
4.3.2 Deletion study 88
4.3.3 Inhibition of CCL8-647 binding to chemokine receptors 89
4.3.4 Design and expression of Hybrid evasins 90
4.3.5 Characterisation of hybrid evasin binding 92
4.3.6 Hybrid evasin inhibition of CCL8 migration 93

4.4 Discussion **94**

4.5 Conclusions **97**

5 Evasin derived multiple chemokine binding peptides ***99***

5.1 Introduction **99**

5.2 Aims **102**

5.3 Results **102**

5.3.1 Hydrogen-Deuterium Exchange mass spectrometry of P672/CCL8 complex 102
5.3.2 Exploration of HDX-MS result 105
5.3.3 Design of P672_PEP 112
5.3.4 Characterisation of P672_PEP chemokine binding 112
5.3.5 Cell based characterisation of P672_PEP 117

5.4 Discussion **120**

5.5 Conclusions **131**

6 Conclusions and future work ***132***

6.1 Summary **132**

6.2 Conclusions **135**

6.3 Future work **136**

7 Materials and Methods ***139***

7.1 Materials 139
7.1.1 Chemicals, oligonucleotides and Enzymes 139
7.1.2 Peptide synthesis 139
7.1.3 Cell lines 139
7.1.4 Plasmid and PCR product preparation kits 140

7.2 Methods 140
7.2.1 PCR 140
7.2.2 Transformation 140
7.2.3 Agarose gel electrophoresis 141
7.2.4 SDS-PAGE Electrophoresis 141
7.2.5 Expression vector construction 141
7.2.6 Site directed mutagenesis 142
7.2.7 Yeast surface display 142
7.2.8 Sequence analysis 143
7.2.9 Protein expression in mammalian cells 143
7.2.10 Protein expression in *E.coli* 144
7.2.11 Deglycosylated protein production 145
7.2.12 MS/MS sample preparation 146
7.2.13 MS/MS data analysis 147
7.2.14 Native mass spectrometry studies 147
7.2.15 Hydrogen-Deuterium exchange mass spectrometry 149
7.2.16 Biolyaer interferometry screening 151
7.2.17 Biolayer interferometry affinity determination 152
7.2.18 Fluorescent ligand/receptor blocking assays 153
7.2.19 Cell migration 154
7.2.20 Fluorescence polarisation assays 155
7.2.21 Homology modelling 156

8 References 157

LIST OF FIGURES

Figure 1.1 View from a crystal structure of CCL8.....9

Figure 1.2 NMR structures of chemokine dimers.....12

Figure 1.3: Chemokine/receptor interaction.....16

Figure 1.4 Representation of a part of the chemokine network.....28

Figure 1.5 View from a crystal structure of the Evasin-1 (green) and CCL3 (red) complex 33

Figure 2.1 BLI assay buffer optimisation.....43

Figure 2.2 Chemokine binding to the reference protein 45

Figure 2.3 Chemokine binding to the unfunctionalized sensor.....46

Figure 2.4 Fluorescent ligand/receptor blocking assay.....50

Figure 2.5 THP-1 cell migration in response to CCL3.....52

Figure 2.6 Chemokine EC_{80} determination in THP-1 cells. 53

Figure 3.1 Yeast surface display screen to identify P672. 60

Figure 3.2 Analysis of P672 primary structure. 62

Figure 3.3 Analysis of glycosylated and deglycosylated P672 by SDS-PAGE and size exclusion chromatography.....64

Figure 3.4 Biolayer interferometry traces for N and C terminally tagged P672 66

Figure 3.5 Characterization of P672 binding to chemokines using biolayer interferometry.....67

Figure 3.6 Biolayer interferometry sensogram for N-tagged deglycosylated P672 binding to different doses of CCL8.....68

Figure 3.7 Functional neutralization of chemokine activity by P672.....69

Figure 3.8 Percentage of migration inhibition by a fixed concentration (100 nM) of P672_CT (C-terminally tagged (filled circles)) or P672_NT (N-terminally tagged (filled squares)) 71
Figure 3.9 Expression and functional testing of recombinant CCL8..... 72
Figure 4.1 Schematic representation of the development of hybrid evasins. 85
Figure 4.2 Analysis of the CCL8-P672 complex using non-denaturing mass spectrometry. 86
Figure 4.3 Homology modelling of the P672/CCL8 complex..... 88
Figure 4.4 Characterisation of P672_17-104 89
Figure 4.5 CCL8-647 blocking assay 90
Figure 4.6 Design of hybrid evasins..... 91
Figure 4.7 Expression of hybrid evasins and Evasin-1. 92
Figure 4.8 BLI binding characterisation of hybrid evasins. 93
Figure 4.9 Inhibition of CCL8 function by a hybrid evasin. 94
Figure 5.1 Sequence coverage of HDX-MS peptides for A. P672 and B. CCL8. 103
Figure 5.2 Percentage of hydrogen/deuterium exchange measured at four incubation time points (5s, 30s, 5 min, 60min) for the P672/CCL8 complex 105
Figure 5.3 Small domain transplantation experiment to explore the hydrogen/deuterium exchange-MS result. 107
Figure 5.4 BLI traces for alanine mutants of P672 110
Figure 5.5 Activity of P672_F32A in a Boyden chamber assay using THP-1 cells 111
Figure 5.6 Fluorescence polarisation characterisation of P672_PEP-FITC 114
Figure 5.7 Fluorescence polarisation characterisation of P672_PEP and P672_PEP-FITC 116

Figure 5.8 Characterisation of P672_PEP binding to CCL8 by non-denaturing mass spectrometry 117
Figure 5.9 Fluorescent ligand blocking assay with P672_PEP 118
Figure 5.10 Cell based characterisation of P672_PEP 119
Figure 5.11 Alignment of P672 binding chemokines 126

LIST OF TABLES

Table 1 Evasin-1 binding affinities determined by SPR and BLI 46

Table 2 Binding parameters for wild type P672, alanine mutants and Evasin-1/P672 hybrid protein to CCL8 as determined using BLI 108

Table 3 Binding parameters for wild type P672, alanine mutants and Evasin-1/P672 hybrid protein to CCL3 as determined using BLI. 108

LIST OF ABBREVIATIONS

ACE	Angiotensin Converting Enzyme
AMI	Acute Myocardial Infarction
ApoE	Apolipoprotein E
BLI	Biolayer Interferometry
BSA	Bovine Serum Albumen
CANTOS	Canakinumab Anti-inflammatory Thrombosis Outcomes Study
cDNA	Complimentary Deoxyribonucleic Acid
CDR	Complimentary Determining Region
CKBPs	Chemokine Binding Protein
COX	Cyclooxygenase
CRS	Chemokine Recognition Site
Da	Dalton
E. Coli	*Escherichia Coli*
EC	Effective Concentration
ECM	Extracellular Matrix
Fab	Fragment antigen binding
FACS	Fluorescence Assisted Cell Sorting

Fc	Fragment crystallisable
Fv	Fragment variable
GAGs	Glycosaminoglycans
GDP	Guanidine Diphosphate
GPCR	G-protein Coupled Receptor
GTP	Guanidine Tri-phosphate
HDX-MS	Hydrogen/Deuterium Exchange Mass Spectrometry
HEK	Human Embryonic Kidney
HEPES	4-(2-Hydroxyethyl)-1-piperazineethanesulfonic acid
HexNac	N-acetylglucosamine
HIV	Human Immunodeficiency Virus
HMG Co-A	3-Hydroxy-3-methyl-glutaryl-coenzyme A
IC	Inhibitory Concentration
JUPITER	Justification for the Use of Statins in Primary Prevention: An Intervention Trial Evaluating Rosuvastatin
LDL	Low Density Lipoprotein
LPS	Lipopolysaccharide
MCP	Monocyte Chemoattractant Protein
MFI	Median Fluorescence Intensity

MIP	Macrophage Inflammatory Protein
mRNA	Messenger Ribonucleic acid
MS	Mass Spectrometry
NMR	Nuclear Magnetic Resonance
NTA	Nitrilotriacetic acid
oxLDL	Oxidised Low Density Lipoprotein
PBS	Phosphate Buffered Saline
PCR	Polymerase Chain Reaction
PPI	Protein-Protein Interaction
RANTES	Regulated on Activation, Normal T cell Expressed and Secreted
scFv	Single-Chain Variable Fragments
SGE	Salivary Gland Extract
SPR	Surface Plasmon Resonance
SUMO	Small Ubiquitin-like Modifier
TNF	Tumour Necrosis Factor
UTR	Untranslated Region
vMIP-II	Viral Macrophage Inflammatory Protein II

1 INTRODUCTION

The molecular arms race between host and pathogen has driven the evolution of molecules that can pharmacologically modulate the normal physiology of the host. For example, ticks have successfully evolved ways to suppress a host's immune system to remain undetected for a number of days whilst they feed[1]. Inflammation, whilst vital for protecting an organism from infection, also plays a role in the pathophysiology of a number of diseases, including cardiovascular disease[2]. This work seeks to unlock how a tick can suppress a host's immune system and hijack this to design compounds that can mimic their mechanism of action to treat cardiovascular disease.

1.1 CARDIOVASCULAR DISEASE

Cardiovascular disease is the reduction in the ability of the heart and circulatory system to transport blood around the body and is the leading cause of death worldwide[3,4]. As people begin to live longer it is reasonable to speculate that the number of deaths resulting from this disease will continue to increase over time. Whilst there are several treatments available for differing forms of heart disease, such as statins, angiotensin converting enzyme (ACE) inhibitors and beta blockers, the high number of deaths associated with this disease suggests that new treatments are still needed. Additionally, there are still several rare forms of cardiovascular disease, such as myocarditis, which have few, if any, available treatments[5]. Despite this clear unmet medical need for new therapies, there has been a recent stagnation in the number of new medical entities approved for the treatment of this disease[6]. As such, there is a great necessity to develop new

medicines to treat cardiovascular disease which can only be achieved through an increase in our understanding of this complex disorder. There are several forms of cardiovascular disease and as examples, atherosclerosis, myocardial fibrosis and myocarditis will be discussed briefly.

1.1.1 ATHEROSCLEROSIS

Atherosclerosis is defined as the build-up of plaque inside the artery wall and the mechanism of this disease has been studied in detail[7]. At sites of endothelial dysfunction due to endothelial cells being placed under stress due to certain blood flow patterns, exposure to toxins, or hypertension, circulating lipids in the form of low density lipoprotein (LDL) move from the circulatory system into the endothelium. This influx of LDL results in the endothelial cells secreting radical oxidising species (ROS) which oxidise the LDL to oxidised LDL (oxLDL). oxLDL induces an inflammatory response in the endothelium resulting in the recruitment of circulating monocytes. These monocytes differentiate into macrophages and attempt to remove the oxLDL through phagocytosis and attempting to break it down intracellularly. This results in the build-up of cholesterol inside the macrophage resulting in the cytoplasm becoming “foamy” as it is so laden with cholesterol, leading to so called foam cell formation. These macrophages laden with cholesterol accumulate inside the arterial wall leading to build up of fatty streaks inside the vasculature. The plaques can grow so large that they can lead to blood vessel occlusion, leading to conditions such as angina, or they can rupture leading to thrombi formation causing a myocardial infarction or stroke.

1.1.2 Myocardial Fibrosis

After severe cardiac injury, such as that following myocardial infarction, the heart undergoes significant remodelling[8]. This is because, unlike some other organs, the heart lacks the ability to regenerate and the dead cardiomyocytes are replaced by scar (fibrotic) tissue[9]. The extracellular matrix (ECM) provides a scaffold for cardiomyocytes as well as the mechanical strength for the contraction of the heart. The ECM is maintained by the cardiac fibroblasts which are specialised cells resident in the heart. Upon significant or persistent trauma to the heart cardiomyocytes become necrotic and need to be removed. Initially, there is a period of inflammation where monocytes, macrophages and neutrophils are recruited to the heart to remove the dead cells[10]. These recruited immune cells also activate cardiac fibroblasts, which begin to produce collagen, resulting in the replacement of cardiomyocytes with fibrotic tissue. Whilst this process is necessary to maintain the structural integrity of the heart, a chronic inflammatory response leads to continued deposition of fibrotic tissue resulting in impaired cardiac function and ultimately heart failure[11].

1.1.3 Myocarditis

Myocarditis is defined as inflammation of the heart's muscle cells and is characterised by the infiltration of immune cells into the myocardium, the thick layer of muscle tissue in between the outer (epicardium) and inner (endocardium) layers of the heart[12]. Typically, myocarditis occurs following a bacterial or viral infection. Infection of the myocardium results in an inflammatory response and, in the process of the recruited immune cells trying to remove the infection, tissue necrosis and damage to the heart can occur. In some cases this can be mild and there are no

obvious symptoms. However, in some cases this can be severe leading to dilated cardiomyopathy and heart failure[13].

1.1.4 The immune system as a target for cardiovascular disease

The immune system is complex and involves many different types of cells acting together to bring about an immune response to provide protection from invading pathogens and to maintain tissue homeostasis. However, what unites several forms of cardiovascular disease is the role of deleterious inflammation in the pathophysiology of the disease. The innate immune system, involving cell types such as monocytes, neutrophils, eosinophils and basophils and the adaptive immune system, consisting of T cells and B cells, have both been shown to play a role in cardiovascular disease[14].

As a result of this, pharmacological studies in humans have suggested that lowering inflammation could be a possible approach to treating cardiovascular disease[2]. Statins are one of the most widely prescribed drugs for treating cardiovascular disease and their mechanism of action is through the inhibition on HMG Co-A reductase[15]. This enzyme is key to the biosynthetic pathway of cholesterol so through the inhibition of HMG Co-A reductase statins lower levels of cholesterol and thereby reduce atherosclerotic plaque build-up in the endothelium. However, it is now widely accepted that the success of statins is due to their pleiotropic effects and not just the cholesterol limiting effect due to HMG Co-A reductase inhibition[16]. One additional mechanism by which statins may work is their effect on the immune system[17]. The JUPITER (Justification for the Use of Statins in Primary Prevention: An Intervention Trial Evaluating Rosuvastatin) clinical trial evaluated whether statins reduced heart attacks and strokes in people with normal

cholesterol levels but also had high levels of C-reactive protein. C-Reactive protein is a biomarker for inflammation and is associated with increased incidence of cardiac events[18]. It was found that patients with a high level of inflammation, but normal cholesterol levels, were protected from deleterious cardiovascular events when given a daily dose of Rosuvastatin[19]. This suggests that the success of statins is due to their ability to lower inflammation, and not just their effect on cholesterol levels, validating the immune system as a target for cardiovascular disease. However, it is likely that Rosuvastatin also lowered lipid levels in this study, so the beneficial outcome may also be due to the inhibition of HMG-CoA reductase to some degree. Further justification for the direct targeting of the immune system, independent of lowering lipid levels, comes from the CANTOS (Canakinumab Anti-inflammatory Thrombosis Outcomes Study) trial[20]. In this study, subjects with a history of myocardial infarction and high levels of C-reactive protein were given a daily dose of canakinumab. Canakinumab is a neutralising monoclonal antibody to interleukin-1β, a cytokine that is involved in driving the immune response. Patients who were given Canakinumab had lowered levels of C-reactive protein, but no change in their circulating lipid levels, yet still had a lower incidence of cardiac events. This study provides direct evidence that reducing inflammation is a valid therapeutic approach to treating atherosclerosis.

These studies suggest that lowering inflammation is worth exploring for the treatment of cardiovascular disease. The immune system involves the concerted action of multiple agents to bring about an immune response. Whether the immune system is driving the pathophysiology of a disease or protecting an organism from an invading pathogen, the timely recruitment and control of immune cell migration is vital. This is controlled, in part, by a family of proteins known as chemokines.

1.2 CHEMOKINES

Chemokines, or chemotactic cytokines, are small (8-12 kDa), generally basic secreted proteins that are known primarily for their ability to bring about the directional migration of various types of leukocytes[21]. The primary amino acid sequence of the different members of this family can be distinct from one another, excepting the location of four highly conserved cysteine residues. These cysteine residues are involved in intra-molecular disulphide bonds where the first cysteine is joined to the third and the second to the fourth[22]. Chemokines are divided into four sub-groups based on the spacing of the N-terminal cysteine residues. This leads to the chemokine ligands being categorised as CCL, CXCL, CX3CL and XCL where X is any amino acid and L denotes that they are chemokine ligands[23]. These ligands signal through G-protein coupled receptors (GPCRs) to stimulate white blood cell migration. The chemokine receptors are generally categorised by the class of chemokine ligand it interacts with, giving rise to the CCR, CXCR, CX3CR or XCR classes of chemokine receptors[23].

Isolated from the supernatants of monocytes activated by the immunostimulator lipopolysaccharide (LPS) from gram-positive bacteria, CXCL8 was one of the first chemokines to be identified and thoroughly characterised[24,25]. This protein was specific for driving neutrophil migration rather than being chemotactic for several types of leukocyte, as was the case for other cytokines known at the time such as TNF-α. N-Terminal sequencing of this protein revealed the “CXC” motif that is now used to categorise chemokines. Not long after this discovery, the chemokine now known as CCL2 was identified in the supernatant of tumour cells and was found to be specific for inducing monocyte migration in a

directional manner[26,27]. This protein was found to have cysteine residues in almost identical locations with CXCL8, except the N-terminal cysteines which had a CC not CXC relationship. These early discoveries showed was that there was a family of proteins responsible for the directional migration of sub-types of leukocyte and these proteins had conserved cysteine residues, suggesting that they may be related to one another.

The first chemokine receptors to be functionally cloned were CXCR1 and CXCR2, which are the receptors for CXCL8[28,29]. Most chemokine receptors possess seven α-helical transmembrane domains that associate with the heterotrimeric guanidine nucleotide binding protein (G-protein)[30]. The G-protein is a membrane-bound protein and is composed of the alpha, beta and gamma subunits[31]. In the inactive state it associated with the receptor and the alpha subunit is bound to guanidine diphosphate (GDP). The conformational change induced in the receptor following ligand binding results in GDP being replaced with guanidine triphosphate (GTP) in the alpha subunit, driving the dissociation of the alpha subunit from the beta and gamma units and placing the protein in an active state[32]. Once in an active state the dissociated subunits can initiate other signalling cascades, such as the production of secondary messengers or the opening of ion channels, resulting in signal transduction across the cell membrane and the appropriate cellular response[32]. In general, the chemokine receptors are approximately 350 amino acids in length, contain a short acidic extracellular N-terminus, three extracellular and three intracellular loops, and an intracellular C-terminus[33]. There is also a highly conserved disulphide bond between the extracellular loops one and two, and the G-protein interacting region is believed to be toward the intracellular C-terminus[33]. There are several amino acid motifs that are conserved across the chemokine

receptors, one being the DRYLAIV motif found in the second intracellular loop, which is also believed to be involved in G-protein coupling to the receptor[34].

Since these seminal discoveries approximately 50 chemokine ligands and 20 chemokine receptors have been functionally characterised. Chemokines perform a variety of physiological functions and can be roughly broken into two categories, homeostatic chemokines and inflammatory chemokines[35]. Homeostatic chemokines are constitutively expressed and are involved in maintaining correct physiological trafficking and positioning of cells. For example, CXCL12 and its receptor CXCR4 are involved in stem cell mobilisation and haematopoiesis[36], and CCL27 and its receptor CCR10 are involved in homing of T-cells for the establishment of immune homeostasis in the skin[37]. Inflammatory chemokine expression is induced in inflamed tissue in response to pro-inflammatory cytokines or in response to pathogenic stimuli. For example, LPS induces CCL2 and CXCL8 expression in macrophages[38,39]. The role of these induced chemokines is to recruit leukocytes to mount an immune response against an invading pathogen. The unifying features of all these proteins is that they stimulate the chemotaxis of white blood cells, signal through GPCRs and possess conserved cysteine residues. The conserved cysteine residues and the resulting disulphide bonds suggest that the chemokine ligands would share a related protein fold.

1.2.1 CHEMOKINE STRUCTURE

Despite chemokines possessing distinct primary amino acid sequences, the overall tertiary structure of the chemokine ligands is highly conserved. Chemokines are composed of a flexible N-terminal region, a 10-20 residue N-terminal loop, a β-sheet composed of three antiparallel β-strands and a C-terminal α-helix (fig. 1.1).

The loops connecting the first and second and second and third β-strands are known as the 30S and 40S loops respectively. The loop connecting the third β-strand to the C-terminal alpha helix is known as the 50S loop. However, most chemokines do not exist as monomers but as dimers or higher order oligomers as shown by their crystal or NMR structures[40,41].

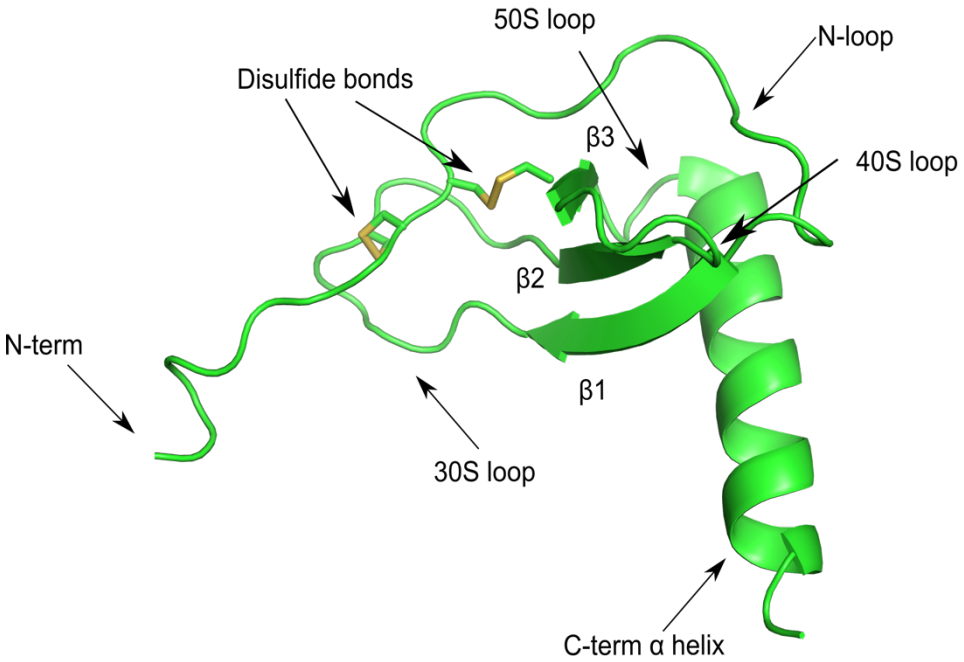


Figure 1.1 View from a crystal structure of CCL8 (PDB ID 1ESR). This is as an example of the typical chemokine structure. The structural features are indicated.

1.2.2 CHEMOKINE DIMERIZATION

Although chemokines all share a similar three-dimensional structure, the quaternary structures formed by chemokines can differ. The quaternary structure of a chemokine roughly depends on the family of ligand it belongs to with CXC and CC chemokines having markedly different dimer structures.

The three-dimensional structure of CXCL8 was solved using NMR spectroscopy and represents the archetypal CXC dimer structure (fig. 1.2A) [40]. It was found to be dimeric with the three β-strands of one subunit coming together with the three β-strands of the other subunit to form a six stranded β-sheet. The dimerization interface is primarily between residues from the first β-strand of each CXCL8 subunit. The C-terminal α-helices sit on top of the β-strands, almost running across the six β-sheets, and are packed to stabilise the dimeric structure. The structure of CCL4 was also solved by NMR spectroscopy and represents the typical CC dimer topology (fig. 1.2B). In contrast to CXCL8, the dimerization interface of CCL4 was found to primarily be between the N-terminal residues, leading to an elongated structure with the C-terminal α-helices at either end[41]. These differences were proposed to be due to the slightly extended C-terminal α-helix found in CXC chemokines verses CC chemokines, allowing for it to partake in dimer stabilisation. Additionally, the slightly more hydrophobic N-terminus of the CC chemokines, as opposed to mainly polar N-terminus of the CXC chemokines, results in more favourable interactions occurring when the CC type dimer is observed for this class of chemokines[41].

Whilst this categorisation may be true for several CC and CXC chemokines, there are exceptions. For example, CXCL10 exists as a tetramer in its crystal structure but can be thought of as dimer of CXCL8 type dimers, so still follows this rule to some extent[42]. The crystal structure of CCL2 was solved and it was found to exist in two crystal forms and accommodate two different quaternary forms[43]. One form was of the CC type dimer observed for CCL4 as expected whereas the other was a tetramer with the dimer of dimers making up this tetramer being much more

similar to the CXCL8 type. However, it should be noted that these structures could be artefacts of the protein being in a crystalline state or from the crystallographic conditions used; when the NMR structure of CCL2 was solved it was found to adopt a typical CC type dimer structure[44]. The biological significance of these quaternary structures is not clear. The dissociation constants for these interactions tend to be in the micromolar range and chemokines are most active in the nanomolar range *in vitro*, suggesting that the active form of the chemokine is the monomeric unit. Moreover, there have been studies where dimerization deficient mutants were found to be able induce chemotaxis in a comparable fashion to wild type also suggesting that it is the monomeric form of the chemokine that is binding the receptor[45,46]. However, studies involving a trapped monomer or dimer of CXCL8 revealed these forms have different recruitment profiles *in vivo,* with both forms still being active but to different extents[47]. To add a further level of complexity, it has also been shown that chemokine ligands can form heterodimers in solution. CCL2 and CCL8 have been found to form a CC type heterodimer preferentially to homodimer formation[48]. What is possible is that the dimerization of chemokines provides a nuance to the regulatory element of the chemokine system, highlighting the complexity of this family of proteins.

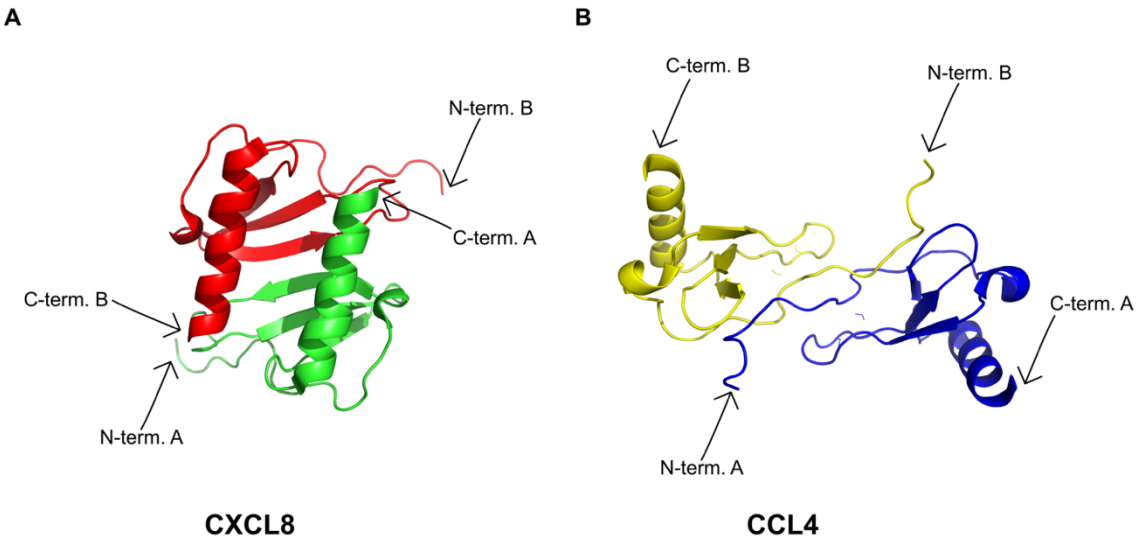


Figure 1.2 NMR structures of chemokine dimers. **A.** NMR structure of CXCL8 (PDB ID: 1IL8). One monomer is shown in green (chain A) and the other in red (chain B). **B.** NMR structure of CCL4 (PDB ID: 1HUM). One monomer is shown in blue (chain A) and the other in yellow (chain B). The N and C termini of each monomer are labelled on the figure.

1.2.3 CHEMOKINE LIGAND/RECEPTOR INTERACTION

The chemokine receptors are membrane bound proteins. Due to the challenges typically associated with membrane protein crystallography most of the insights into the determinants of the chemokine/receptor interaction have arisen through truncation and mutagenesis studies.

Initial truncation studies on CCL2 revealed that the N-terminus is essential for receptor activation[49]. A CCL2 truncation with residues 9-76 acted as antagonist of CCL2 activity, indicating that this protein can still bind the receptor but is unable to activate it. Further evidence for the importance of the N-terminus for receptor activation is the observation that addition of a methionine residue at the N-terminus of CCL5 (Met-RANTES) also functions as a receptor antagonist[50]. This again highlights the importance of the N-terminus of the chemokine in receptor activation. However, mutation of several residues at the N-terminus of CCL2 to alanine did not

dramatically effect signalling, indicating that the exact chemical nature of the N-terminus is not important for receptor activation[51]. Mutagenesis studies have highlighted the importance of the N-terminal loop region in receptor binding. In the context of CCL2, a Y13A CCL2 mutant had a lowered affinity for the CCR2 receptor[52]. This tyrosine (or the similar aromatic amino acid phenylalanine) is highly conserved across the CC chemokine family, suggesting it is a conserved receptor binding residue. A study supporting this hypothesis showed that a F13A mutant of CCL4 also had a reduced receptor affinity[53]. Furthermore, alanine mutants of R18, K19 and R24 of CCL2 all had reduced affinity for CCR2, indicating the importance of the N-terminal loop region in receptor binding[52]. What these studies suggest is that there are two distinct regions in chemokine ligands that are involved in receptor binding and activation. The N-terminus is important for receptor activation whereas the N-terminal loop region is important for receptor binding.

Many of the molecular insights into the determinants of regions within the chemokine receptors that are responsible for ligand binding have been from domain swap experiments. Swapping the extracellular N-terminal sections of CCR1 and CCR3 or CXCR1 and CXCR2 showed that these regions are vital for binding by their target ligands[54,55]. Expression of the 35 amino acid tail of the N-terminus of CCR2 fused to the transmembrane domain of CD-8 to anchor it in the plasma membrane was enough to drive high affinity binding of CCL2 to cells expressing this fusion protein[56]. What these studies revealed is that the extracellular N-terminus of the chemokine receptor is crucial for chemokine ligand binding. Activation of the receptor is primarily driven by the N-terminus of the ligand interacting with the transmembrane portion and the extracellular loops of the receptor. Mutation of residues in the transmembrane domain of CCR5 revealed that these residues were

critical for receptor activation and swapping the N-termini of various CCR5 ligands showed that it was this section of the ligand interacting with this region on the receptor[57]. Moreover, swapping various extracellular loops between CXCR1 and CXCR3 and evaluating the binding and functional effects of the CXCR3 ligands CXCL9, CXCL10 and CXCL11 indicated that these extracellular portions form a binding site for the N-terminus of the ligand and are important for receptor activation[58]. What these studies indicate is the existence of two domains on the chemokine receptor, one that is responsible for ligand binding and one that is responsible for activation by the ligand (fig. 1.3). This has led to the two-site binding model for chemokine receptor activation involving chemokine recognition site 1 (CRS1) and chemokine recognition site 2 (CRS2) on the receptor[59]. CRS1 involves the N-terminus of the receptor interacting with the N-loop region of the ligand whereas CRS2 involves the transmembrane pocket/extracellular loops of the receptor interacting with the N-terminus of the ligand. Through the combined action of these sites, chemokine ligands interact with their target receptors to bring about their functional effects.

Post-translational modification of the chemokine receptors has also been shown to play a role in chemokine recognition. For example, sulfation of tyrosine residues at the chemokine receptor N-terminus is important for chemokine ligand binding[60]. The sulfotyrosine group interacts with residues in the N-loop region on the ligand, helping to facilitate the chemokine/receptor binding interaction[61].

To determine how chemokine ligand binding to a receptor drives cell signalling and provide more information on how the chemokine receptors function a shotgun mutagenesis approach was used[62]. In this study, all residues of CXCR4 were mutated randomly and the effect of these mutations on CXCL12 signalling

studied. What this revealed was that when CXCL12 binds to the transmembrane pocket on CXCR4, this initiates the conformational change of the receptor driven by the formation of a hydrophobic bridge along the transmembrane helices, resulting in the release of the G-protein subunits. This study provided an insight into how chemokine binding can result in the transmission of a signal to the inside of a cell.

Despite the challenges associated with membrane protein crystallography, the crystal structure of CXCR4 in complex with a viral chemokine vMIP-II has been solved[63]. CXCR4 regulates cell migration for immune surveillance and the development of the hematopoietic, cardiovascular and central nervous systems[64,65]. vMIP-II is a chemokine ligand mimetic and is an antagonist of several CC and CXCR receptors that is used by Kaposi's sarcoma-associated herpesvirus to avoid detection by the host's immune system[66]. This structure confirmed the experimental evidence highlighted previously that led to the suggestion of the two-site binding model for the chemokine receptor/ligand interaction. This model also revealed that the interaction involves a contiguous surface involving every residue from the N-terminus to the N-loop region of the ligand interacting with the receptor. The lack of a boundary between the CSR1 and CSR2 interacting sites on the ligand led to the creation of an intermediary chemokine recognition site 1.5 (CRS1.5). Thus, the interaction is defined as follows: The N-terminus of the receptor (residues 23-27; CSR1) interacts with the N-terminal loop and first beta sheet of the ligand (residues 13-16), the next five residues of the receptor (residues 27-31; CRS1.5) interact with five residues toward to the N-terminus (residues 8-12), and the remaining N-terminal ligands interact with a pocket formed by the transmembrane helices, stabilised by a number of hydrogen bonds. What this study also highlighted was the importance of positive residues at the N-terminus of CXC ligands (R8 in CXCL12,

highly conserved across CXC chemokines but not CC chemokines) and positive residues in the N-loop region of CC chemokines (K22 in CCL5, highly conserved across CC chemokines but not CXC chemokines) for receptor binding and specificity. The studies described above have revealed the mechanism for chemokine ligand binding to its target receptors, involving the CRS1 CRS1.5 and CRS2 binding sites on the receptor and the N-terminus and N-loop region on the ligand.

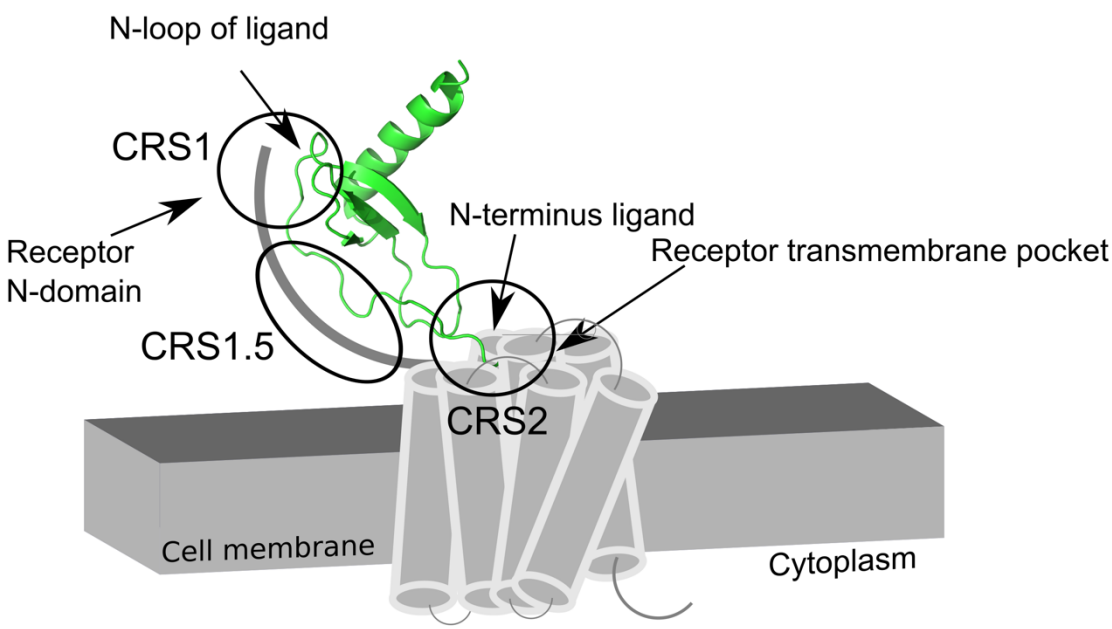


Figure 1.3: Chemokine/receptor interaction. The features of the interaction are labelled in the figure.

1.2.4 Chemokine oligomerisation and GAG binding

Chemotaxis is the directional migration of cells in response to a soluble agent whereas haptotaxis is the migration of cells in response to an immobilised agent and initial experiments revealed that chemokines can drive white blood cell migration through both mechanisms[67]. Subsequent experiments have shown that chemokines not only interact with chemokine receptors and themselves to form

dimers, but also glycosaminoglycans (GAGs) on the surface of endothelial cells and heparin[68]. This immobilises the chemokine to the endothelial cell surface and this interaction was shown to induce chemokine oligomerisation[68]. The heparin binding sites were found to be different to the receptor binding sites of CXCL8 as they were primarily toward the C-terminus of this ligand[69]. Additionally, a BBXB (where B is a basic amino acid and X is any amino acid) motif in the 40S loop on CCL5 was shown to be the binding site for heparin and this is distinct from the receptor binding sites on this ligand. Whilst mutation of this motif to alanine did lead to impaired heparin binding, a decreased affinity for CCR1 but not CCR5 was also obseved[70]. The latter may be explained by the crystal structure of CCL5 in complex with oligomers of heparin which showed that the BBXB motif in the 40S loop is indeed involved in GAG binding. However, this structure also revealed that there are some interactions with the positive residues in the N-terminal loop of CCL5, suggesting that there is some degree of overlap with the receptor and GAG binding sites[71,72]. The difference in CCR1 and CCR5 receptor binding noted above for the BBXB mutants highlights the differential importance of residues for binding to different receptors. Nonetheless, what these studies show is that chemokines interact with GAGs and this results in a change in the oligomerisation state of the chemokine, possibly affecting its activity.

The *in vivo* importance of the chemokine/GAG interaction was highlighted when GAG binding-deficient mutants of CCL3, CCL4 and CCL5 were unable to recruit cells when injected peritoneally despite being active *in vitro*[73]. In addition to this, mutants of these chemokines which could not oligomerise but could bind heparin were also shown to be active *in vitro* but not *in vivo*[73]. What this suggests is that for some ligands, chemokine/GAG binding and chemokine oligomerisation is

essential for activity *in vivo*. The interaction with cell surface GAGs immobilises the chemokines to specific sites, thereby creating local high concentration of chemokine, and also creating a concentration gradient of chemokine at specific sites to drive directional white blood cell movement. Therefore, this interaction provides a regulatory element to the chemokine system by localising and presenting the chemokine to circulating leukocytes to drive their physiological function.

1.2.5 Atypical chemokine receptors

The chemokine system is also regulated by a series of non-signalling or atypical chemokine receptors[74]. These are similar to the "typical" chemokine receptors as they have seven transmembrane domains but crucially they lack the DRYLAIV motif found on the second intracellular loop that is involved in G-protein coupling. The lack of this motif prevents these receptors from becoming activated in the "classical" sense of G-protein activation and do not signal *via* this route. These atypical chemokine receptors therefore do not drive cell migration or any of the other functions that are typically associated with the activation of chemokine receptors. To date four atypical chemokine receptors have been identified and characterised and these have been given the Atypical Chemokine Receptor X (abbreviated to ACKRX) nomenclature where X is a number[75]. These receptors were once known as: Duffy antigen receptor for chemokines (DARC) now ACKR1, D6 now ACKR2, CXCR7 now ACKR3 and CC chemokine receptor like 1 (CCRL1) now ACKR4.

Currently, these receptors regulate chemokines by two mechanisms. The first is by controlling the level of chemokines present through receptor internalisation after chemokine binding to the ligand and the subsequent degradation of the chemokine[76]. The second is through supporting chemokine trafficking by delivering

the chemokine to the necessary sites for optimal function[77,78]. These functions modulate the levels of chemokines at specific locations thereby providing instruction for this system. This is necessary for the chemokine system as deletion of these regulatory receptors in mice leads to the presentation of deleterious phenotypes. For example, ACKR2 was found to be protective against sepsis[79]. The possible lack of regulation of the chemokine system resulted in excessive chemokine accumulation and in turn excessive neutrophil recruitment, leading to tissue damage[79]. Moreover, ACKR2 was shown to regulate the inflammatory response during psoriasis in mice and expression of this receptor was higher in skin close to psoriatic lesions in humans, suggesting it plays a regulatory role in the surrounding skin. Atypical chemokine receptors add a further nuance to the chemokine system, along with chemokine dimerization, GAG binding and oligomerisation.

1.3 CHEMOKINES AND CARDIOVASCULAR DISEASE

Chemokine dimerization, GAG binding and the activity of atypical chemokine receptors exemplify the complexity of the chemokine system. These salient features point to a system that is highly complex and tightly regulated as chemokines are major players in the immune response. When this system is dysregulated, aberrant chemokine expression can drive a number of cardiovascular disease pathologies[80].

Atherosclerosis is the build-up of fatty plaques in the arteries. When LDL moves from the circulatory system into the arteries it is oxidised by macrophages to oxLDL[81] and this has been shown to upregulate the production of CCL2 from these cells[82]. Moreover, elevated expression of CCL2 was present in atherosclerotic lesions in hypercholesterolemic non-human primates[83] and was also found in macrophage-rich atherosclerotic regions in humans[84]. The recruited monocytes

differentiate into macrophages and contribute to the formation of fatty lesions through foam cell formation. Monocytes were found to require CCR2, CCR5 and CX3CR1 for recruitment to the atherosclerotic plaque[85] and CCR1, CCR2, CCR3, CCR4, CCR5 and CXCR3 expression was increased in mRNA from atherosclerotic aortas[86]. Additionally, patients with a non-functional mutation in the CCR5 receptor were protective against an early episode of myocardial infarction, possibly attributed to a delayed inflammatory response[87]. When CCR2, the receptor for CCL2, was knocked out in a mouse model of atherosclerosis there was a decrease in the size of the lesion formed despite no effect on circulating lipid levels[88]. Additionally, overexpression of CCL2 from macrophages in a mouse model of atherosclerosis resulted in an increase in atherosclerotic lesion size and greater macrophage recruitment to fatty plaques[89], indicating a role for this chemokine in plaque development. A number of other chemokines have been shown to be present in atherosclerotic plaques of humans including CCL3, CCL4 and CCL5[90]. CCL3 knockout mice displayed decreased lesion formation in a mouse model of atherosclerosis[91]. However, this result was attributed to the effect on neutrophil recruitment and human neutrophils typically do not respond to CCL3 whereas mouse neutrophils do. OxLDL was found to drive CXCL8 production in monocytes[92] and in a mouse model of atherosclerosis with the CXCL8 receptor CXCR2 removed a decrease in atherosclerotic lesion size was observed[93]. These studies suggest that chemokines play a role in the pathophysiology of atherosclerosis and, moreover, provide validation for chemokines as therapeutic targets for this form of heart disease.

Following a period of sustained and severe cardiac ischaemia, such as that following a heart attack, cardiomyocytes ultimately die and due to the lack of

regeneration capacity of the heart are replaced with fibrotic or “scar tissue", resulting in hearth failure[94]. Whilst this initial collagenous scar tissue formation is vital for preventing heart rupture following cardiomyocyte necrosis, the remodelling of surrounding non-infarct areas during reperfusion primarily contribute to the development of heart failure following ischaemia[95]. Therefore limiting infarct size following reperfusion would be desirable to prevent severe heart failure from occurring. The process of repairing the infarcted myocardium roughly involves three phases: the inflammatory phase when dead cardiomyocytes are removed by monocytes and neutrophils; the proliferative phase when the recruited leukocytes are removed and collagen deposition initiated; and the maturation phase where the collagenous matrix is cross linked and more remodelling occurs[96]. At each stage, the timely recruitment of leukocytes is required and as regulators of cell recruitment chemokines have been shown to play a role. Neutralisation of CCL2 in a rat model of myocardial ischemia by an antibody reduced infarct size following reperfusion[97]. PA508, a non-agonist mutant of CCL2 that was also engineered to have a higher affinity for GAGs than wild type CCL2, was shown to reduce infarct size, monocyte infiltration and collagen deposition in a mouse model of ischaemic reperfusion injury[98]. Patients with acute myocardial infarction (AMI) presented higher serum levels of CCL3, CCL4 and CCL5 compared to healthy controls and the AMI patients who presented severe ventricular remodelling also had a higher serum level of CCL3[99]. Moreover, administration of a GAG binding deficient mutant of CCL5 that acted as an antagonist of this chemokine reduced early reperfusion injury in mice[100]. These studies show that chemokines play a role in reperfusion injury and cardiac remodelling and targeting these chemokines may present a therapeutic strategy to treat these diseases.

Myocarditis is defined as inflammation of the myocardium and is associated with the development of cardiomyopathies[101]. Following a bacterial or viral infection, the chronic recruitment of leukocytes to the myocardium results in tissue damage and heart failure[102]. The pathophysiology of this disease is driven by excessive white blood cell recruitment and there have been studies showing that chemokines play a role. For example, CCL5, CXCL9, CXCL10, CCL17, CCL19 and their receptors were upregulated in the myocardium and disease severity directly correlated with CXCL9 expression[103]. Moreover, CXCL9 and CXCL10 polymorphisms in the 5'-UTR of these chemokines, which may affect gene expression, were associated with a less severe form of myocarditis[103]. CCL3 has been shown to be an important mediator of viral-induced inflammation and CCL3 null mice displayed resistance to Coxsackievirus-induced myocarditis compared to wild type[104]. Myocarditis therefore may be a disease which could be treated through the inhibition of chemokine action.

These diseases represent only a selection of cardiovascular diseases that possess a significant chemokine element to their pathophysiology. The studies outlined above suggest that chemokines are associated with these forms of cardiovascular disease. Moreover, the knockout or knock in studies in the animal models described above provide validation for targeting chemokines for these diseases. However, this element is not only limited to cardiovascular diseases. Several other inflammatory disorders such as arthritis, inflammatory bowel disease and psoriasis have all been shown to be driven by chemokine action[105-107]. As chemokines appear to be validated therapeutic targets for these diseases, there have been several clinical and preclinical trials evaluating chemokines in inflammatory disorders.

1.4 CLINICAL AND PRE-CLINAL STUDIES OF COMPOUNDS THAT TARGET CHEMOKINES

The chemokine system is highly complex and consequently there are few therapeutics that target this system. However, there are some success stories, such as Maraviroc and Plerixafor which are small molecules that target chemokine receptors[108]. Targeting CCR5 for the treatment of HIV is one of the greatest success stories regarding the targeting of the chemokine system for therapeutic benefit. It was discovered that individuals with a non-functional mutation in their CCR5 gene were resistant to HIV infection[109] and CCR5 was shown to be a co-receptor for HIV entry into the cell[110]. This led to development of small molecules to target CCR5 with the intention of inhibiting HIV entry into the cell. Through the use of a high-throughput radio ligand binding screen for hit identification and subsequent optimisation the drug Maraviroc was created, which prevented the development of HIV and AIDS through inhibition of virus entry to the cell via binding of CCR5[111]. Plerixafor is a drug that is used to treat haematological malignancies such as non-Hodgkin's lymphoma and acts as an antagonist of CXCR4, blocking the interaction of this receptor with CXCL12. CXCR4 was also shown to be a co-receptor for HIV entry[112] and consequently small molecules able to bind to this receptor that could inhibit HIV entry were screened. This identified the molecule Plerixafor, which was evaluated for its ability to provide resistance to HIV infection[113]. Despite not being pursued as an HIV treatment due to the requirement for systemic delivery, it was noted that test subjects had an increased level of circulating haematopoietic stem cells[113]. This was found to be due to Plerixafor inhibiting the action of CXCL12, the only ligand of CXCR4, which is responsible for the homing of haematopoietic stem cells to the bone marrow[114]. This observation led to Plerixafor being developed to

mobilize haematopoietic stem cells for transplantation into patients following chemotherapy to treat diseases such as non-Hodgkin's lymphoma. What these studies show is that the chemokine system is able to be pharmacologically modulated. However, these molecules do not elicit their effect through the lowering of inflammation. Considering that chemokines are "master controllers" of white blood cell migration[115] one would expect more drugs to be available that target chemokines for the lowering of inflammation to treat disease.

There have been several preclinical studies of chemokine inhibitors performed in inflammatory disease, along with a few clinical trials involving these types of compounds against inflammatory disease in humans. However, the overarching theme of these studies is that there is generally a positive outcome in the animal studies but then failure in the clinical stage. For example, there have been several pre-clinical studies involving the inhibition of chemokine action in arthritis. Arthritis is inflammation of the joints and chemokines have been shown to recruit leukocytes to the inflamed synovium[105]. Inhibition of CX3CL1, CCL2, CCL5 and CXCL12 by antibodies has been shown to reduce disease severity in mouse models of arthritis[116-119]. However, a clinical trial of a neutralising antibody to CCL2 did not result in improved clinical outcomes for patients with rheumatoid arthritis[120]. Moreover, a clinical trial involving a blocking antibody of the receptor CCR2 showed no improvement in outcomes for arthritis patients[121]. There have been several preclinical studies investigating the effect of inhibiting chemokine action in atherosclerosis. For example, inhibition of CCL5 activity has been shown to lower atherosclerotic plaque size in animal models of atherosclerosis[122,123] and a small molecule inhibitor of CCR5 was found to have a similar effect[124]. A neutralising antibody to CCL2 and CCL12 was shown to reduce plaque formation and leukocyte

infiltration in ApoE$^{-/-}$ mice[125]. A CCR2 neutralising antibody was able to lower C-reactive protein in humans, an important biomarker for atherosclerosis, but the efficacy of this antibody in treating this disease was not reported[126]. Moreover, clinical trials investigating a CCR1 inhibitor for psoriasis and endometriosis, a CCR3 inhibitor for asthma and allergic rhinitis or a CXCR3 inhibitor for psoriasis were either halted, no longer reported or deemed to have failed[127]. Taken together, these studies show that targeting a single chemokine ligand or receptor in the chemokine pathway for inflammatory diseases yields compounds that provide no efficacy in humans despite showing promise in pre-clinical models of disease. This highlights a lack of translation between animal models and humans and suggests a possible erroneous approach to neutralising the chemokine system.

1.5 Challenges in targeting the chemokine system

1.5.1 Animal models

All drugs need to be tested in some animal model before entering into clinical trials and the mainstay of pre-clinical models is rodents. Whilst chemokines are conserved across all vertebrates, subtle differences are present across these organisms. For example, human neutrophil recruitment is primarily driven by CXC chemokines such as CXCL8, signalling through the receptors CXCR1 and CXCR2[25,29]. However, murine neutrophils do not express CXCR1 but express CCR1, possibly to make up for the lack of this receptor. This gives a role to the ligands of this receptor, such as CCL3, in neutrophil recruitment that may not be seen in humans. However, it must be noted human neutrophils treated with CXCL12 will begin to express CCR1 and CCR3 indicating that this difference is not absolute[128]. Nonetheless, there are difference between what receptors are primarily

responsible for neutrophil recruitment in mice and humans, indicating that studies in mice may be different to what the situation is in humans. Moreover, the chemokine receptor sequences can differ quite substantially between the murine and human counterparts, for example CCR2 and CCR5, suggesting that what works well in mice may not translate into humans[129]. Additionally, animal models of disease are used to inform the selection of targets for therapeutic development. As several different models in mice can be used to study a single disease that is present in humans, this may produce subtle variations in the pathophysiology observed. Coupled with the differences in the human and murine chemokine system this may result in a suboptimal choice in target selection giving rise to the failure of compounds in the clinic[130]. Whilst therapeutics do need to be tested in a living system prior to being tested on human subjects, the lack of translatability of animal models to human disease for the chemokine system may be a possible reason for the relative high level of failure of clinical trials involving chemokine inhibitors observed thus far.

1.5.2 THE CHEMOKINE NETWORK

One of the most fundamental and intriguing properties of the chemokine system is that the chemokines operate through a robust network[131]. This means a single chemokine ligand can bind multiple receptors and a single chemokine receptor can bind multiple ligands. This “one-to-many” binding that is observed in the chemokine system offers a robust network that serves to drive the chemokine response. This network is not merely a series of overlapping degenerate and redundant interactions as the effect of the same chemokine binding to different receptors may drive different responses and *vice versa*. For example CCR7 has two

ligands, CCL19 and CCL21 but only CCL19 induces receptor internalisation[132]; CXCL8 has two target receptors, CXCR1 and CXCR2 yet both are internalised to different extents upon ligand binding[133]. These studies highlight how the chemokine response can differ depending on which ligand is activating the receptor or which receptor is being activated. Moreover, the studies highlighted above where chemokine ligands or receptor levels were determined in the atherosclerotic plaque revealed that multiple receptors and ligands were present in the diseased area[86,90], this suggests it is the combined action of multiple ligands and receptors driving the diseased state. To add further complexity to the chemokine network, single cells can express multiple chemokine receptors and depending on the location of the cell different receptors can be expressed[134,135]. Additionally, feedforward loops exist whereby chemokine expression can drive further expression of different chemokines and can lead to multiple chemokines being expressed in inflamed tissues[136]. The combined action of multiple chemokine receptors and ligands brings about the recruitment of multiple leukocytes to offer up a robust immune response. This robust network, driven by a series of “one-to-many” interactions, possibly renders the targeting of a single chemokine ligand or receptor by a therapeutic agent ineffective as the network can withstand an intervention such as this.

The temporal and spatial expression of chemokines may also render the chemokine a challenging system to inhibit through the targeted inhibition of a single chemokine ligand or receptor[137]. The expression of chemokine ligands and their receptors may change over time in the inflamed area. Yet, due to the “one-to-many” binding of the chemokine receptors and ligands, leukocyte migration can still be initiated. This means that the inhibition of a single ligand/receptor at one time point

may be effective, however over time this will become ineffective as other chemokines will be expressed and the white blood cells will still be recruited.

What these observations point to is a system that is challenging to target by conventional methods i.e. a therapeutic that operates by the “one drug one target” paradigm that is observed for many drugs. Perhaps taking a different approach, possibly one that is inspired by chemokine blocking agents that are found in nature which have arisen through evolution, may be able to deliver a therapeutic that can overcome the robustness of the chemokine system.

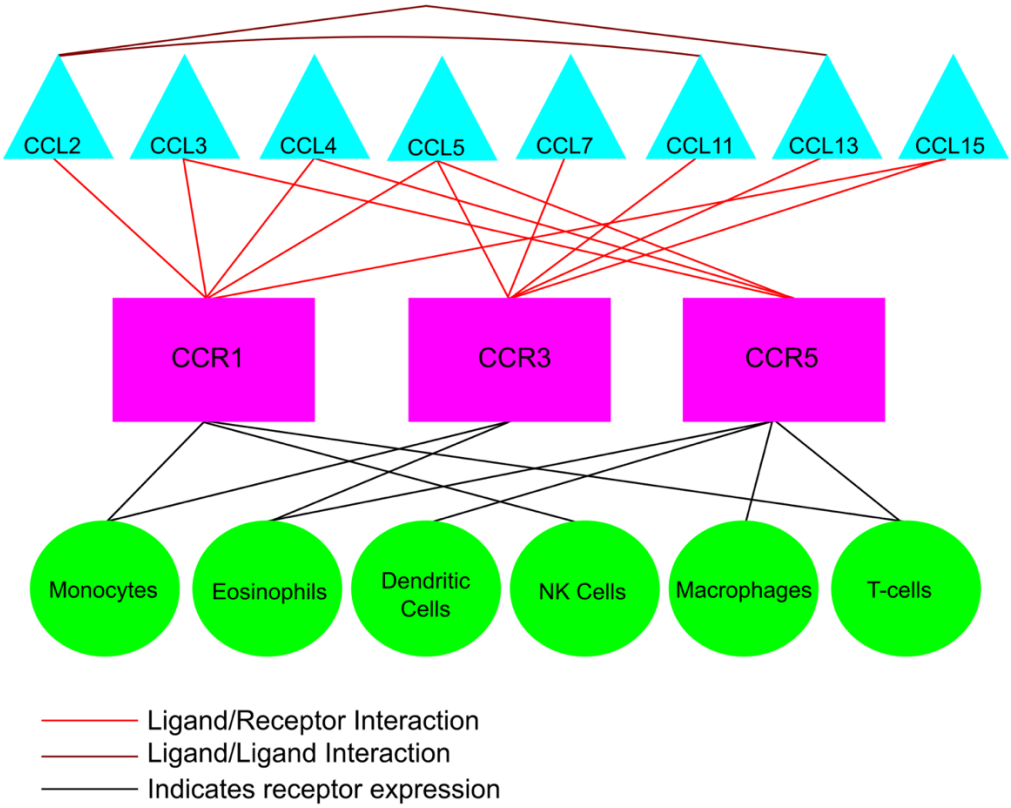


Figure 1.4 Representation of a part of the chemokine network. Ligand/receptor and receptor expression data for CCR1 (entry P32246), CCR3 (entry P51678) and CCR5 entry (P51681) taken from the UniProt database. Ligand/ligand interaction data from reference[48].

1.6 EVASINS

Ticks are blood feeding ectoparasites that to draw a decent blood meal must remain attached to their host for a number of days. This extended host residence time is most likely to produce inflammatory, haemostatic and immune responses. Consequently, ticks have evolved a number of anti-coagulant, anti-inflammatory and immunomodulatory factors to prevent detection by the host organism[138-140]. It has also been demonstrated that ticks are able to modulate or inhibit the activity of a variety of cytokines[141]. For example, tick salivary gland extracts (SGEs) has been shown to inhibit the activity of the pro-inflammatory cytokine TNF-α[142], suggesting that ticks suppress the host's immune system to remain undetected whilst they feed.

As discussed above, chemokines are key mediators in the immune response through their major role in the recruitment of various type of leukocytes, including monocytes and neutrophils, to sites of inflammation[143,144]. CXCL8 is a major driver of neutrophil recruitment[145] and studies have indicated that tick saliva is able to inhibit neutrophil function[146]. Through a combination of ELISA, radioligand-binding and chemotaxis assays it was initially shown that tick salivary gland extracts (SGE) had anti-CXCL8 activity[147,148]. CCL2, CCL3, CCL5 and CCL11 are potent regulators of monocyte, macrophage and eosinophil recruitment[143,149,150] and similar studies demonstrated that tick saliva can interact with and inhibit these chemokines[151]. In these experiments, unrefined SGE and fractionated SGE were shown to possess anti-chemokine activity suggesting that ticks target the chemokine system to suppress the host's immune system and allow them to remain undetected for a number of days.

The agents responsible for the anti-chemokine activity in tick saliva were characterised and these were proteins that have been termed “Evasins”. The first evasin to be described, Evasin-1, was identified using an expression-cloning approach[152]. A cDNA library was prepared from the salivary glands of feeding *Rhipicephalus sanguineus* (common brown dog tick) and this was cloned into a mammalian expression vector to create a library of tick salivary protein expression vectors which could then be expressed in HEK293 cells. Through cross linking studies to ^{125}I-CCL3, this library was deconvoluted to a single secreted protein from the library that was able to bind CCL3; this was termed Evasin-1. Evasin-1 was produced in HEK293 mammalian and TN5 insect cells and was found to be glycosylated and form a 1:1 complex with CCL3. Using surface plasmon resonance it was shown to bind CCL3, CCL4 and CCL18, but not CCL1, CCL2, CCL5, CCL1, CCL11, CCL13, CCL15, CCL17, CCL22, CCL26, CXCL1, CXCL4, CXCL7, CXCL8, CXCL9, CXCL10, CXCL11, CXCL12, CXCL13, XCL1 and CX3CL1 indicating that it only binds CC-type chemokines and is highly selective for the CC type chemokines that it binds. This work identified one of possibly several proteins responsible for anti-chemokine activity in tick saliva, where its mechanism of action was to bind chemokines in a “one-to-many” fashion i.e. one evasin binds many chemokines.

It is likely that *Rhipicephalus sanguineus* saliva contains more evasins as Evasin-1 was only shown to bind a small subset of one class of chemokine and previously it was discussed how multiple chemokines from the different chemokine sub-families work together to drive the inflammatory response. Subsequently, two more evasins, Evasin-3 and Evasin-4, were identified using a similar approach to that used to identify Evasin-1[1]. Cross-linking studies with ^{125}I-CXCL8 and the tick

transcriptome library described above identified Evasin-3 and deconvolution of the library after incubation with ^{125}I-CCL5 and ^{125}I-CCL11 identified Evasin-4. All three of the evasin proteins have a molecular weight below 11 kDa. Evasin-3 was found to be unrelated to Evasin-1 and was selective for CXC class chemokines. However, it was similar to Evasin-1 in the sense that it was highly selective for the CXC chemokines it could bind, binding only CXCL1 and CXCL8. Evasin-4 was found to be related to Evasin-1 due to the presence of conserved cysteine residues and only binding CC class chemokines. However, this protein was different to Evasin-1 as it had a much broader chemokine selectivity, binding CCL1, CCL3, CCL4, CCL7, CCL8, CCL11, CCL13, CCL14, CCL15, CCL16, CCL17, CCL18, CCL19, CCL21, CCL22, CCL23, CCL24, CCL25 and CCL26 but, interestingly, not CCL2 and the related protein CCL13[153]. The identification of evasins 1, 3 and 4 indicated that *Rhipicephalus sanguineus* has evolved several proteins that target multiple chemokines in a "one-to-many" fashion. Moreover, evasins can discriminate between the different classes of chemokine and have differing selectivity within the chemokine class they target. Evasin-1 and 4 only target CC class chemokines with Evasin-1 being much more selective than Evasin-4, and Evasin-3 binds only CXC class chemokines and is selective for the chemokines within this class that it binds[1,152,153]. It is likely that the tick uses the evasins to neutralise chemokine driven white blood cell migration to prevent the bite site from becoming inflamed. This indicates that the tick has evolved a way to successfully neutralise the chemokine network and the evasins may therefore also be useful for inhibiting chemokine action in diseases where they are implicated[154].

Evasins have been assessed in a number of pre-clinical disease models including lung fibrosis, colitis, post infarction myocardial injury and myocardial

reperfusion injury[155-158]. The success of the evasins in these disease models suggests that they could be used as therapeutics for the treatment of disease where chemokines have been shown to play a role. The success of the evasins at alleviating the disease phenotype in these models may be due to their "one-to-many" binding mechanism. This is because neutralising multiple chemokines at the same time prevents the chemokine network from being able to initiate the recruitment of white blood cells to inflamed tissue. This approach to neutralising the chemokine network that has arisen through evolution may be able to succeed at delivering an anti-chemokine therapeutic as, outline above, compounds that typically inhibit single chemokine ligands or receptors have not been successful in the clinic.

As evasins possess a novel mechanism of action for neutralising the chemokine network and are active in pre-clinical models of disease, a thorough understanding of their binding mode could be useful for the design of neutralising molecules towards chemokines to generate anti-inflammatory therapeutics. To this end, the crystal structure of Evasin-1 in complex with CCL3 has been solved (fig.1.5)[159]. This revealed that the N and C termini of Evasin-1 engage with the N-terminus of CCL3. At the C-terminus, W89 of Evasin-1 interacts with F29 of CCL3. The N-terminal residues D3-L9 of Evasin-1 interacts with the side-chains of CCL3, namely T16-S17-R18. There are several N-terminal contacts involving many hydrophobic interactions, one of which is a π-π interaction between F14 from Evasin-1 and F13 from CCL3. These observations suggest that Evasin-1 targets the chemokine receptor binding residues of CCL3 in the N-terminal loop region of this chemokine. An increase in K_d from 8nM to 32nM and a four-fold loss of affinity was observed when a F14A/ W89A Evasin-1 double mutant was tested against

immobilised CCL3; an F14A single mutant had little effect on the binding affinity. This work revealed that Evasin-1 targets the receptor binding region of CCL3 using its N and C-termini, and thus most likely exerts its anti-CCL3 effect by blocking the binding of CCL3 to its target receptors.

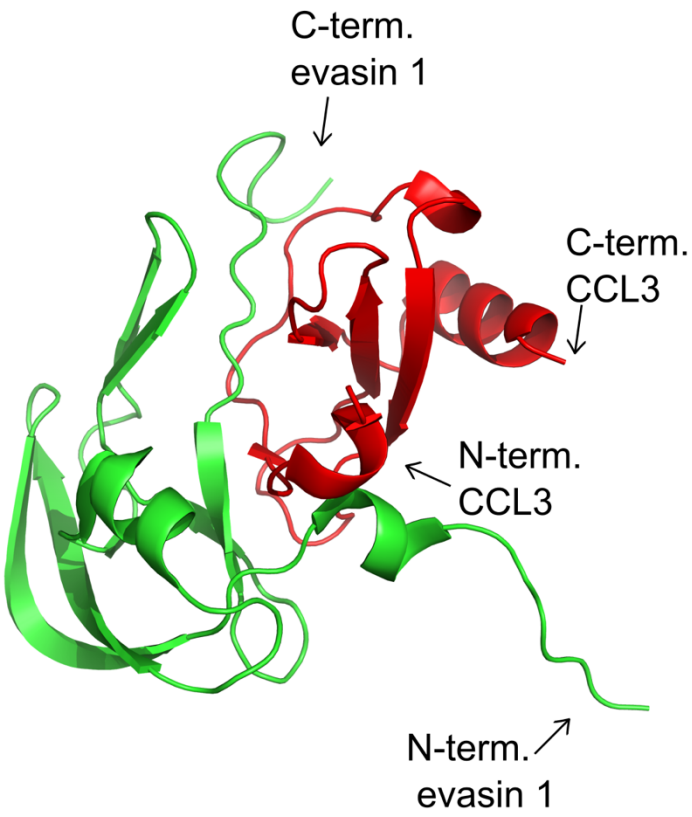


Figure 1.5 View from a crystal structure of the Evasin-1 (green) and CCL3 (red) complex. PDB ID 3FPU

Further work to elucidate the mechanism of evasin binding was achieved through the display of Evasin-1 and 4 on filamentous phage[160]. Using the crystal structure of Evasin-1 and CCL3, a homology model of Evasin-4 in complex with CCL3 was generated. Based on this a series of alanine mutants of putative interacting residues were then displayed on the surface of phage. This allowed for rapid screening of these mutants for chemokine binding. These studies revealed

that, unlike Evasin-1, Evasin-4 utilises solely the N-terminus to target CCL3, CCL5 and CCL8 with Glu16 and Tyr19 making key contacts with these chemokines, as revealed by a reduction in binding affinity when these residues were mutated to alanine. Moreover, the double mutant Y28Q/N60D was shown to reduce the binding affinity to these chemokines. It was also revealed that Evasin-4 had a lower affinity for T8P and F12A CCL5 mutants, but not the CCL5 alanine mutants when the mutated residues were in the 20S, 30S, 40S or 50S loop regions of this chemokine[160]. These observations provide further evidence that evasins target the chemokine N-terminus to bring about their inhibitory effects.

This initial work identified and characterised the moieties in the saliva from a single tick species that are responsible for the anti-chemokine activity observed in SGEs of these parasites. The agents responsible are proteins that, at least for the case of evasins 1 and 4, target the receptor binding region of their target chemokines. Furthermore, the evasins bind the chemokines in a “one-to-many” fashion. This may be because, as mentioned previously, chemokines signal through a network with “one-to-many” interactions between the ligands and receptors so the only way to successfully inhibit this network is to neutralise multiple ligands at the same time. The success of this novel mechanism of action, as outline above, is exemplified by evasins being active in several pre-clinical models of inflammatory disease and this novel mechanism of action may also be able to influence the design of anti-chemokine therapeutics going forward.

Despite the clear potential evasins offered as anti-chemokine therapeutics, only these three evasins from a single tick species were described in the literature. However, it was reported that a cDNA library constructed from the salivary gland of *R. sanguineus* contained five more putative evasins[161] and cDNA libraries

constructed from other tick species, such as *Amblyomma maculatum* and *Amblyomma ameicanum* were also found to contain DNA sequences that would correspond to putative evasins[162,163]. Notwithstanding several tick salivary gland transcriptome libraries being shown to contain putative evasin sequences, there still remained a relative paucity of recombinantly expressed and characterised evasins in the literature.

The next generation of evasins were identified using a yeast surface display approach[164]. In this work a library of over 350 putative evasin sequences were identified from the publicly available transcriptome datasets from Prostriate and Metastriate ticks using the sequence homology to evasins 1, 3 and 4 using psiBLAST. These putative evasin sequences from multiple tick species were then cloned into a yeast surface display vector to generate a library of evasins that could be expressed on the surface of yeast, thereby linking genotype to phenotype. This library was then screened against a number of fluorescent CC class chemokines to pull out chemokine binding sequences using fluorescent assisted cell sorting (FACS). Using this technology 26 evasin sequences were identified, 10 of which were characterised in detail through recombinant expression of these sequences in HEK293 cells. Using a combination of biolayer interferometry (BLI) and Boyden chamber assays these proteins were shown to bind and neutralise multiple chemokines *in vitro*[164]. This work highlights that evasin sequences identified bioinformatically are able to bind to and neutralise chemokines when produced recombinantly. Moreover, this work shows that it is possible to display functional evasins on the surface of yeast thereby generating a technology that allows for the rapid identification of evasins that can target specific chemokines.

The work described above highlights that bioinformatic identification of evasin sequences is possible approach to identify functional evasins from multiple tick species. This is exemplified further by a piece of work where over 250 putative evasin sequences were identified from the UniProtKB protein sequence database and the tick genomic and transcriptomic data in VectorBase[165]. Of these sequences, nine were successfully expressed and refolded from an *E. coli* expression system and using a fluorescence polarisation assay these proteins were shown to bind CCL2, CCL7, CCL8, CCL11, CCL24 and CCL26[165]. By measuring the levels of cAMP, a secondary messenger involved in chemokine signalling, induced by CCL2, CCL8, CCL11 and CCL24 with and without prior incubation of these chemokines with recombinant evasins it was demonstrated that these evasins can inhibit signalling due to these chemokines. This work highlights further the utility of identifying evasin sequences through sequence homology.

To date, approximately 20 CC binding evasins and one CXC binding evasin have been identified and characterised in detail from the salivary transcriptomes of multiple tick species. The CC binding evasins are all related proteins that share eight conserved cysteines and possibly four disulphide bonds, suggesting they all have a similar secondary structure, whereas the CXC binding evasin, Evasin-3, only has six cysteines and three disulphide bonds. This has led to the classification of the evasins as follows: CC binding evasins are termed 8-cys evasins and CXC binding evasins are termed 6-cys evasins[165].

The “one-to-many” binding observed for the evasins presents a novel mechanism of action to neutralise the chemokine network. This is in contrast to the mechanism of action of monovalent antibodies which typically target a single chemokine, which may explain the failure of this modality in the clinic. Combined

with the efficacy of evasins in pre-clinical models, evasins, or agents that can mimic the evasin “one-to-many” chemokine binding mechanism, may present a route to a possible anti-chemokine therapeutic.

1.7 FURTHER EVIDENCE OF THE “ONE-TO-MANY” MECHANISM

It is not only ticks that have evolved chemokine binding proteins with a “one-to-many” chemokine binding mechanism. Other pathogens that require extended host residence times such as viruses and parasitic worms have also convergently evolved multiple chemokine binding proteins (CKBPs).

Poxviruses produce CKBPs that are able to block the activity of several chemokine ligands, including CCL2, CCL3, CCL5, CCL7, CCL11 and CCL23, by inhibiting the engagement of the chemokine with its target receptor[166]. The structure of a poxvirus CKBP in complex with CCL2, CCL3 and CCL7 revealed that in a similar fashion to Evasin-1 it binds the N-terminal loop region of the chemokine and thereby blocks the interaction of the chemokine with its target receptors[167]. Incubation of egg secretions from the parasitic work *Schistosoma mansoni* with chemokines identified a protein capable of binding multiple chemokine ligands, CXCL8, CX3CL1, CCL2, CCL3 and CCL5, and was shown to be efficacious in *in vivo* inflammatory models of disease[168].

The capability for all these evolved proteins to bind multiple chemokines suggests that this “one-to-many” mechanism of action is able to overcome the network robustness of the chemokine system. Targeting multiple chemokines prevents the chemokine network from being able to initiate the recruitment of white blood cells, thereby inhibiting the immune response. As chemokines play a role in

several diseases where inflammation is driving the pathophysiology, this approach may be able to inhibit the chemokine system and deliver new agents that will be able to treat these types of diseases. As there has not been much success using the "one-drug-one-target" mechanism that is associated with most drugs, exemplified by the failure of the anti-body clinical trials outline above, perhaps the targeted inhibition of multiple chemokines will be able to deliver a therapeutic that is inspired by nature and is active in inflammatory diseases in humans.

1.8 NATURE AND THERAPEUTICS

Nature has provided a wealth of biologically active compounds, several of which have been converted into drugs[169]. For example, morphine, salicylic acid and digoxin are the active ingredients in plant extracts that have been used to treat diseases for possibly thousands of years. Moreover, nature has not only provided the ingredients for a drug but has also provided inspiration for drug mechanisms of action. Fentanyl is a synthetic opioid which works in a similar manner to morphine by binding to the opioid receptors[170]. Additionally, celecoxib, a selective COX-2 inhibitor, targets the same enzyme that is inhibited by aspirin to act as an anti-inflammatory and painkiller[171]. These drugs have their origins in nature but are synthetic, indicating that through the understanding of a naturally pharmacologically active compound it is possible to generate a drug that can be inspired by nature's mechanism of action.

It is not only small molecule drugs that have their origins in nature; several biological therapeutics have their origins from natural source as well. Hirudin, an anti-coagulant drug, was originally isolated from leech saliva and is now used in the clinic[172]. Moreover, conversin, a C5 complement inhibitor[173], is being evaluated in

clinical trials and was originally isolated from tick saliva. In a similar fashion to celecoxib and fentanyl there are also several small molecule drugs that have been inspired by the mechanism of action of biologics found in nature. Captopril, an ACE inhibitor used for treating cardiovascular disease, works in the same manner as Pit viper venom to lower blood pressure[174] and tirofiban, an antiplatelet agent, also mimics snake venom biologics[175]. These drugs were discovered through the deconvolution of protein-protein interaction to a protein-peptide interaction and finally to a small molecule protein interaction. Taken together, these examples show that it is possible to use a natural biologic as a drug, or through the understanding of a biologic found in nature it is possible to generate a therapeutic with a mechanism of action inspired by a natural agent. Evolution has had billions of years of natural selection to determine the best mechanism of action for a compound to have the most potent biological effects and by exploiting this it may be possible to deliver new therapeutics with novel mechanism of action to treat diseases where conventional approaches have failed.

This rationale may be extended to the evasins found in tick saliva. The “one-to-many” binding mechanism that has evolved in the evasins may suggest that these proteins are able to successfully inhibit the chemokine system, so they could be used as anti-chemokine drugs. However, small molecules or peptides that present the same mechanism of action as evasins, that is the inhibition of multiple chemokines through “one-to-many” binding, may also be able to successfully target the chemokine system. Through the study of an evasin/chemokine complex it may be possible to deliver a peptide or small molecule that has a mechanism of action inspired by these tick proteins that is able to successfully neutralise the chemokine system.

1.9 AIMS OF THIS WORK

The studies outlined above suggest that evasins may be a class of biologic that could be used to treat disease where chemokines are implicated. The aim of this work is to build upon the yeast surface display approach outlined above to identify new evasins[164]. The library will be screened against the chemokine CCL8 to identify an evasin capable of binding this chemokine. This evasin will have its chemokine binding profile determined and will be evaluated for the ability to functionally inhibit chemokine driven cell migration.

Protein therapeutics such as evasins would require parenteral delivery and are associated with high manufacturing costs, and therefore designing an entity that has the same “one-to-many” mechanism of action as an evasin which can be chemically synthesised would be highly advantageous. To achieve this it is envisioned that the newly identified evasin/CCL8 complex interface will be characterised to aid in the design of peptides that mimic the evasin mechanism of action.

This work seeks to unlock how nature is able to target multiple chemokines and use this to design therapeutics that have their mechanism of action inspired by the work of evolution.

2 ASSAY DEVELOPMENT

2.1 INTRODUCTION

Chemokines are proteins that are responsible for immune cell trafficking. They bind to and activate GPCRs on white blood cells, thereby providing a migrational cue[176]. Evasins are proteins found in tick saliva that bind chemokines and inhibit their action[1] and having quantitative, robust and reproducible assays is a prerequisite for the development and characterisation of inhibitors. Therefore, assays that can monitor chemokine/evasin binding, the inhibition of chemokine binding to chemokine receptors and the functional inhibition of chemokines by evasins need to be developed.

Previous techniques used to characterise evasin/chemokine interactions have included surface plasmon resonance (SPR), chemokine/receptor equilibrium binding assays and Boyden chamber assays[152,153]. SPR allows for the characterisation of evasin/chemokine binding, equilibrium binding assays can show chemokine/receptor binding inhibition and Boyden chamber assays can indicate whether a chemokine is being functionally inhibited. In this chapter the development of a biolayer interferometery (BLI) binding assay, a fluorescent chemokine/receptor blocking assay and cell migration assay will be described.

2.2 BIOLAYER INTERFEROMETRY BINDING ASSAY

Biolayer interferometry (BLI) is a technique which is similar to SPR and allows for the binding between two interacting proteins to be measured in real time[177]. In this technique a functionalised biosensor is loaded with one of the binding partners. This loaded biosensor is then placed into a solution of the other binding

partner to allow for the association between the two proteins to be monitored. It is then placed into a solution of buffer to allow for the dissociation of the two partners to be monitored. The BLI instrument allows for 384 well plate format, allowing for the rapid characterisation of binding interactions.

The biosensor is made of glass fibre and when white light is sent down the biosensor it is reflected back along the sensor and this is monitored. As a binding partner binds to the biosensors (or to a binding partner already bound to the sensor), the thickness of the tip changes and this impacts the wavelength of the reflected light. This wavelength shift serves as a measure of the degree of binding and is monitored as a function of time and thus can inform on kinetic parameters such as association (k_a) and dissociation rate constants (k_d), and thermodynamic parameters such as binding association (K_a) and dissociation constants (K_d), thereby giving an indication of the strength of an interaction.

One of the main issues facing BLI is non-specific binding of a protein to the biosensors. In this experiment, an Ni-NTA charged biosensor is loaded with his-tagged evasin. This loaded biosensor is placed into a well containing chemokine and the binding monitored. What became apparent after initial experiments is that chemokine binding to the sensor was an issue and the assay needed to be optimised to prevent this (fig. 2.1). CCL5 appeared to bind to the unfunctionalized biosensor, indicated by the large increase in the wavelength shift as the biosensor was placed into the CCL5 solution; CCL2 and CCL3 also showed some binding to the sensor. The manufacturers recommended buffer is phosphate buffered saline (10mM Na-Phos, 137mM NaCl, 2.7mM KCl) with 0.01% BSA and 0.002% TWEEN-20 to act as blocking agents to limit non-specific interactions. In an attempt to limit the binding of the chemokine to the sensor a buffer screen was performed (fig. 2.1).

This revealed that increasing the sodium chloride concentration to 500mM dramatically lowered the chemokine binding to the sensor, thereby suggesting that these conditions were suitable for measuring evasin/chemokine interactions. The Ni-NTA biosensors can be thought of as essentially a positively charged sheet that can electrostatically interact with other moieties. The higher salt concentration was investigated as increasing the ionic strength of the solution could shield this positively charged sheet, thereby preventing the binding of the chemokine to the sensor.

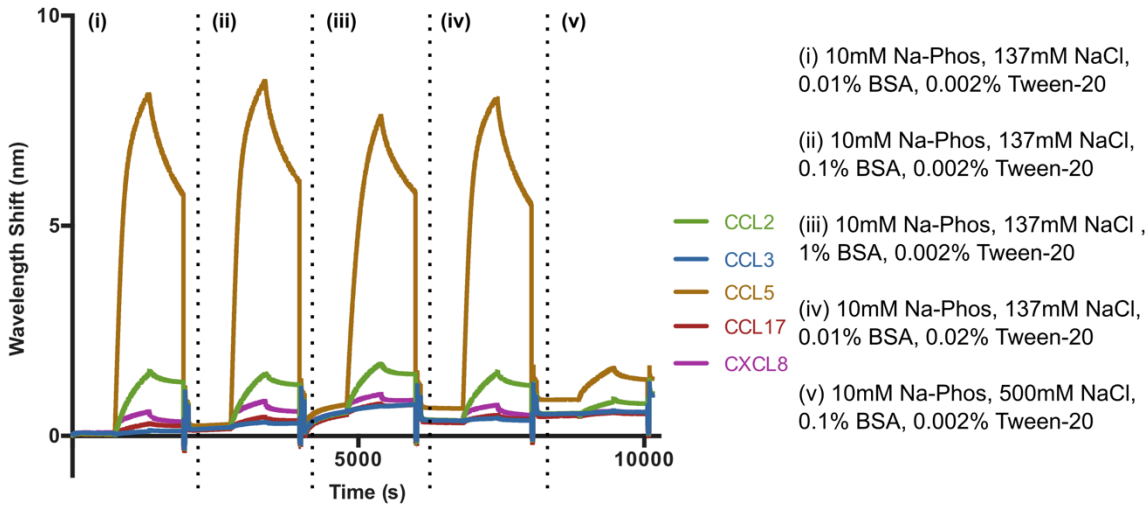


Figure 2.1 BLI assay buffer optimisation. Biolayer interferometry sensors were exposed to chemokine (300nM) for 600s and then buffer for 600s prior to being regenerated. Regeneration was performed by the sensors being stripped and then reloaded with nickel. Nickel was removed by placing the sensors into 10mM glycine pH 1.7 for five seconds followed by buffer for five seconds three times, and nickel was charged onto the sensor by the sensor being placed into 10mM $NiCl_2$. Each condition tested is separated by a dotted line on the figure with the buffer composition indicated by (i)-(v). The chemokine tested is indicated by the colour displayed in the legend. Y-axis displays wavelength shift (nm), x-axis display times (seconds).

One important aspect of the biolayer interferometry assay is comparing the binding interaction of two proteins to a binding experiment where one of the proteins is replaced with a protein that is not expected to bind. This negative control

experiment is performed every time a binding experiment is performed and is subtracted from the binding signal to account for non-specific interactions. A reference protein with the sequence: DGGQRNAICRLPPDEGICRASIPRFYFNPAEGKCSFFIYGGCEGNENNFETIEEC EKTCGEPERPSDFEGADFETGCAPKPQRGFCKGFLDHWFFNVTSGECEAFLYS GCGGNDNNYESKEECEIACKLTGGASAWSHPQFEKLEHHHHHHHH was chosen. This protein is also found in tick saliva and is an inhibitor platelet activation. It was chosen because it has a his-tag so it can be immobilised to the sensor and could be expressed to high levels using the same expression system as the evasins to be tested[164]. Crucially, it was not expected to interact with any chemokines. Using the optimised buffer conditions binding of all commercially available chemokines to this protein were tested (fig. 2.2).

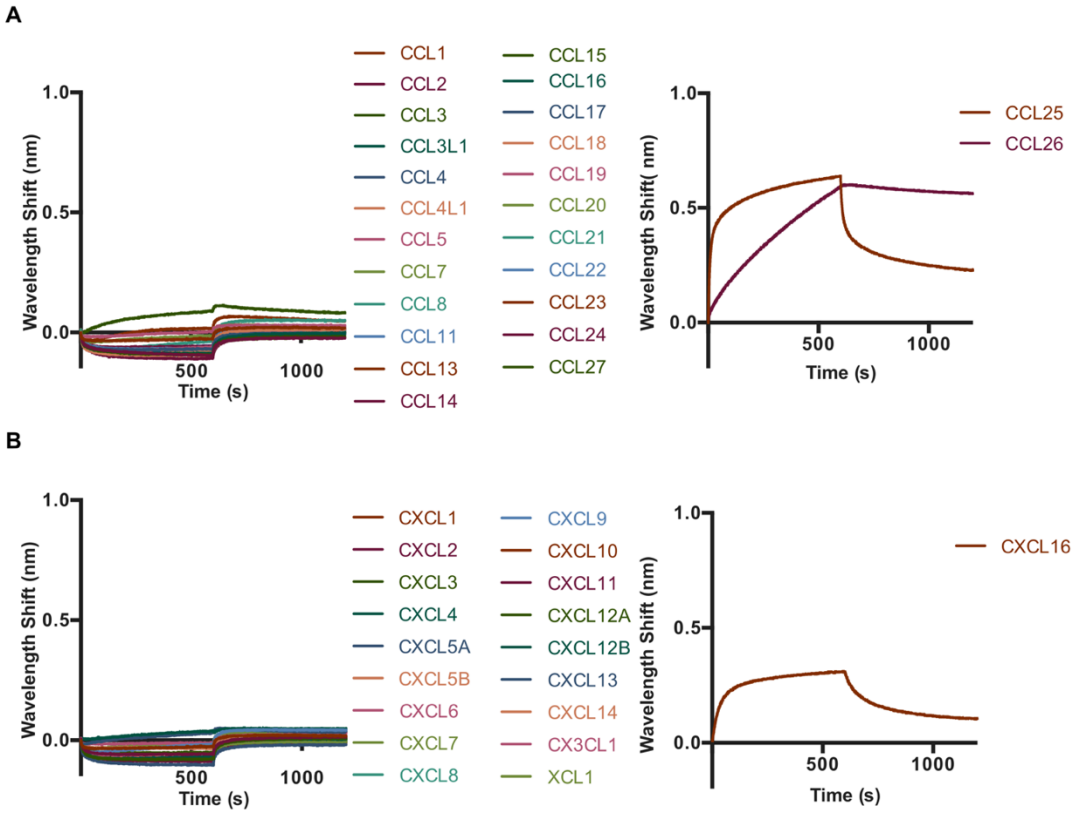


Figure 2.2 Chemokine binding to the reference protein. the Reference protein was loaded onto the biosensors for 500s (not shown). This was then placed into a solution containing the chemokine (300nM) for 600s followed by buffer for 600s. The chemokine tested is indicated by the colour displayed in the legend. **A.** *Left panel* – CC class chemokines that did not display a binding signal. *Right panel* – CC class chemokines that displayed a binding signal. **B.** *Left panel* – CXC, CX3C and XC class chemokines that did not display a binding signal. *Right panel* – CXC, CX3C and XC class chemokines that displayed a binding signal. Y-axis displays wavelength shift (nm), x-axis display times (seconds).

This cross binding experiment revealed that all chemokines tested, apart from CCL25, CCL26 and CXCL16, did not bind to the reference protein under these conditions. CCL25, CCL26 and CXCL16 still displayed binding to the unfunctionalized sensor under these conditions (fig. 2.3), which probably explains the binding signal that was observed to the reference protein, so were excluded from the BLI assay.

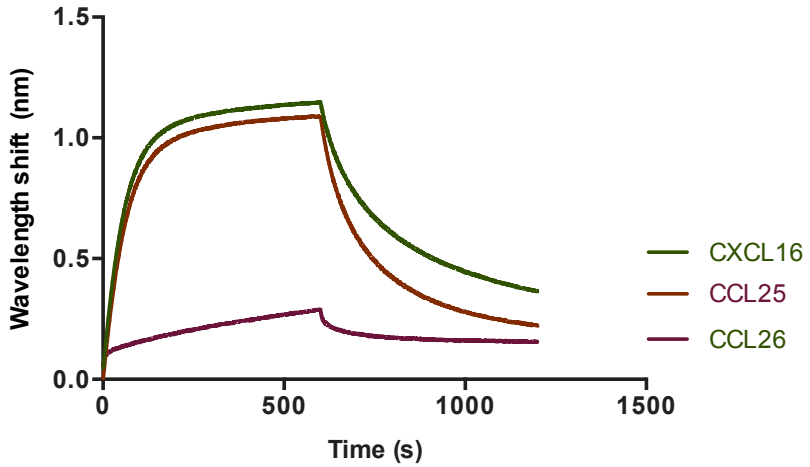


Figure 2.3 Chemokine binding to the unfunctionalized sensor. The sensor was placed into a solution containing the chemokine (300nM) for 600s followed by buffer for 600s. The chemokine tested is indicated by the colour displayed in the legend. Y-axis displays wavelength shift (nm), x-axis display times (seconds).

To validate the assay the chemokine binding profile of Evasin-1 was investigated using these conditions and the affinities of the binding chemokines determined. Evasin-1 was screened against the panel of chemokines which did not display binding to the reference protein at 300nM and for those which displayed a binding signal the affinity was determined (table 1).

	SPR[152]		BLI	
Chemokine	**K_d (M)**	**Error**	**K_d (M)**	**Error**
CCL3	*1.30E-10*	*8.00E-11*	*7.28E-09*	*5.15E-11*
CCL3L1	*ND*	*ND*	*2.24E-08*	*1.78E-10*
CCL4	*8.10E-10*	*3.00E-10*	*2.33E-07*	*6.23E-09*
CCL4L1	*ND*	*ND*	*7.79E-08*	*1.87E-09*
CCL14	*ND*	*ND*	*1.08E-07*	*1.89E-09*
CCL18	*3.21E-09*	*1.95E-09*	*2.02E-09*	*1.49E-10*

Table 1 Evasin-1 binding affinities determined by SPR and BLI

Evasin-1/chemokine interactions were previously characterised using SPR and the chemokines that displayed a binding signal in the BLI experiment were in good agreement to those published previously[152]. A binding signal to CCL14 was observed and this has not been reported before but Evasin-1 was not tested for binding to this chemokine previously. Evasin-1 was also tested against CCL3L1 and CCL4L1 which are isoforms of CCL3 and CCL4 and this was not shown before. Expectedly, Evasin-1 was able to bind these chemokines. The K_d values are in the nM range when determined by BLI whereas by SPR the K_d values were all sub-nanomolar. The rank order of the affinities determined by BLI also differs to the order determine by SPR. The SPR rank order of decreasing affinity was CCL3, CCL4 then CCL18 whereas by BLI it was CCL18, CCL3, CCL4. These differences may be due to the different techniques used and the different conditions that the binding experiments were performed under. Nonetheless, the expected chemokine interactions were observed for Evasin-1 and the K_d values could readily be determined.

This BLI assay was further optimised to screen an evasin against a panel of 42 chemokines in under three hours in an entirely automated fashion. This assay can also be used for the rapid determination of affinity constants, where approximately 20 K_d values can be determined in a day. However, this assay does require the protein tested to be immobilised through a poly-histidine tag which may not truly represent the binding event that occurs when both binding partners are in solution. Nonetheless, this assay offers the ability to rapidly and robustly characterise evasin/chemokine interactions with minimal input from the experimenter and thus was used as an assay of choice for K_d determination in chapters 3, 4 and 5.

2.3 FLUORESCENT LIGAND/RECEPTOR BLOCKING ASSAY

Chemokines signal through GPCRS and inhibition of this interaction should prevent chemokine signalling. Previous experiments used to characterise chemokine/receptor binding inhibition by evasins have included the use of radioactive chemokine/receptor binding assays[152]. In this work, to characterise CCL8 binding to chemokine receptors and the subsequent inhibition of this interaction, a fluorescent chemokine/receptor blocking assay was developed. This experiment involved incubating human monocytic THP-1 cells, which are known to express chemokine receptors CCR1, CCR2 and CCR5[178], with CCL8 conjugated to a fluorophore (purchased from Almac), herein referred to as CCL8-647. When CCL8-647 binds to the chemokine receptors, this should result in the cells becoming fluorescent. This can then be monitored using fluorescence assisted cell sorting (FACS) where the median fluorescence intensity of the cells (MFI) can serve as a measure for chemokine/receptor binding. If an evasin can inhibit an increase in MFI, this would suggest that it is inhibiting the CCL8/receptor interaction.

Incubating THP-1 cells with varying concentrations of CCL8-647 results in a dose dependent increase in the MFI of the cells (fig. 2.4A). Interestingly, this would reproducibly produce a binding curve that appeared to reach an initial plateau and then begin to increase again (fig. 2.4A). This could be because at higher concentrations of CCL8-647 the target receptors are becoming internalised and recycled to the cell surface[179]. The fluorescent chemokine would remain in the cell whereas the receptor would now be on the cell surface able to bind another molecule of CCL8-647, thereby causing a greater increase in MFI than would be expected. Also, CCL8 can bind CCR2 and CCR5 and it is possible that there is one

high affinity binding event followed by a second lower affinity binding event to these receptors, thereby giving a bi-phasic binding curve. Nonetheless, CCL8-647 appears to be binding to THP-1 cells as evidenced by the increase in MFI.

To determine the concentration of CCL8-647 to be used in a blocking assay, the four highest concentrations points were removed from the curve and an EC_{80} value determined (fig. 2.4B). This means the concentration of CCL8-647 used will be in the linear range, allowing for effects on chemokine binding to clearly be observed.

To investigate if CCL8-647 binding could be inhibited, an evasin (P672) and "cold" CCL8 (CCL8 not conjugated to a fluorophore) were pre-incubated with CCL8-647 and the effect on MFI determined. This revealed that cold CCL8 could prevent CCL8-647 from binding, indicating that this is a specific interaction. Moreover, an evasin was able to block an increase in MFI, indicating that this assay can be used to probe chemokine/evasin interactions.

This assay can be performed in a 96 well plate, does not require the use of radioactive chemokines and as it uses THP-1 cells it does not require the isolation of membranes from cells. However, as it is using endogenous chemokine receptors on a cell and the cell still has receptor recycling and degrading mechanisms it is not clear what receptors are being inhibited and is not a direct chemokine/receptor equilibrium binding assay. Nonetheless, this assay is able to probe the effect of an evasin on chemokine/receptor binding in a rapid and robust fashion.

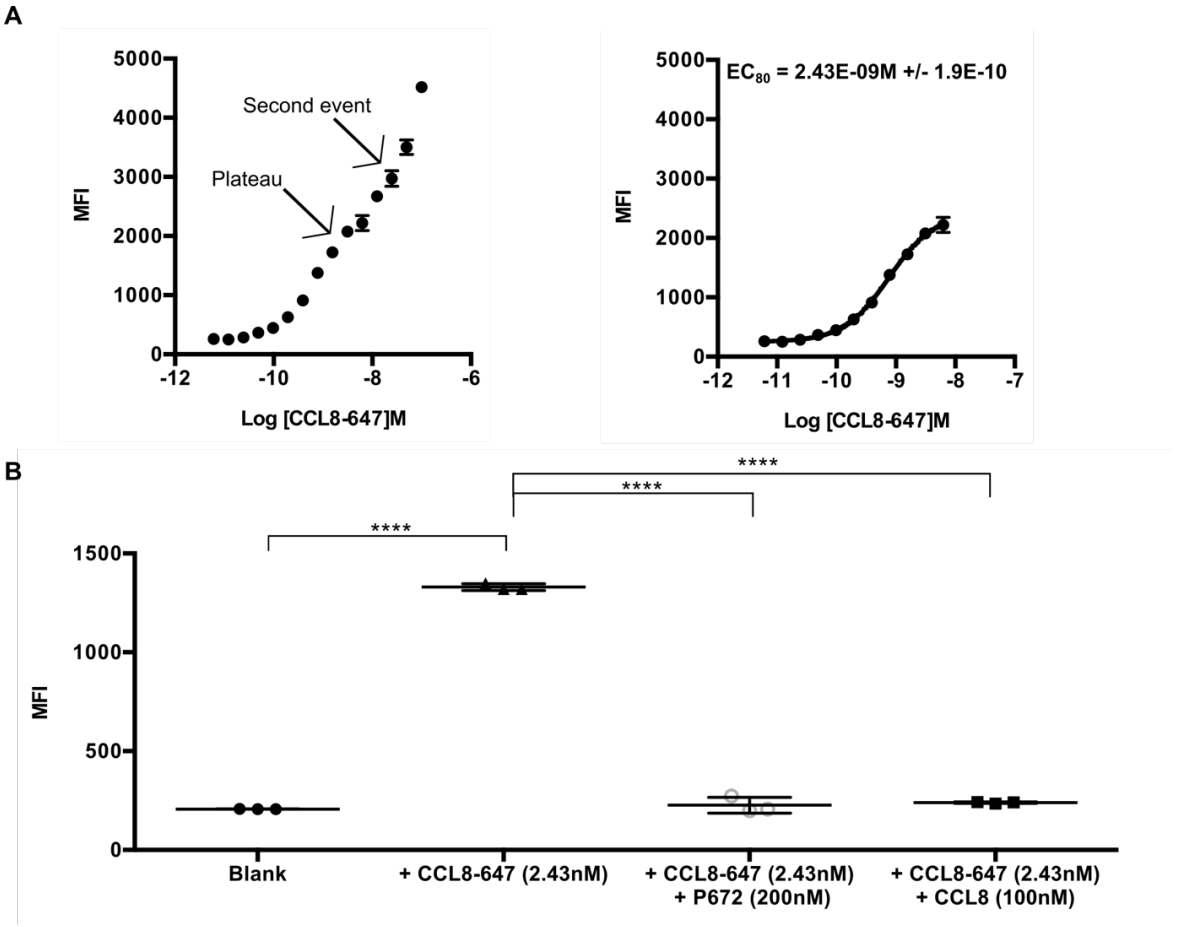


Figure 2.4 Fluorescent ligand/receptor blocking assay. **A.** *Left panel* - Median fluorescence intensity (MFI) of THP-1 cells as a function of CCL8-647 concentration. The two binding events are indicated on the curve. X-axis display Log[CCL8-647]M and Y-axis displays MFI. *Right panel* - Representative EC_{80} determination for CCL8-67 binding to THP-1 cells. Experiment was performed in technical triplicate with error bars shown as SEM. EC80 is the average of three independent experiments carried out in triplicate; error shown as SEM. Curve was fit using a four-parameter fit in Graph Pad Prism 6. **B.** Effect of an EC_{80} worth of CCL8-647 on THP-1 cells and the effect of preincubating this either with an evasin (P672) or cold CCL8. Data is one experiment carried out in triplicate with mean and SEM shown. Statistical significance calculated using a one-way ANOVA with Sidak's correction for multiple comparisons. **** = $p < 0.000005$.

2.4 CELL MIGRATION ASSAY

It is essential to have a robust and quantitative assay to assess the effect of chemokine-neutralising evasins on chemokine-driven white blood cell migration. Cell migration is typically monitored using a Boyden chamber assay and this has been used previously to characterise chemokine/evasin interactions[153]. This

experiment essentially involves incubating cells in a well that contains a membrane with pores in it. The cells are placed above the membrane and the chemokine or chemokine/evasin mixture below. This is then incubated for a period of time and the cells arriving below the membrane are counted. The protocol here is a modified version of one that has been described previously[73].

Initially, a varying dose of CCL3 was placed in the lower chamber and the migration of THP-1 cells was monitored. THP-1 cells express chemokine receptors and have been shown to respond to various chemokines[180]. To allow for the rapid determination of the number of arriving cells this assay was performed in a 96 well plate where the cell count was determined using a flow cytometer attached to an autosampler. Initially, the dose response of CCL3 produced a bell-shaped curve (fig. 2.5A). This is expected as at high concentrations there is desensitisation of the cell due to the high concentration of chemokine and therefore no cell migration observed. Compared to vehicle, CCL3 was able to induce a significant increase in cell migration at 3.54nM (fig. 2.5B).

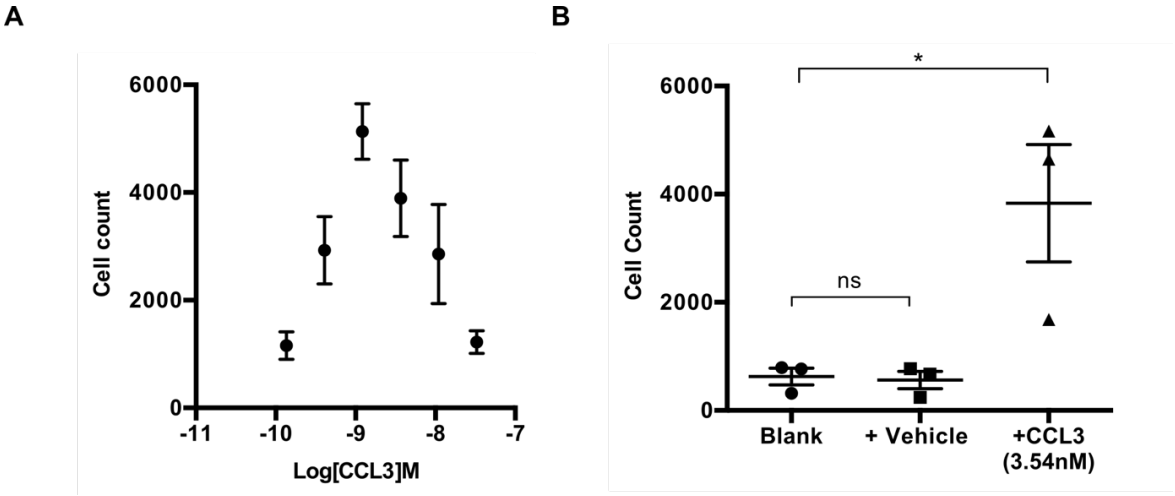


Figure 2.5 THP-1 cell migration in response to CCL3. **A.** Migration of THP-1 cells in response to different concentrations of CCL3. Experiment was carried out in triplicate, with mean and SEM shown. X-axis is Log[CCL3]M, Y-axis is cell count. **B.** Effect of a single concentration of CCL3 on cell migration compared to vehicle (PBSA). Experiment carried out in triplicate where each data point is the average of one experiment carried out in technical triplicate. Statistical significance was determined using a one-way ANOVA with Sidak's correction for multiple comparisons. NS = not significant, * = $p<0.05$.

With careful selection of chemokine concentration a sigmoidal-dose response curve can be obtained. This allows for EC_{80} determination to be carried out. This is important as the concentration of chemokine chosen for experiments needs to be in the linear range, so any inhibition of chemokine activity will result in a clear drop in the number of cells migrated. THP-1 cells were found to respond to CCL2, CCL3, CCL3L1, CCL5, CCL7 and CCL8. The EC_{80} values for cell migration were determined (fig. 2.6). EC_{80} determination experiments for CCL3 and CCL3L1 were carried out by the candidate, CCL2, CCL5, CCL7 and CCL8 EC_{80} determination experiments were performed by Mr Graham Davies. This revealed that the EC_{80} values were in the low nM region which is expected for these chemokines[73].

Evasins are the proteins in tick saliva responsible for inhibiting white blood cell migration and this is achieved through the inhibition of chemokines. This cell

migration assay can monitor THP-1 cell migration in response to various chemokines and therefore the inhibitory effect of the evasins on these chemokines can be evaluated.

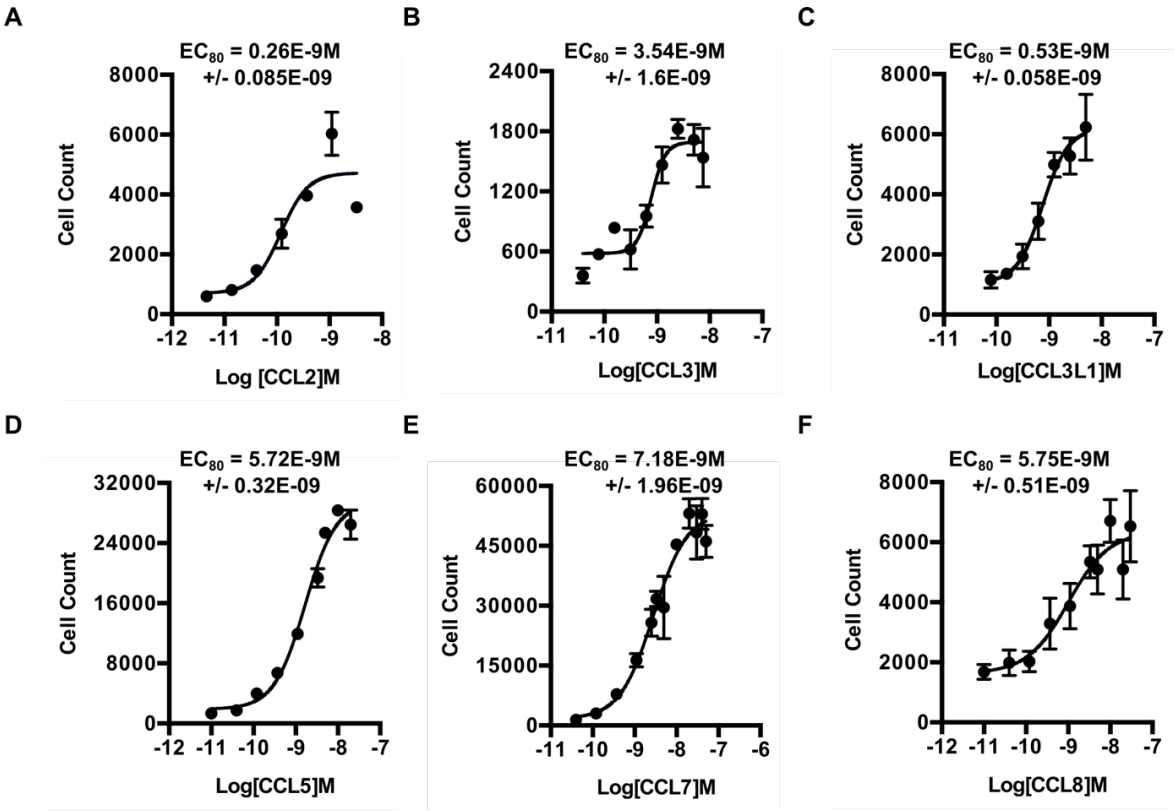


Figure 2.6 Chemokine EC_{80} determination in THP-1 cells**. A.** Representative EC_{80} curve for CCL2 THP-1 migration. **B.** Representative EC_{80} curve for CCL3 THP-1 migration. **C.** Representative EC_{80} curve for CCL3L1 THP-1 migration. **D.** Representative EC_{80} curve for CCL5 THP-1 migration. **E.** Representative EC_{80} curve for CCL7 THP-1 migration. **F.** Representative EC_{80} curve for CCL8 THP-1 migration. In each case, representative experiment was performed in technical triplicate with mean and SEM shown for each data point. EC_{80} values were determined using a four-parameter fit in Graph Pad Prism 6. EC_{80} values displayed are the average of three independent experiments each carried out in technical triplicate with error as SEM. X-axis is Log[chemokine]M and Y-axis is cell count. Data for parts A, D, E and F were collected by Mr Graham Davies and not the candidate.

2.5 SUMMARY

In this chapter, the development of three assays to characterise evasin/chemokine interactions have been described. The BLI assay can readily

screen an evasin for chemokine binding and can subsequently be used to determine the strength of an interaction. The fluorescent chemokine/receptor blocking assay can inform whether an evasin is able to inhibit chemokine/receptor binding. The cell migration assay allows for the functional effect of an evasin on chemokine action to be probed. Moreover, all of these assays are performed in microplate format allowing for the rapid and robust acquisition of data. These assays were used as described in subsequent chapters for characterising evasins.

3 CHARACTERISATION OF P672

3.1 INTRODUCTION

The immune system is vitally complex as under healthy conditions a variety of factors act concertedly to protect a host from invading pathogens whilst maintaining acceptance toward self-proteins. However, chronic and unregulated inflammation can drive the pathology and progression of several diseases, including atherosclerosis, myocardial infarction and stroke. It would therefore be desirable to have a therapeutic agent that could lower levels of inflammation to slow the progression or even prevent these diseases[181]. Evidence for this approach comes from the success of the recent CANTOS trial where an antibody to the inflammatory molecule IL-1β was shown to reduce cardiac events in patients with a risk of myocardial infarction[20]. This trial strongly suggests that targeting inflammation is a validated approach that is independent of lowering lipid levels to treating cardiovascular disease. Other diseases, such as arthritis[182], are also driven by an inflammatory mechanism, indicating the broad applicability that a potent inhibitor of inflammation could have.

Physiological and pathological inflammation is driven, in part, by a family of chemotactic cytokines known as chemokines[183]. Chemokines are small (7-12 kDa), secreted proteins that share a conserved secondary structure, typically imparted to them by a tetra-cysteine motif. The relationship between the N-terminal cysteines, which can be CC, CXC, CX3C and XC (where X is any amino acid), serves as the basis of their nomenclature[184]. This results in the chemokine ligands being classed as either CCL, CXCL, CX3CL or XCL type ligands. The structure of these ligands is typically composed of a disordered N-terminus followed by the di-cysteine motif,

an N-loop, a three-stranded ß-sheet with 30S (between ß1-ß2) and 40S (between ß2-ß3) loops, and a C-terminal alpha helix[40]. Chemokine ligands signal though the chemokine G-protein coupled receptors (GPCRs), which are classified based on the type of chemokine it interacts with. GPCRs that interact with CCL type chemokines are termed CCR receptors whereas those that interact with CXCL, CX3CL or XCL ligands are termed CXCR, CX3CR or XCR respectively. Binding of a chemokine ligand to a chemokine receptor brings about the directional migration of white blood cells to sites of inflammation[185]. Due to their key role in the regulation of the immune system, chemokines are validated therapeutic targets for diseases where pathologic inflammation is driving the disease mechanism[186,187]. For example, deletion of the chemokine receptor CCR2 was shown to be protective against atherosclerosis[88] and the CCR2 ligand CCL2 was shown to drive the progression of atherosclerosis in ApoE knockout mice[89]. High levels of chemokine ligands, including CCL7 and CCL8, and cells expressing chemokine receptors were found in the synovium of rheumatoid arthritis patients[188] and treatment with an anti-CCL2 antibody decreased macrophage infiltration and swelling in a rodent model of arthritis[189]. Despite the clear role chemokines play in driving the pathophysiology of these diseases there remain no therapeutics that target chemokines in inflammatory disorders. This may be explained, in part, by the differences between pre-clinical (rodent) models of disease and clinical (human) systems[129] and the robustness of the chemokine network[127]. Chemokine ligands bind their receptors in a “one-to-many” fashion where each ligand can bind multiple receptors, and each receptor can bind multiple ligands. Antibodies targeting single chemokines have been developed and evaluated in clinical trials, but these did not result in a significant reduction in disease severity[120,190]. However, administration of multiple chemokine

antagonists did result in reduction of disease severity in a rat model of arthritis, compared to dosing with a single chemokine anatagoist[191]. This suggests that the targeting of a single chemokine ligand or receptor, as is the typical mechanism of most drugs, is not enough to overcome this network robustness and other approaches must be sought.

Whilst humans have only relatively recently began designing compounds to effect biological function, evolution has had billions of years of natural selection to design compounds that can successfully manipulate complex biological systems. This is illustrated by viruses and parasites who, to successfully invade a host or continue propagating, must evade their host's immune response and have consequently evolved agents with novel mechanisms of action to achieve this. As chemokines form a major part of a host's defence system, evolutionary pressure in these pathogens has resulted in the convergent evolution of proteins that are able to overcome the robustness of the chemokine network. A uniting feature of all of these proteins is that they all bind to and neutralise multiple chemokine ligands or receptors. Poxviruses produce multiple chemokine binding proteins (CKBPs) that are able to block the activity of several chemokine ligands, including CCL2, CCL3, CCL5, CCL7, CCL11 and CCL23[166] to overcome the chemokine network. Cross linking studies from the egg secretions of the helminth *Schistosoma mansoni* identified a protein capable of binding multiple chemokine ligands, CXCL8, CX3CL1, CCL2, CCL3 and CCL5, and was shown to be efficacious in *in vivo* inflammatory models of disease[168]. Using an expression cloning approach, a CKBP termed Evasin-1 was identified from a cDNA library derived from the salivary glands of the tick species *Rhipicephalus sanguineus*[152] and was shown to bind CCL3, CCL4 and CCL18. Further screening of the cDNA library resulted in the

identification of two additional CKBPs, namely Evasin-3 and Evasin-4, which were shown, along with Evasin-1, to be efficacious in preclinical models of inflammatory disorders[1,153]. Interestingly, the viral and helminth CKBPs have a molecular weight between 30-40 kDa[166,168] whereas the tick CKBPs have a remarkably smaller size, between 7-12 kDa, when compared to the other CKBPs. Moreover, the tick CKBPs are selective for either CC or CXC type chemokines and are also highly selective within the type of chemokine family they bind. Evasin-1 was reported to only bind three CC-type chemokines whereas Evasin-4 could bind 18 of the CC-type chemokines tested. The small size of evasins may lead to better tissue distribution[192] and their ability to bind multiple chemokines in a somewhat selective manner means they may be able to successfully neutralise the chemokine network in a targeted fashion. Due to these unique features, evasins present a possible new route to a novel therapeutic for inflammatory disorders[154].

Evasin-1 and 4 are classified as “8-cys” evasins due to their conserved eight cysteine residues and selectivity for CC-type chemokines. Evasin-3 is an unrelated protein and is selective for CXC-type chemokines, namely CXCL1, CXCL2 and CXCL8; this evasin contains only six cysteine residues and is therefore classed as a “6-cys” evasin. Whilst Evasin-1 and 4 do bind several CC-type chemokines there remains some chemokines which they do not bind, such as CCL2 and CCL13. The selectivity of these evasins may also not be optimal for a particular disease state. This is because sites of deleterious inflammation are characterised by the expression of multiple chemokines, where the pattern of chemokines expressed can vary wildly between diseases[193]. It would therefore be desirable to have an arsenal of evasins, each with unique chemokine binding patterns, to allow for the selection of the most appropriate evasin for a particular disease. Until recently, evasins 1, 3

and 4 were the only known CKBPs found in ticks and these were only from a single species. However, as targeting chemokines seems to be a conserved approach for avoiding a host's immune system it is likely that other tick species have also evolved evasins. Using a yeast surface display approach, where putative evasins identified by sequence homology to evasins 1, 3 and 4 were displayed on the surface of yeast, approximately ten more 8-cys evasins were identified, including some that could bind CCL2 and CCL13[164]. Following this, eight more 8-cys evasins were identified, based on sequence homology to evasins 1, 3 and 4, and were characterised for their ability to bind multiple chemokines[165]. All of these evasins possessed a distinct chemokine binding pattern, suggesting one could be chosen for a specific disease where only certain chemokines are implicated. Despite ten more 8-cys evasins being identified using the yeast surface display approach, there still remained over 300 putative evasins in this library which had not been characterised, meaning there were still evasins to be discovered.

Prior to this study commencing, to identify an evasin which was capable of binding CCL8, a library of evasins expressed on the surface of yeast was screened against this chemokine. The library was designed to express 352 putative evasins with either an N-terminal (AGA2) or C-terminal (SAG1 or AGA2) surface display tags. The library was transformed as a pool into yeast and cells labelled with biotinylated CCL8 and streptavidin-AF647. The sorting gate was determined by fluorescent assisted cell sorting (FACS) analysis of the yeast cells binding to streptavidin-AF647 alone to exclude yeast cells displaying background fluorescence generated by streptavidin-AF647 binding to yeast (fig. 3.1A). Labelled cells were sorted by two rounds of FACS (fig. 3.1B, C) to enrich for cells that could bind CCL8. After the second sort, cells were plated at low density to allow for

individual yeast clone to be picked and re-tested by labelling with biotinylated CCL8 and streptavidin-AF647. The clones picked were compared to control yeast expressing the relevant surface display tag (Fig. 3.1 D). In these experiments, only a proportion (30.8%) of the clonal yeast population would bind CCL8. Two independent clones, both with an N-terminal surface display tag, were recovered in this screen and encoded a novel tick CKBP, P672_RHIPU (P672; accession JAA60789.1).

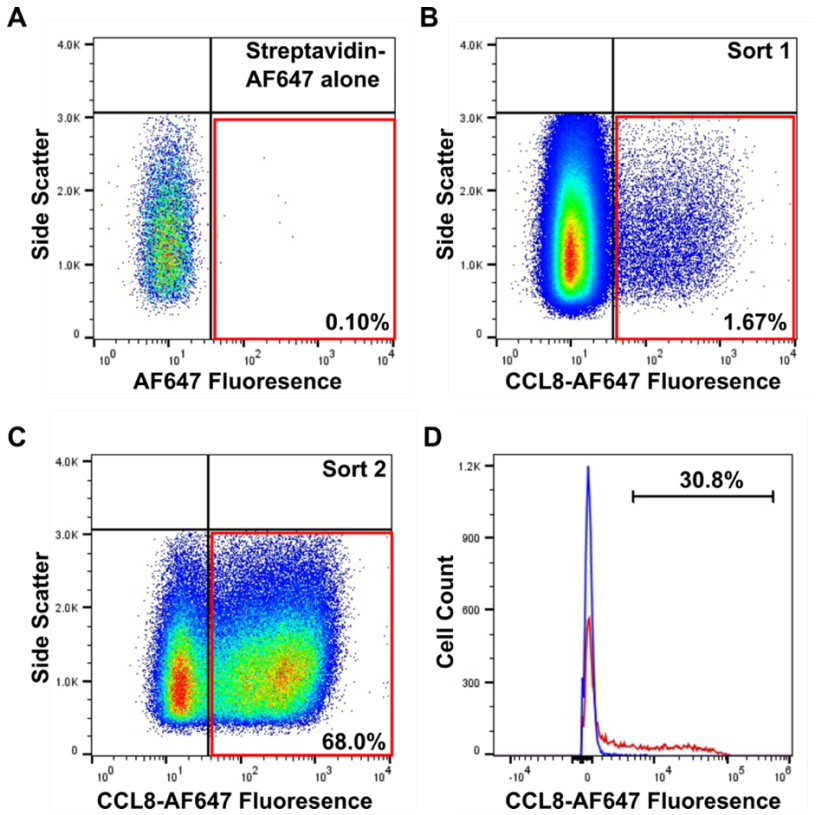


Figure 3.1 Yeast surface display screen to identify P672. **A**. Fluorescence profile of yeast surface display library expressing putative tick evasins incubated with streptavidin-AF647 alone. The *red outlined box* indicates the sorting gate. **B.** Yeast surface display library incubated with biotinylated CCL8 plus streptavidin-AF647. The sorting gate was identified from the negative control and was used to sort CCL8-binding yeast from the library. **C.** Second round sorting of CCL8-binding yeast identified above. The proportions of cells within the sorting gate are indicated as a percentage. **D.** Binding of P672 to CCL8. Yeast expressing P672 are shown in *red*, and control yeast bearing empty vector surface display plasmid are shown in *blue*. The *y* axis shows cell count and *x* axis the fluorescence intensity on a $\log_{10}$ scale. The proportion of cells exceeding background is indicated as a percentage. This data was acquired by Ms Yara Alenazi.

3.2 AIMS

The aims of the work described in this chapter were:

(i) to analyse the P672 primary structure in the context of the other known evasins

(ii) to recombinantly express P672

(iii) to recombinantly express CCL8

(iv) to determine the chemokine binding pattern of P672

(v) to determine if P672 can inhibit chemokine migration *in vitro*

3.3 RESULTS

3.3.1 SEQUENCE ANALYSIS OF P672

To confirm that P672 is related to the previously identified evasins, analysis of the P672 primary structure was performed. P672 is composed of 104 amino acid residues with a predicted molecular mass of 11.7 kDa and a predicted isoelectric point of 4.45. Analysis of the sequence using NetNGly and NetOGlyc predicts several N-linked glycosylation sites and a single O-linked glycosylation site[194]. Protein sequence alignment with Evasin-1, Evasin-4 and the other 8-cys evasins identified by yeast surface display (fig. 3.2A) shows that P672 is an 8-cys evasin as it retains the eight cysteine residues that form disulphide bonds in Evasin-1. Furthermore, P672 shares a cluster of acidic amino acids at the N-terminus which seems to be present in all 8-cys evasins. All other evasins, bar Evasin-4 and P672, have a proline residue immediately following the first cysteine; in P672 and Evasin-4 this is exchanged for a tyrosine residue. P672 is also similar to Evasin-4 in that it ends immediately after the final cysteine residue with a tryptophan, all other evasins

appear to have an extended C-terminus. Phylogenetic analysis of P672 (fig 3.2B) shows that Evasin-4 is the most closely related evasin, with which it shares a 36% identity over an alignment length of 105 residues. It shares only a 29% identity with Evasin-1 over an alignment length of 89 residues.

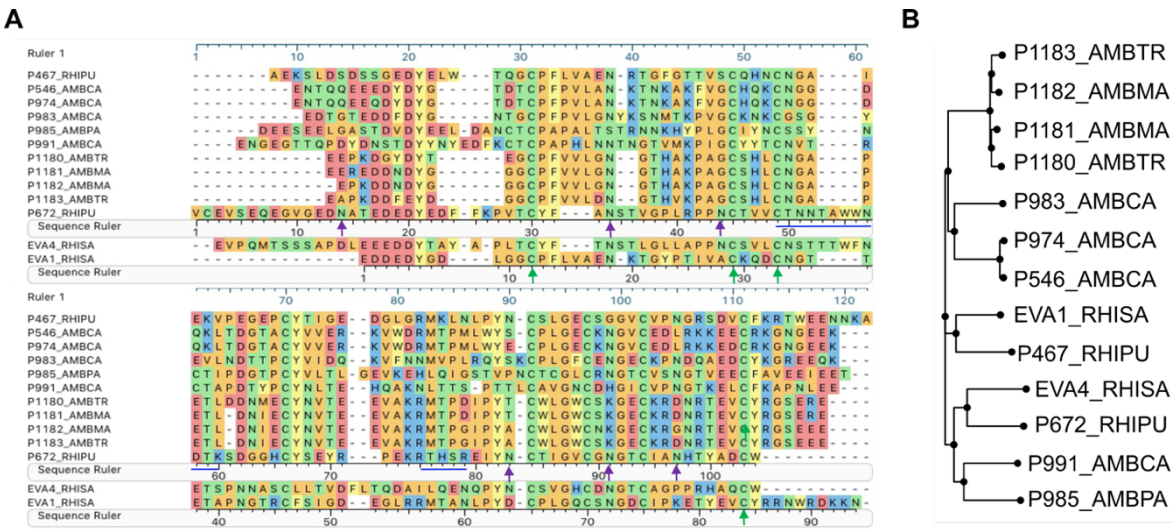


Figure 3.2 Analysis of P672 primary structure. **A.** Sequence alignment of P672 with CC-binding evasins. The peptide sequence prefix indicates the identity, and suffixes indicate the tick species as follows: RHISA and RHIPU, *Rhipicephalus sanguineus* and *R. pulchellus*, respectively; AMBPA, AMBCA, AMBMA, and AMBTR, *Amblyomma parvum*, *Amblyomma cajennense*, *Amblyomma maculatum*, and *Amblyomma triste*, respectively. Amino acid residues are color-coded according to physicochemical properties: *yellow*, aromatic (*F*, *W*, and *Y*); *red*, acidic (*D* and *E*); *blue*, basic (*R*, *H*, and *K*); *orange*, nonpolar aliphatic (*A*, *G*, *I*, *L*, *M*, *P*, and *V*); *green*, polar neutral (*C*, *N*, *Q*, and *T*). The *green arrows* indicate disulphide bond positions in EVA1. *Magenta arrows* indicate the six *N*-glycosylated residues identified in P672 by mass spectrometry. The *blue lines* indicate the regions of P672 not covered by elastase and tryptic digest bottom-up mass spectrometry. Sequence rulers of P672, EVA1, and the alignment (ruler 1) are indicated. **B.** Phylogenetic tree of CC-binding evasins.

3.3.2 Expression of P672

P672 was expressed from the pHLsec vector which is optimised for production of secreted proteins in mammalian expression systems[195]. A mammalian system was chosen as it had previously been shown to produce biologically active evasins[153]. It was purified using a two-step procedure of nickel affinity followed by

size exclusion chromatography as described previously[164] to give the protein in suitable yield (~4mg/L) and of acceptable purity as assessed by SDS-PAGE. The P672 construct contained either a C-terminal or N-terminal StrepII-His purification tag with the sequence detailed in the materials and methods section. P672 was expressed with both an N- and C- terminal tag because all other evasins identified previously had been produced with a C-terminal purification tag. However, P672 was only recovered in the N-terminally tagged orientation in the yeast surface display screen so the N-terminally tagged expression construct was produced to determine whether tag location had any effect. The purified protein in each case migrated as a smear at a much higher molecular weight (30-40 kDa) than expected (14.5 kDa) which is indicative of glycosylation (fig. 3.3A). This would be expected based on the sequence analysis presented above. Glycosylation was confirmed by digestion of the protein with the glycosidases Endo F1 and PNGase F, which produced a protein which ran much closer to the expected molecular weight on SDS-PAGE and produced a corresponding change in retention volume on size exclusion chromatography (fig. 3.3A, 3.3B).

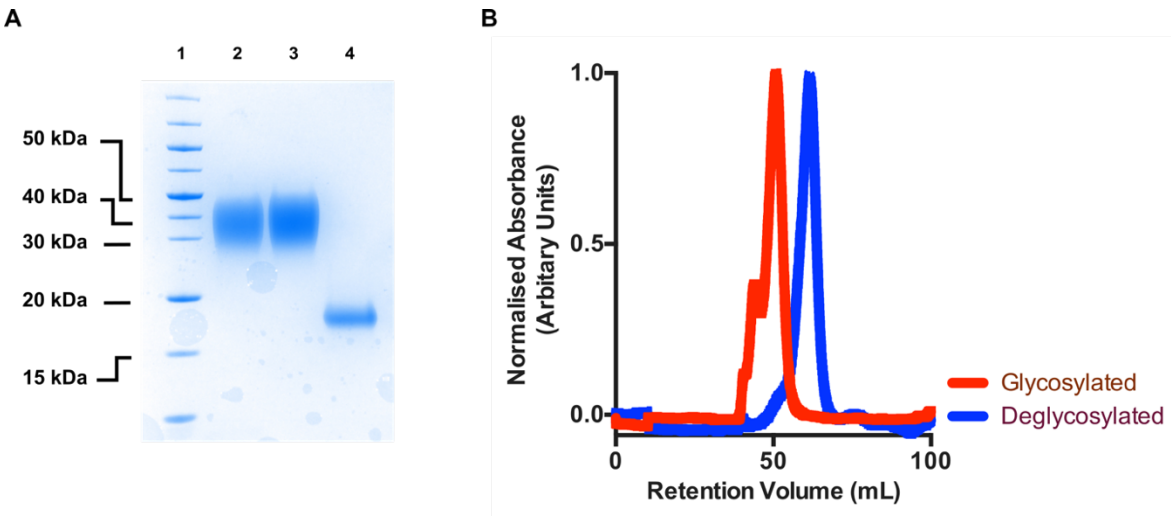


Figure 3.3 Analysis of glycosylated and deglycosylated P672 by SDS-PAGE and size exclusion chromatography. **A.** SDS-PAGE gel stained with colloidal Coomassie blue showing: 1. Molecular weight marker 2. N-terminally tagged P672 protein 3. C-terminally tagged P672 protein 3. C-terminally tagged P672 protein 4. N-terminally tagged P672 protein treated with Endo F1 and PNGase F. All proteins were purified by nickel affinity followed by size exclusion chromatography **B**. Size exclusion chromatography traces of N-terminally tagged glycosylated (red) and deglycosylated (blue) P672 protein.

3.3.3 Tandem mass spectrometry identification of glycosylation sites in P672

To confirm the sequence of the recombinantly expressed protein and to aid in the identification of glycosylation sites, tandem mass spectrometry of P672 at the peptide level was performed. PNGase F and Endfo F1 treated P672 was analysed by tandem mass spectrometry (MS/MS) at the peptide level where 87% coverage was achieved, excepting the residues indicated in figure 3.2A. This result confirms the protein sequence of the recombinantly expressed protein (see PRIDE partner repository with the dataset identifiers PXD008025 and 10.6019/PXD008025). There were several residues that had converted from asparagine to aspartate, corresponding to a mass shift of +0.98 Da in NX(S/T) motifs. Deamidation of asparagine is a characteristic feature of N-glycosylation cleavage by PNGase F and suggests that these residues are glycosylated[196]. There were several peptides that

were carrying N-acetylglucosamine and/or N-acetylglucosamine (HexNAc) moieties, suggesting that deglycosylation was only partial. The presence of HexNAc can be explained by the EndoF1 cleavage. The identified N-glycosylation sites are indicated on figure 3.2.

3.3.4 BINDING OF P672 TO CHEMOKINES

With access to high levels of purified P672, the N- and C- terminally tagged protein was explored using biolayer interferometry (BLI)[164]. P672 was immobilised on the sensor through the N- or C- terminal his-tag and screened against a panel of 42 chemokines at 300nM (fig. 3.4 A, C). This revealed that P672 only bound CC-type chemokines and the location of the tag effected binding. N-terminally tagged P672 was able to bind CCL1, CCL2, CCL3, CCL3L1, CCL7, CCL8, CCL11, CCL13, CCL14, CCL15, CCL16, CCL18 and CCL23. C-terminally tagged P672 was only able to bind CCL3, CCL3L1, CCL8, CCL18 and CCL23. No binding was detected to CXC, CX3C or XC type chemokines. Binding affinities (K_d) values were determined using BLI studies against chemokines which displayed a binding signal at 300nm (fig. 3.4 B, D; fig. 3.5). Using the dissociation rate constants it was possible to calculate retention time for the target chemokines. For N-tagged P672 these ranged from 31.39 minutes for CCL3 to 1.59 minutes for CCL7, suggesting that for some chemokines the P672/chemokines complex was stable as some antibody/antigen complexes. Whilst the retention times for the C-tagged protein were also on the order of minutes they were all less than that of the N-tagged protein, ranging from 15.20 minutes for CCL3 and 2.55 minutes for CCL18.

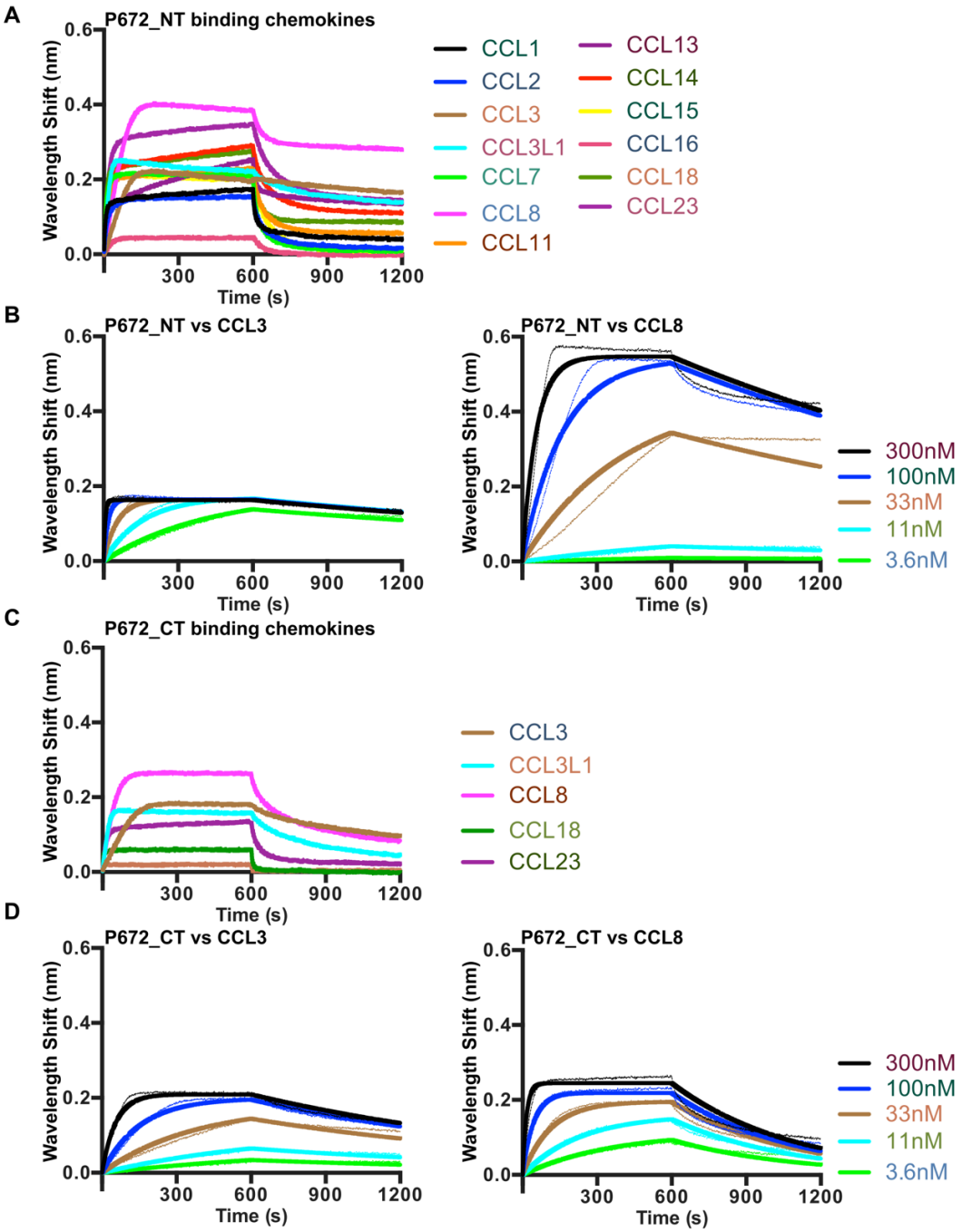


Figure 3.4 Biolayer interferometry (BLI) traces for N and C terminally tagged P672. **A.** BLI sensogram for N-terminally tagged P672 (P672_NT) of chemokines that displayed a binding signal at 300nM in cross binding screen. **B.** BLI sensogram for N-tagged P672 binding to different doses of CCL3 (*left panel)* or CCL8 *(right panel)*. **C.** BLI sensogram for C-terminally tagged P672 (P672_CT) of chemokines that displayed a binding signal at 300nM in cross binding screen. **D.** BLI sensogram for C-tagged P672 binding to different doses of CCL3 (*left panel)* or CCL8 *(right panel)*. Plots display wavelength shift (y axis, nm) verses time (x axis, second). For K_d determination, dotted lines indicate collected data, solid lines indicate modelled data.

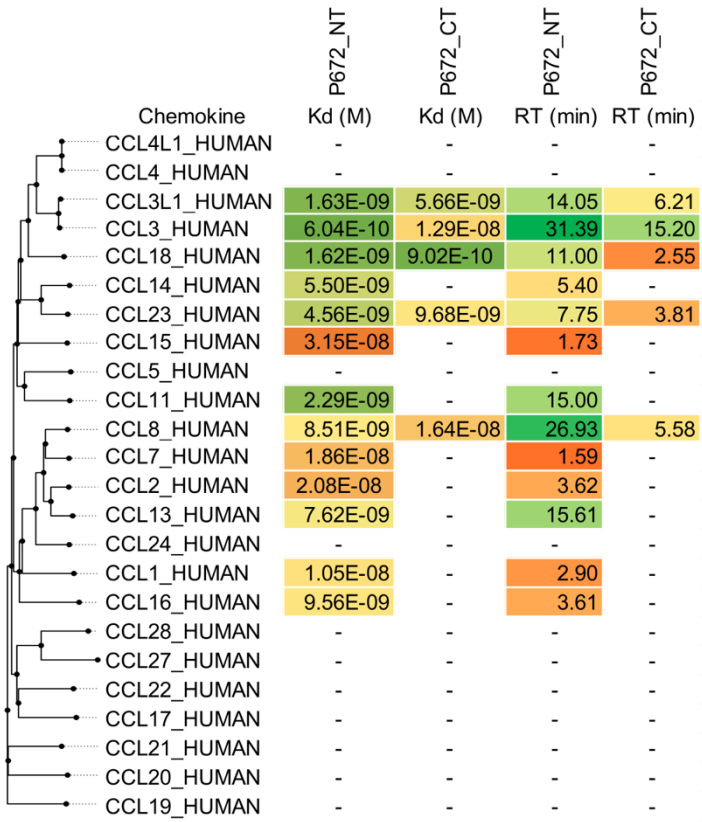


Figure 3.5 Characterization of P672 binding to chemokines using biolayer interferometry. **A.** Binding affinities (K_d, M) and target residence times (RT, minutes) of immobilized P672 (either N- or C-terminally tagged as indicated) to human CC-chemokines using biolayer interferometry. High-affinity binding and longer residence times are indicated as shades of *green*, medium affinity as *yellow*, and low affinity as shades of *orange*. Chemokines are arranged by sequence similarity–based phylogeny. A *dash* (—) indicates that binding was not detected at 300 nM chemokine concentration.

3.3.5 Binding of deglycosylated P672 to CCL8

It has been shown for some antibodies that glycosylation is important for fuction[197]. To determine if this was the case for P672, the binding of N-tagged deglycosylated P672 to CCL8 was examined using BLI. It was found that the K_d increased to 72.5E-08M, compared to 8.51E-09M for the glycosylated form, and there was a corresponding decrease in retention time for the complex from 26.93 minutes to 3.76 minutes, indicating that the deglycosylated protein had a lower affinity for CCL8 compared to the glycosylated form.

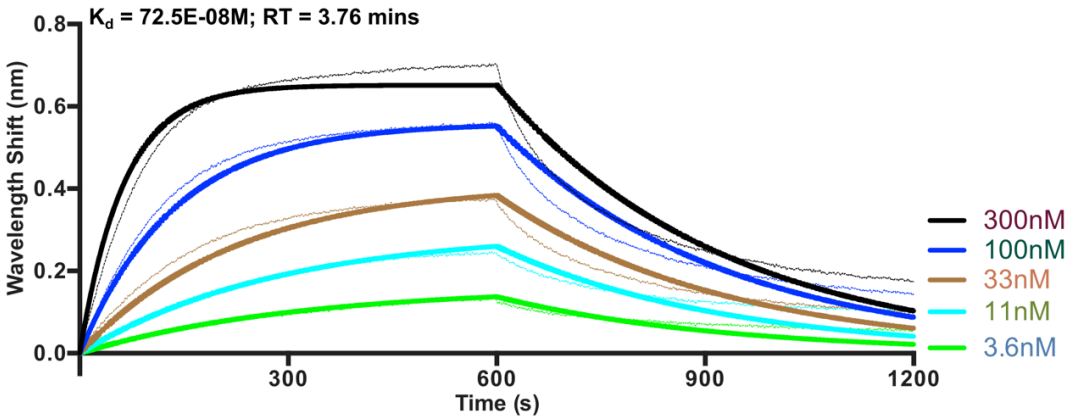


Figure 3.6 Biolayer interferometry sensogram for N-tagged deglycosylated P672 binding to different doses of CCL8. Plots display wavelength shift (y axis, nm) verses time (x axis, second). Dotted lines indicate collected data, solid lines indicate modelled data.

3.3.6 Neutralisation of chemokine migration by N-tagged P672

The ability of N-terminally tagged P672 to inhibit chemokine function was examined using a 96-well Boyden chamber assay to monitor THP-1 human monocyte cell migration in response to human CC chemokines. The effects of titrating in progressively increasing doses of P672 at the effective concentration (EC) dose, EC_{80} (the determination of which is described in chapter 2), for CCL2, CCL3, CCL3L1, CCL7 and CCL8 (chemokines purchased from Peprotech) and found that P672 inhibits THP-1 cell migration in response to CC chemokines with IC_{50} values <10nM for CCL3, CCL3L1 and CCL8 and values <30nM for CCL2 and CCL7.

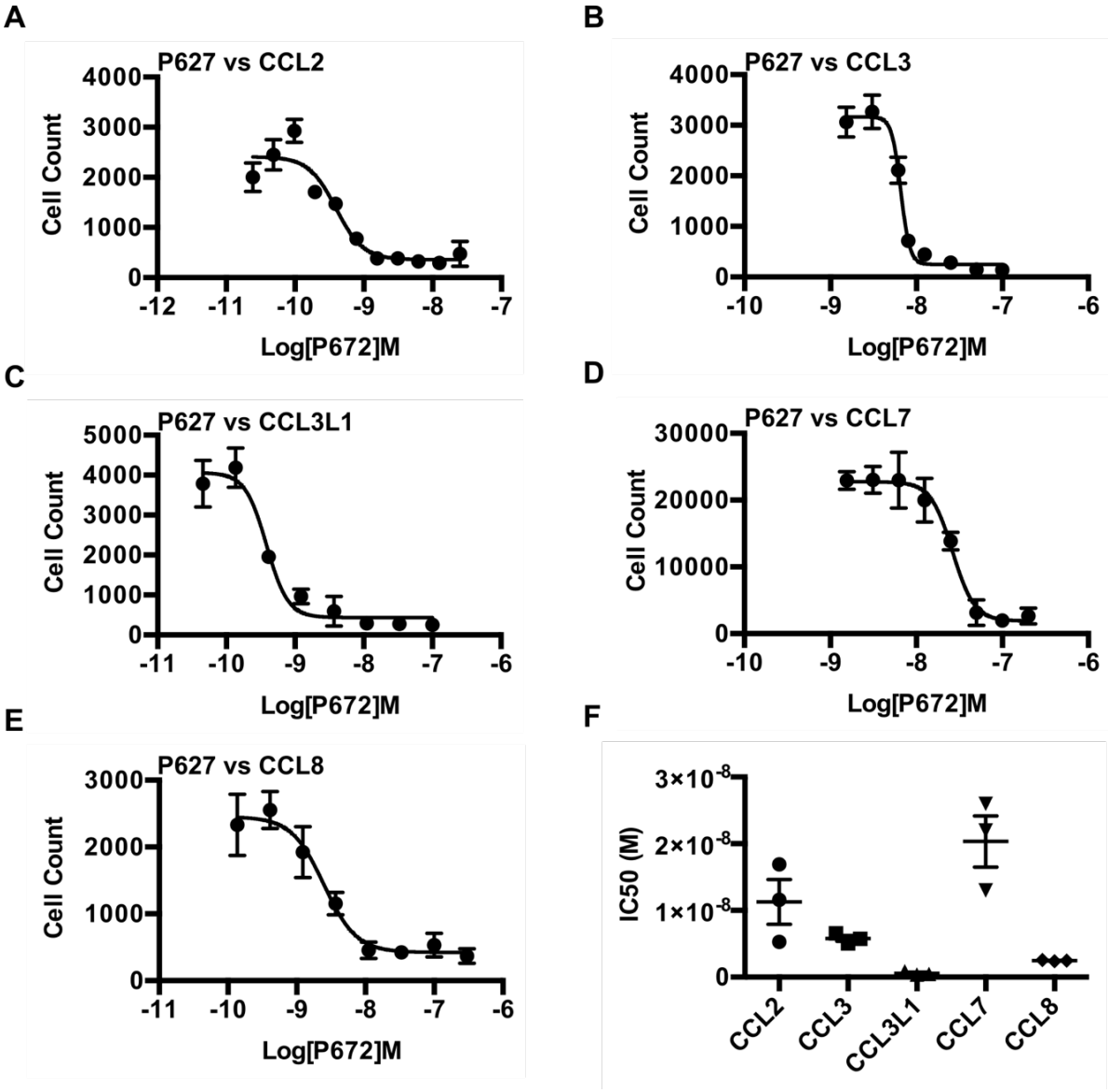


Figure 3.7 Functional neutralization of chemokine activity by P672. **A, B, C, D, E.** Representative IC_{50} curves for the neutralisation of CCL2 (A), CCL3 (B), CCL3L1 (C), CCL7 (D) and CCL8 (E) induced THP-1 cell migration by N-terminally tagged P672. The y axis shows cell count of THP-1 cells migrating through to the bottom chamber in response to an EC_{80} dose of the indicated chemokines. Data (three technical replicates) are shown as mean ± S.E. The x axis shows P672 concentration (log_{10} molar). The IC_{50} indicated was estimated by fitting an agonist response curve with four parameters. **F.** Summary of N-terminally tagged P672 IC_{50} data (M, mean ± S.E. of three biological replicates analysed as above) for chemokines that induce THP-1 cell migration. The EC_{80} doses of the indicated chemokines were as follows: CCL2, 0.52 nM; CCL3, 3.55 nM; CCL7, 7.18 nM; CCL3L1, 0.52 nM; and CCL8, 5.75 nm.

3.3.7 COMPARISON OF N- AND C- TERMINALLY TAGGED P672 IN A CELL MIGRATION ASSAY

Motivated by the observation that N- and C- terminally tagged P672 displayed differing CC chemokine selectivity by BLI, the inhibitory effect of N and C terminally tagged P672 was examined at a single concentration, 100nM, against CCL2, CCL3, CCL3L1, CCL7 and CCL8 driven THP-1 migration in a Boyden chamber assay. The BLI result indicated that for these chemokines N-terminally tagged P672 was able to bind all of them whereas C-terminally tagged P672 was only able to bind CCL3, CCL3L1 and CCL8. In this assay both interacting partners are in solution, as opposed to having one of the binding partners immobilised as is the case with the BLI assay, and this would determine if the effect of the tag is an artefact of immobilisation or the difference in binding selectivity is inherent to the protein. At 100nM N-terminally tagged P672 was able to inhibit all these chemokines to less than ~20% of chemokine alone. However, C-terminally tagged P672 was able to inhibit CCL3, CCL3L1 and CCL8 at a similar level to N-terminally tagged P672 but was unable to reduce migration as well as the N-terminally tagged protein for CCL2 and CCL7.

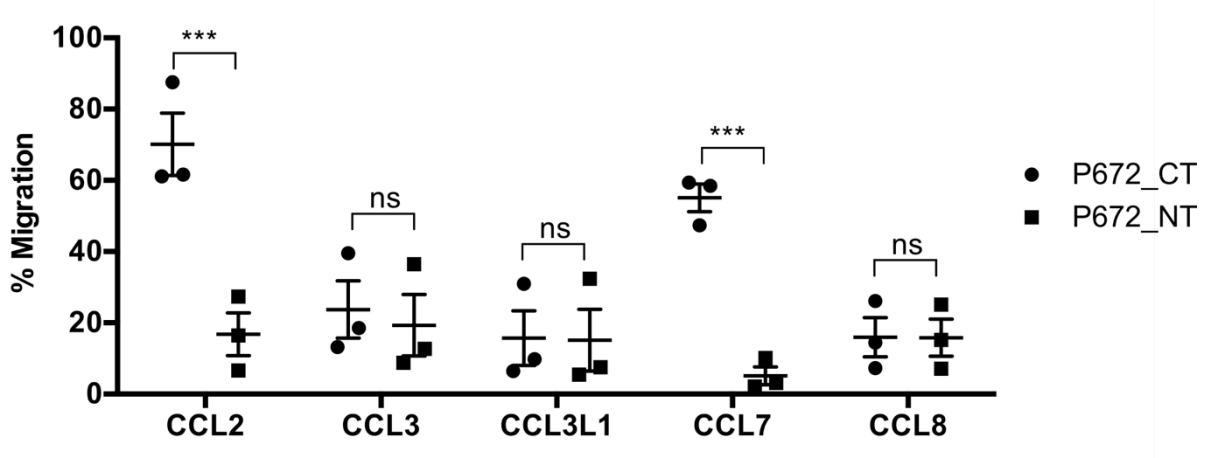


Figure 3.8 Percentage of migration inhibition by a fixed concentration (100 nM) of P672_CT (C-terminally tagged (filled circles)) or P672_NT (N-terminally tagged (filled squares)). The experiment was performed at an EC_{80} concentration of the chemokines indicated. Data (three technical and three biological replicates) were normalized to chemokine-alone control to account for day to day variation. Data were analysed with one-way analysis of variance and corrected for multiple comparisons with the Sidak method. ***, $p < 0.001$.

3.3.8 Expression of CCL8

Having access to large amounts of CCL8 could subsequently allow for the interaction of P672 and CCL8 to be studied in detail. To this end, CCL8 was expressed as a SUMO fusion in a pNIC-BIO3 *E. coli* expression vector. This vector backbone adds an Avi-tag to the protein, allowing for the straightforward addition of biotin to the protein. This can be achieved through co-transforming and expressing biotin ligase (BirA) in the *E.coli*. However, in this instance biotin was not added. The SUMO-CCL8 fusion protein expressed well in the soluble fraction of RosettaGami 2 *E.coli* and could be purified in three steps using nickel affinity chromatography, cation exchange chromatography and size exclusion chromatography (fig. 3.9 A). The purified recombinant CCL8 was assessed for the ability to migrate THP-1 human monocytes in a Boyden chamber assay as was found to induce migration in a similar manner to that of the commercial CCL8 (fig 3.8 B).

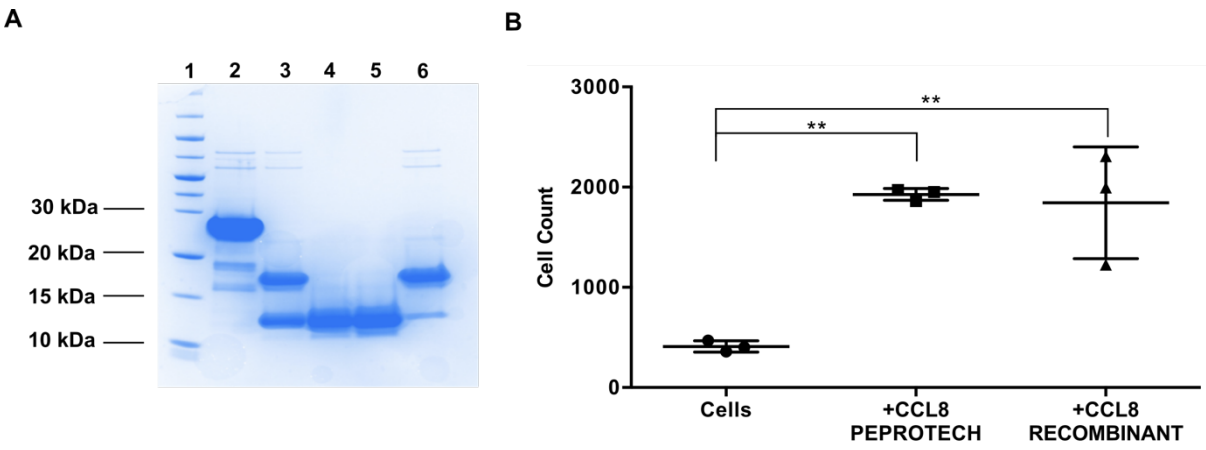


Figure 3.9 Expression and functional testing of recombinant CCL8. **A.** SDS-PAGE stained with colloidal Coomassie blue showing: 1. Molecular weight marker 2. Nickel affinity purified SUMO-CCL8 fusion 3. SUMO protease treated SUMO-CCL8 4. Cation exchange chromatography elution of CCL8 5. Size exclusion chromatography purified CCL8 6. Flow through from cation exchange chromatography step. **B.** Human monocytic THP-1 cell migration in response to commercial CCL8 (Peprotech) or recombinant CCL8. The concentration tested of both was 5.75nM. Data (three technical and three biological replicates) were analysed with one-way analysis of variance and corrected for multiple comparisons with the Sidak method. **, $p < 0.01$

3.4 Discussion

The combined action of multiple chemokine ligands serves to bring about a chronic inflammatory response. As a consequence of this, therapies targeting single ligands tend to be unable to successfully neutralise deleterious inflammation. As suppression of a host's immune system is vital for the survival of an invading pathogen, several viruses and parasites have evolved an elegant strategy to overcome this problem; CKBPs that are able to bind to and neutralise the effect of multiple chemokines[198]. Previous efforts to identify CKBPs in ticks (evasins) have involved cross linking studies[152] or the identification of putative evasins based on sequence homology[165]. The work presented here builds upon combining the identification of putative evasins through sequence homology to the evasins identified through cross linking studies and the ability to link genotype to phenotype

using yeast surface display[164]. This approach allows for the screening of putative evasins against a defined target to identify CKBPs that can neutralise a specific chemokine.

A library of putative evasins displayed on the surface of yeast was screened against the chemokine CCL8 to yield a novel CC chemokine binding evasin sequence termed P672. Alignment of the P672 sequence with other CC chemokine binding evasins previously identified revealed that, expectedly, it was an 8-cys evasin, with four disulphide bonds predicted to be in its structure due to alignment of the cystine residues in P672 with those found in Evasin-1. P672, along with the other 8-cys evasins, has a cluster of acidic amino acids at its N-terminus. This negatively charged cluster in Evasin-1 and 4 has been suggested to interact with a positively charged cluster on CCL3[160], and it may perform a similar role in P672. This charge complementarity may provide an insight into the mechanism by which the evasins are able to bind to their target chemokines as chemokines are mostly basic proteins so will possess a positive charge at physiological pH. P672 shares a 36% identity with Evasin-4, the 8-cys evasin it is most closely related to. These are the only two evasins identified to date that end immediately following the terminal disulphide-forming cysteine residue on a tryptophan. These are also the only two evasins that have a tyrosine residue instead of a proline immediately following the first disulphide-forming cysteine residue. This proline in Evasin-1 has been shown to target the conserved disulphide bond in CCL3[199] and this tyrosine was suggested not to be important for CCL5 binding in Evasin-4[160] so the role of this substitution in P672 is, as yet, unclear because P672 does not bind CCL5.

P672 was identified in a screen against CCL8. CCL8 is a part of the Monocyte Chemoattractant Protein (MCP) subfamily where CCL2, CCL7 and

CCL13 are also members. N-terminally tagged P672 was shown to bind these related chemokines that signal through the common receptor CCR2. This receptor is a key regulator of monocyte and macrophage migration[200] and when knocked out resulted in decreased atherosclerotic lesion formation in ApoE$^{-/-}$ mice[88]. P672 was also able to bind several other monocytic chemoattractant proteins, including CCL3, CCL14 and CCL23 suggesting that the role of P672 in *R.pulchellus* may be to block the host's monocyte recruitment to allow the tick to remain undetected. N-terminally tagged P672 was also shown to bind CCL1, CCL3L1, CCL11, CCL15, CCL16, and CCL18. P672 does not bind CCL4, which is a part of the Macrophage Inflammatory Protein (MIP) subfamily, whereas it does bind CCL3, CCL15, CCL18 and CCL23 which are the other chemokines which make up this group. This illustrates that the tick CKBPs are not only selective between class of chemokines, i.e. for CC type chemokines, but are also selective within the subgrouping of these classes, i.e. only binding certain members of the MIP family. P672 was also unable to bind CCL5 at concentrations below 300nM which is surprising considering it could bind the related proteins CCL11 and CCL15 (fig. 3.5). This may be because *R.pulchellus* utilises other evasins, such as P467_RHIPU (P467) [164], to target this chemokine. P467 was shown to also bind several other chemokines including CCL2, CCL3, CCL7 and CCL8, which P672 was also able to bind despite coming from the same species of tick. This is also observed for the evasins from *Rhipicephalus sanguineus* as both Evasin-1 and 4 bind some of the same chemokines despite also coming from the same species of tick. The presence of multiple evasins that can bind the same chemokines in a single tick species may be a mechanism that ticks use to effectively suppress the target chemokines. This "cross reactivity" between evasins from the same species may also be a mechanism by which the tick can avoid the generation

of antibodies to evasins. This is because having complimentary evasins prevents continual exposure to a single antigen, potentially lowering the likelihood of an antibody being generated.

Other mechanisms to avoid immunogenicity is the use of a glycan shield to prevent the formation of neutralising antibodies and may be a mechanism by which evasins avoid the generation of antibodies[154,201]. P672 was predicted to be glycosylated based on the identification of several *NX(S/T)* motifs and this was confirmed by the recombinant protein running as a smear on SDS-PAGE, collapsing of this smear to a single band upon treatment with the glycosylases PNGase F and ENDO F1 and bottom up proteomics. This is the same as other evasins produced in eukaryotic systems as were also found to be glycosylated[152,164]. The affinity of deglycosylated protein for CCL8 was investigated by BLI and it was found to bind with a lower affinity compared to that of the glycosylated protein. It is possible that the resulting N to D mutations that occurs upon deglycosylation by PNGase F may destabilise the complex resulting in a lower affinity or that the glycans themselves were stabilising the interaction. It is also possible that upon deglycosylation the protein becomes less stable so is unable to bind CCL8 in a comparable manner to the glycosylated form. Evasin-1 was shown to have similar biological activity regardless of glycosylation[152,202] however a Y28Q/N60D double mutant of Evasin-4[160] was shown to have a lowered affinity for CCL5. The single mutants were not tested, however, so it is difficult to say whether the N60D mutation alone is enough to bring about a reduction in affinity and thus if there is any precedent for an N to D mutation effecting chemokine binding by an evasin. The bottom up proteomics reveals how heterogenous the deglycosylated sample is, with the same peptide presenting an N to D mutation, a single HexNac sugar attached or the presence of

an unmodified asparagine residue. This heterogeneity makes it difficult to say absolutely what is responsible for the reduction in binding affinity.

Interestingly, the location of a StrepII-his tag markedly effected the behaviour of P672. The C-tagged protein was only able to bind 5 chemokines whereas the N-tagged protein was able to bind 13 chemokines. Moreover, the affinity for the chemokines both the N- and C-tagged proteins could bind were all lower for the C-tagged construct. In addition to this, the ability of the C-tagged protein to inhibit CCL2 and CCL7 in solution, as assessed by a Boyden chamber assay, was considerably lower than for the N-tagged protein, which is to be expected based on the BLI screen. Taken together these results suggest that the immobilisation of the protein is not responsible for the change in binding selectivity seen in BLI and that this purification tag is preventing binding in some way, possibly by obscuring the chemokine binding residues in the C-tagged construct. It has been shown that the location of an Fc-domain on Evasin-4 did not affect the selectivity of Evasin-4 but did lower the affinity for the target chemokines slightly when it was placed at the C-terminus[153] and for other non-evasin proteins the location of a purification tag did effect binding[203]. This change in binding selectivity provides a powerful reagent that can rapidly assess the effect of different chemokines in disease models. The C-tagged protein can serve as a strong negative control and any difference in efficacy observed when compared to the N-tagged protein would suggest a role of the chemokines the C-tagged protein does not bind. It is interesting how dramatically the binding profile of P672 is altered simply by the location of the purification tag. Whilst at the C-terminus the binding profile is such more similar to that of Evasin-1, which is quite selective for the chemokines that it interacts with. Conversely, when the tag is at the N-terminus the binding profile is more similar to the of Evasin-4

which, although fairly selective, binds many more CC chemokines. Crucially, N-tagged P672 is able to bind and neutralise CCL2 and CCL13; two chemokines that neither Evasin-1 or 4 were able to inhibit. In a broader sense, the observation that a purification tag can alter the binding properties of this evasin suggests that it is possible to engineer evasins with tailored chemokine binding patterns. Whilst the difference in binding properties of the N- and C- tagged properties was more of a serendipitous discovery here, similar approaches have been used to engineer antibodies with desired features[204] and this work shows for the first time that it is possible to do something similar with evasins. In the future, careful application of steric hindrance from a tag could be used to design evasins with optimised chemokine binding patterns.

CCL8 was produced recombinantly as SUMO fusion in *E. coli* and was found to induce THP-1 migration in a similar fashion to the commercial (Peprotech) protein. CCL8 was produced recombinantly because having access to large amounts of protein would make it easier to study the P672/CCL8 interaction in future studies. The production of chemokines as SUMO fusions has been reported before[205] and is an elegant strategy for producing chemokines with a native N-terminus as a correct N-terminus is important for the biological activity several chemokines[206]. However, cation exchange chromatography has not been used for separating the chemokine from the SUMO tag previously. Cation exchange chromatography relies on the isoelectric point (pI) of a protein and this governs the charge on a protein at a specified pH. All chemokines, apart from CCL3 and CCL4, have a basic pI meaning that at pH 7.4 they will have a positive charge, whereas the SUMO tag has an acidic pI meaning it will have a negative charge at this pH. This means that a cation exchange column will capture only the chemokine, as can

be seen by the flow through containing only the SUMO tag and the elution containing only the chemokine in figure 3.9A. Furthermore, a step elution was used to elute the protein off the column as this elutes the captured protein in a small volume (2mL) which can be injected directly onto the size exclusion column. This purification protocol saves time and reduces the possibility of losing protein whilst concentrating.

The ability of the N-tagged protein to inhibit chemokine driven migration was assessed using a Boyden chamber assay and revealed that this protein was able to inhibit chemokine migration with IC_{50} values in the low nM range. Interestingly, the IC_{50} value for CCL8 inhibition is close to the K_d value determined by BLI for this interaction. CCL8 binds as an agonist to the chemokine receptors CCR1, CCR2, CCR3, and CCR5, and these receptors are known to act synergistically to activate cell migration[207]. Based on this, one explanation for this observation is that titration of CCL8 by P672 may prevent the synergistic effects at a cellular level that occur following binding of CCL8 to its receptors. This could have larger effects on cell migration than are predicted by the K_d. An alternative explanation is that affinity measured by BLI may be underestimated as it involves immobilization of the evasin, and this does not happen in the cell migration assay.

The effect of untagged P672 on chemokine binding has not been assessed here. This is because the StrepII-his tag is crucial for the purification of the protein and if it were to be removed a new purification scheme would have to be developed. It is likely, however, that untagged P672 would share a chemokine binding pattern similar to that of the N-tagged protein. This is because it is unlikely that the StrepII-his tag is conferring chemokine binding and is much more likely to be preventing chemokine binding in the C-tagged protein. However, this has not been tested here

and although it would be interesting if the untagged protein did share a similar pattern to that of the C-tagged protein, it is hard to do anything other than speculate with the data presented.

3.5 CONCLUSIONS

Using a yeast surface display screen of putative evasins against CCL8 the novel evasin sequence P672 was pulled out and shown to bind CCL8 when on the surface of yeast. This protein was expressed recombinantly using HEK293 cells and was found to be heavily glycosylated, as shown by running as a smear on SDS-PAGE, collapsing of this smear to a single band after treatment of the protein with glycosylases and sequence analysis using bottom up proteomics. The recombinant protein was produced with either an N- or C- terminal StepII-his tag and both had their chemokine binding profile determined by BLI. It was found that the N- and C-tagged proteins differed in the chemokine binding profile, with the N-terminally tagged protein binding CCL1, CCL2, CCL3, CCL3L1, CCL7, CCL8, CCL11, CCL13, CCL14, CCL15 CCL16, CCL18 and CCL23 whereas the C-terminally tagged protein was much more selective binding only CCL3, CCL3L1, CCL8, CCL18 and CCL23. Deglycosylated P672 had a slightly lower affinity for CCL8 when compared to the glycosylated form. N-terminally tagged P672 was able to inhibit CCL2, CCL3, CCL3L1, CCL7 and CCL8 migration in human monocytic THP-1 cells with low nM IC_{50} values. When comparing the inhibition of 100nM N- or C- terminally tagged protein the C-tagged protein was unable to inhibit CCL2 or CCL7 as well as the N-tagged protein. This result indicates that the difference in binding observed in the BLI experiment was not due to immobilisation and that the tag is actively preventing the C-tagged protein from binding these chemokines. This work shows that it is

possible to mine a library of putative evasins using yeast surface display and has resulted in the identification of a new tick evasin termed P672. P672 is able to bind and neutralize multiple chemokines *in vitro.* Furthermore, this work shows that it is possible to alter the binding properties of an evasin with the simple addition of a purification tag, suggesting that it is possible to engineer evasins to have altered properties.

4 ENGINEERING OF HYBRID EVASINS

4.1 INTRODUCTION

Understanding of antibody-antigen interactions has led to the development of several antibody fragment derived therapeutics including single-chain variable fragments (scFv), fragment variable (Fv) and antigen binding fragments (Fab)[208]. These developments were possible due to the Nobel prize winning work of Porter and Edelman in the 1960s where they showed that an antibody could be broken down into a crystallizable fragment (Fc domain) that did not possess the capacity to bind an antigen and two fragments that retained antibody binding (Fab domains)[209].

Chemokine binding proteins (CKBPs) are similar to antibodies in that they can recognise their target chemokines (in this case the antigen) with high affinity[210]. However, unlike antibodies, these proteins are structurally diverse and have arisen in several unrelated pathogens such as viruses[166], helminths[168] and ticks[1]. Moreover, what is also unique to this group of proteins is that they are able to bind to and neutralize multiple chemokine ligands, rather than possessing high affinity and specificity for a single antigen, a feature that is typically associated with most antibodies.

The convergent evolution of proteins that all target chemokines by the same mechanism strongly suggests that this approach is a viable way to successfully inhibit this system. This propensity to bind multiple chemokines may have arisen because chemokines signal through a robust network with “one-to-many” interactions between chemokine ligands and their receptors where a chemokine ligand can bind multiple receptors and a single receptor can bind multiple ligands[131]. These “one-to-many” interactions essentially render the chemokine system

resistant to the neutralisation of a single chemokine ligand or receptor, thus providing a strong immune system that is resistant to attack.

Chemokines drive the inflammatory response through the recruitment of various forms of leukocytes, including monocytes, neutrophils and T-cells, to sites of inflammation[185]. This family is divided into four subgroups based on the spacing of the N-terminal cystine residues which leads to the CC, CXC, CX3C and XC groupings that classify these proteins. A conserved pattern of disulphide bonds found in this family leads to a conserved secondary structure composed of a disordered N-terminus, an N-terminal loops region, an ordered central β-sheet region and a C-terminal alpha helix. Chemokine ligands bind to the chemokine G-protein coupled receptors (GPCRS) through a two site binding model, involving chemokine recognition sites 1 (CRS1) and 2 (CRS2) on the receptor[211]. CRS1 involves interactions between the N-terminus of the receptor and the "binding domain" of the globular core of the chemokine, whereas CSR2 involves the N-terminal "signalling domain" of the chemokine ligand interacting with the transmembrane binding pocket on the receptor[63]. Chemokines also interact with glycosaminoglycans (GAGs) on the surface of endothelial cells to form chemokine gradients to bring about high, localised concentrations of chemokine to initiate the directional migration of chemokines to sites of inflammation and these interactions are necessary for chemokine action *in vivo*[73].

Evasins are the CKBPs found in ticks that are possibly utilised by the tick to suppress the host's immune response, so they can feed for several days or weeks without eliciting an immune response[152]. Evasins are unique compared to other CKBPs from other pathogens due to their small size and their specificity. This is because different classes of evasins only bind CC or CXC chemokines and there is

selectivity for chemokines within these classes[1,164]. The crystal structure of Evasin-1, a CC binding evasin, in complex with the chemokine CCL3 has been solved and it revealed that Evasin-1 has a 1:1 stoichiometry with this chemokine, with N and C terminal residues being shown to interact with N-terminus and N-loop of CCL3[159]. As these regions are involved in receptor binding and activation, the targeting of these receptor binding and activating domains of the chemokine by Evasin-1 suggests that this evasin prevents the interaction of the chemokine with its receptor, explaining the inhibitory effect of this evasin. *In silico* modelling and mutational studies of Evasin-4, another CC binding evasin, revealed that it targeted the N-terminus of CCL5 and utilised only its N-terminal residues to bind CCL3, CCL5 and CCL8[160].

Previous work has largely focused on the role of single residues found in evasins that interact with their target chemokines. However, as the evasin/chemokine interaction is a protein-protein interaction it is likely that the combined effect of several residues is responsible for chemokine binding, leading to the suggestion of a “chemokine binding domain” in evasins. This could be thought of as being analogous to the Fab domain found in an antibody that uses its paratope to recognise the epitope on the antigen. From the crystallographic and mutational studies of Evasin-1, it is likely that the binding domain, or paratope, is composed of residues found at both the N and C termini that come together to wrap around the N-terminus of CCL3 (fig. 4.1 A), leading to the creation of a “conformational paratope” in this protein. That is the binding surface is created by the protein folding to bring the N and C termini together to create the chemokine recognition surface. However, the studies on Evasin-4 suggested that this protein utilises solely its N-

terminus to bind target chemokines, suggesting the presence of a linear binding domain, or linear paratope, in this protein.

In the previous chapter, the new evasin P672 was identified and characterised. This evasin could have its binding properties markedly altered by the presence of a purification tag, suggesting that it is possible to engineer evasins to have altered properties. P672 was most closely related to Evasin-4, suggesting that like Evasin-4 it may solely use its N-terminus to bind to target chemokines. Further evidence for a single N-terminal binding domain comes from the sequence analysis of P672 as it does not possess an extended C-terminus. This was not the case for Evasin-1 which possessed an extended C-terminus and some of the CCL3 interacting residues were found to be in this region.

Conveniently, Evasin-1 does not bind CCL8 whereas P672 does. This provides a suitable framework to test whether there are domains in evasins as if a CCL8 binding domain in P672 can be identified, this could be transferred to Evasin-1 and therefore confer CCL8 binding properties to this “hybrid evasin”. The aim of this chapter is to identify domains in evasins to investigate whether it is possible to engineer evasins with altered properties (fig 4.1 B).

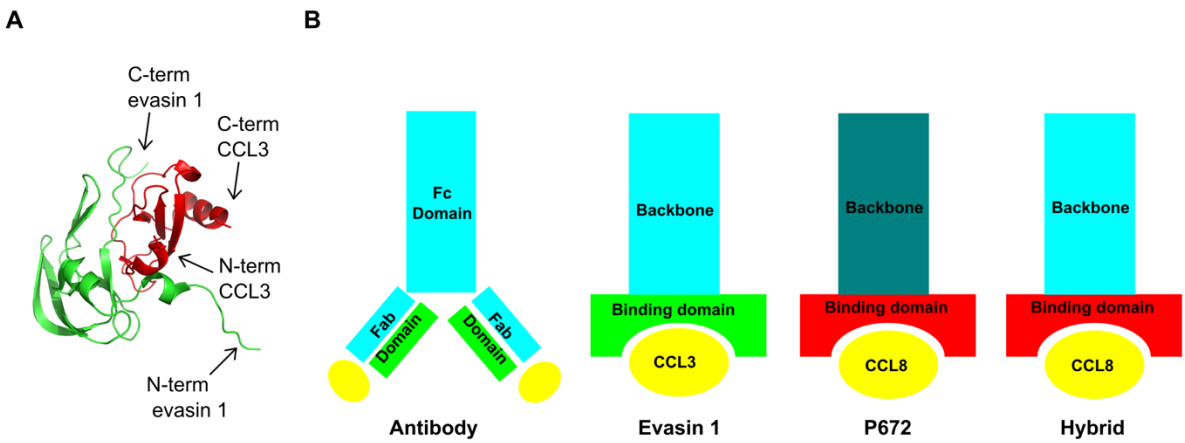


Figure 4.1 Schematic representation of the development of hybrid evasins. **A.** Crystal structure (3FPU) of Evasin-1(green) in complex with CCL3 (red). **B**. Schematic of the domains in an antibody and representation of putative chemokine binding domains in evasins.

To begin to explore how P672 binds CCL8, with the help of a collaborator, the non-denaturing mass spectrum of this complex was determined (fig. 4.2). Initially these proteins were characterised in isolation and it was found that P672 is a monomer in solution whereas under these conditions CCL8 exists as a homodimer. Incubation of P672 and CCL8 together revealed that, like Evasin-1 and CCL3, P672 forms a 1:1 complex with CCL8, disrupting CCL8 homodimerization.

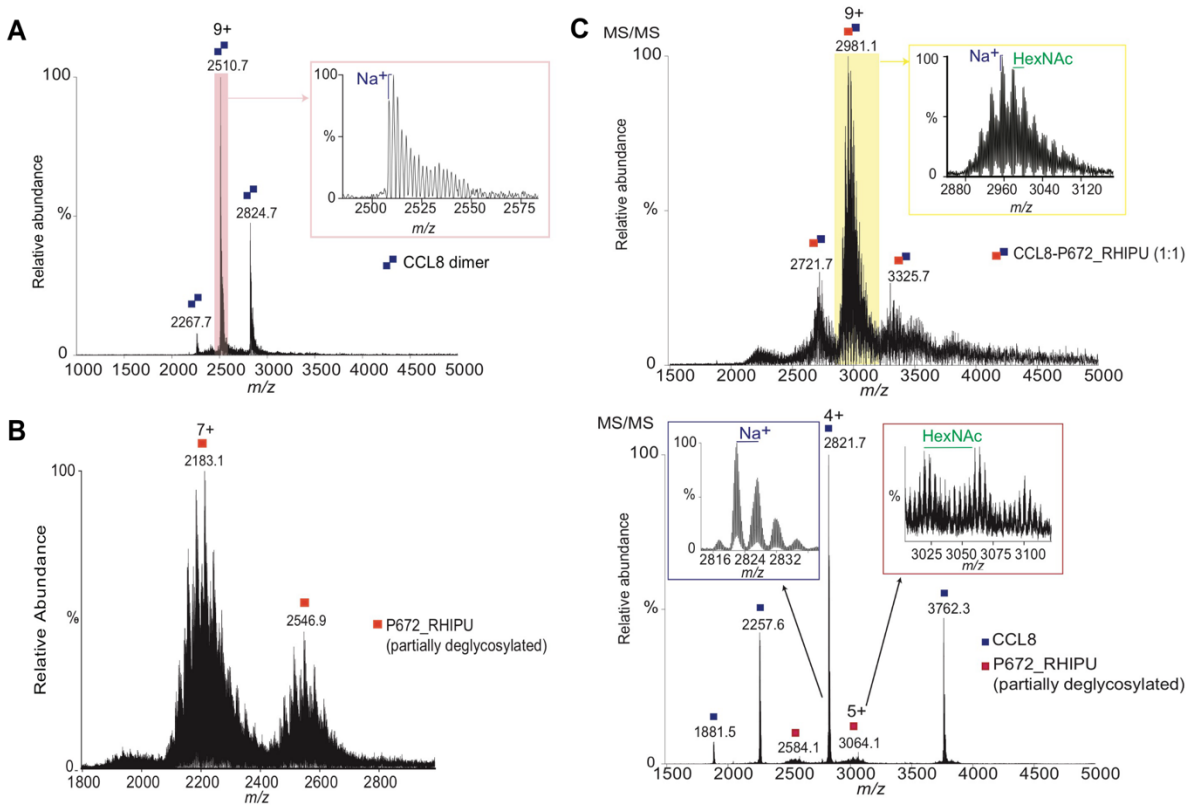


Figure 4.2 Analysis of the CCL8-P672 complex using non-denaturing mass spectrometry. **A.** Non-denaturing MS of CCL8 homodimer. *Inset* shows sodium adducts of the homodimer. **B.** Non-denaturing MS of partially deglycosylated N-terminally tagged P672. **C.** *Top panel* and *inset*, native MS of P672-CCL8 complex. CCL8 and P672 were mixed at a 1:1 ratio (final concentration of 2.5 M) and incubated for 1h at 4 °C. Peaks corresponding with a glycosylated and sodiated CCL8-P672 heterodimer (lowest intensity average mass observed is 25,915.3 1.4 Da) are indicated (*inset*). *Bottom panel*, HCD fragmentation at 100 V of the *m*/*z* 2956 isolated using a 100 *m*/*z* isolation window. Peaks corresponding to sodiated CCL8 (*top left inset*) and a partially glycosylated P672 (*top right inset*) are indicated. In all sections of this figure, the peaks are indicated as CCL8 (*blue squares*) or P672 (*red squares*). Monomers are indicated as a *single square* and homo- or heterodimers as *double squares*. The *y* axis indicates relative abundance, and the *x* axis indicates the *m*/*z* (mass/charge) ratio. This data was acquired by Dr Lucia Geis-Asteggiante.

4.2 AIMS

Knowing that P672 forms a 1:1 complex with CCL8, the aims of the work described in this chapter were:

(i) To gain some insight into how P672 inhibits CCL8

(ii) To identify the CCL8 binding domain in P672

(iii) To generate an expression construct that has this domain transplanted into Evasin-1 to give a "hybrid evasin"

(iv) To recombinantly express this hybrid evasin

(v) To evaluate whether this hybrid evasin with the putative CCL8 binding domain can bind and neutralise CCL8

4.3 RESULTS

4.3.1 HOMOLOGY MODELLING OF THE P672/CCL8 COMPLEX

In an attempt to understand how P672 binds CCL8 a homology model of the P672/CCL8 complex was generated. The published structure of Evasin-1 in complex with CCL3 has a 1:1 stoichiometry[159], the same stoichiometry that was determined for the P672/CCL8 complex using non-denaturing mass spectrometry (fig. 4.2). Using this structure as a template it was possible to generate a homology model for the P672/CCL8 complex using MODELLER[212] (fig. 4.3). The model suggested that P672 had the same disulphide topology as Evasin-1. The Arpeggio web server[213] was used to calculate interchain interactions and to help identify the CCL8 binding domain in P672 (fig. 4.2 B and E). The model suggested that the N-terminal residues, Glu-17 to Asn-44, in P672 form a binding surface that interacts with the N-terminus of CCL8. The model does not provide a role for the extended N-terminus of P672 as this region shares no homology to the residues in Evasin-1.

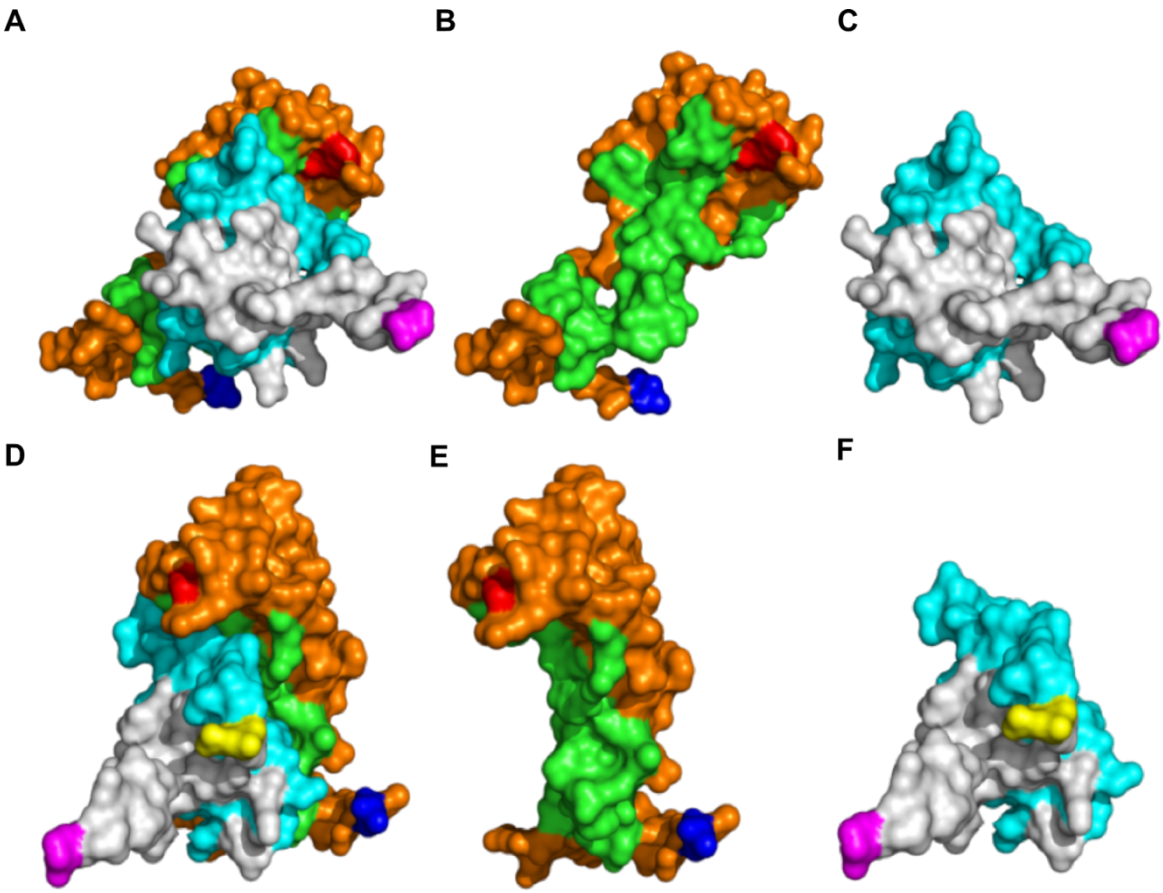


Figure 4.3 Homology modelling of the P672/CCL8 complex. This is a 3D structural model of P672 (*orange* and *green*) and CCL8 (*grey* and *cyan*) modelled as a 1:1 complex using the EVA1-CCL3 structure (Protein Data Bank ID 3FPU) as template and MODELLER with default parameters after alignment with the MUSCLE algorithm. The residues forming the binding surfaces predicted using Arpeggio are indicated in *green* (P672) and *cyan* (CCL8). The N terminus residue of P672 (Val-1) is indicated in *blue* and the C terminus residue (Trp-104) in *red*. The N and C termini of CCL8 are indicated in *yellow* and *magenta*, respectively. **A** and **D.** P672-CCL8 complex shown in two orientations. **B** and **E.** P672-alone shown in two orientations. **C** and **F**. CCL8 alone shown in two orientations.

4.3.2 Deletion study

As the homology model could not provide a role for the extended N-terminus of P672, a deletion study was performed. An expression construct was generated that started with the first residue in P672 (E17) that shared some homology with Evasin-1 and the protein was produced in HEK293 cells in the same fashion as full

length P672 (fig. 4.4A). The affinity of this protein for CCL8 was determined using BLI and a modest decrease in binding affinity was observed, the full-length affinity was 1.63E-08M whereas when the N-terminal residues were deleted the affinity became 30.4E-08M. This result suggests the N-terminal residues may contribute to binding CCL8.

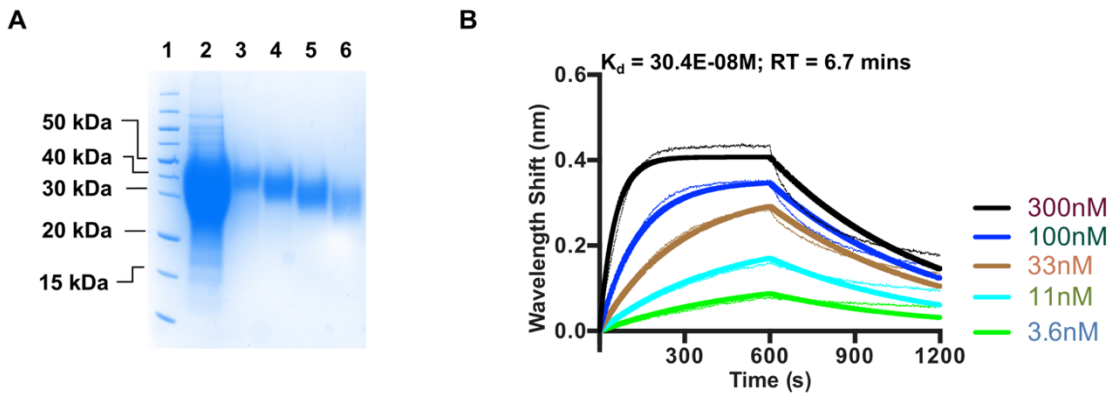


Figure 4.4 Characterisation of P672_17-104. **A.** SDS-PAGE stained with colloidal Coomassie blue showing: 1. Molecular weight marker 2. Nickel affinity purified deletion. 3-6 size exclusion chromatography fractions of affinity purified protein. **B.** Biolayer interferometry sonogram for P672_17-104 binding to different doses of CCL8. Plot displays wavelength shift (y axis, nm) verses time (x axis, second). Dotted lines indicate collected data, solid lines indicate modelled data.

4.3.3 Inhibition of CCL8-647 binding to chemokine receptors

The homology model predicted that P672 binds CCL8 at its N-terminus. This region in CCL8 is responsible for binding to and activating its target receptors[211]. Therefore, the mechanism for the inhibitory effect for P672 on CCL8 could possibly be that it blocks the binding of CCL8 to its target receptors. To explore this hypothesis the effect of P672 on fluorescently labelled CCL8 (CCL8-647) binding to human monocytic THP-1 cells was investigated. CCL8-647 binding to the chemokine receptors on these cells results in an increase in the fluorescence of these cells which can be monitored by FACS (fig. 4.5A). The reference protein used

for BLI studies acted as a negative control and had no effect on CCL8-647 induced fluorescence at 600nM whereas P672 at this concentration appeared to totally prevent CCL8-647 binding (fig. 4.5A). Titrating in decreasing amounts of P672 lead to a dose dependent increase in CCL8-647 fluorescence and gave an IC_{50} of 1.8E-10M (fig. 4.5B). This result suggests that P672 blocks the CCL8/receptor interaction, thus going some way to explaining the inhibitory activities of P672.

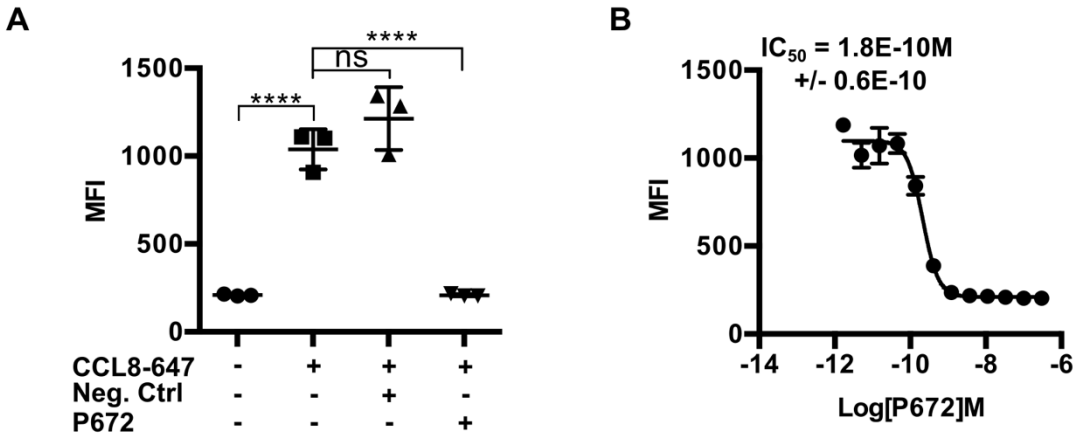


Figure 4.5 CCL8-647 blocking assay. **A.** Median fluorescence intensity (MFI) observed for THP-1 cells alone, when incubated with CCL8-647 (2.5nM), CCL8-647 (2.5nM) and the reference protein from BLI studies (600nM), and CCL8-647 (2.5nM) and P672 (600nM). Each data point is the average of one single experiment carried out in triplicate. **B.** Representative IC_{50} curve for titrating in different doses of P672. Curve was fitted using a four-parameter fit in Graph Pad Prism 6. IC50 value is the average of three independent experiments carried out in triplicate with error displayed as standard error of the mean.

4.3.4 Design and expression of Hybrid evasins

The homology model and deletion study suggested that a binding region at the N-terminus of P672 was responsible for CCL8 binding. Fortuitously, Evasin-1 does not bind CCL8 whereas P672 does. This provides a suitable framework to test this hypothesis as if these residues are responsible for CCL8 binding then when the N-terminal residues of Evasin-1 are exchanged for those of P672 a hybrid evasin

should be generated which can bind CCL8. The alignment of P672 with Evasin-1 (fig. 3.2) indicated that these residues are proximal to the second conserved cysteine in P672 and constructs were designed to maximise the predicted binding interface (fig. 4.6). The first 29 residues of Evasin-1 were replaced by the equivalent residues of P672. Also, more extended hybrid molecules were designed, where longer regions of Evasin-1 were replaced with the corresponding residues of P672.

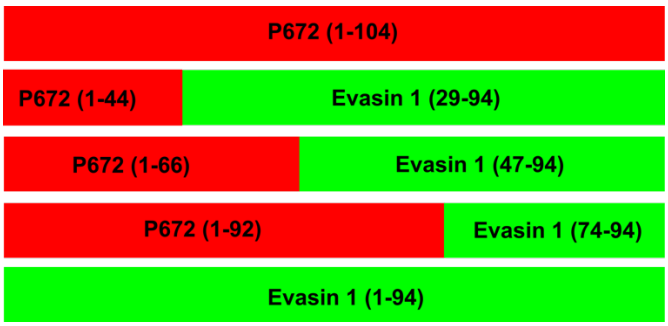


Figure 4.6 Design of hybrid evasins. Hybrid evasins were constructed based on the schematic above. The P672 sequence is represented by the red boxes, the Evasin-1 sequence by the green boxes and the residues present are indicated in brackets.

The hybrid evasins were expressed in HEK 293 cells and purified using the same strategy as for P672 using nickel affinity chromatography and size exclusion chromatography (fig. 4.7). The StrepII-his tag was placed at the C-terminus so that the changes made at the N-terminus were not confounded by the changing distance between the N-terminal residue and the purification tag. The protein ran as a smear at a much higher molecular weight than expected on SDS-PAGE, as was observed for full length P672. Evasin-1 was also expressed using the same system.

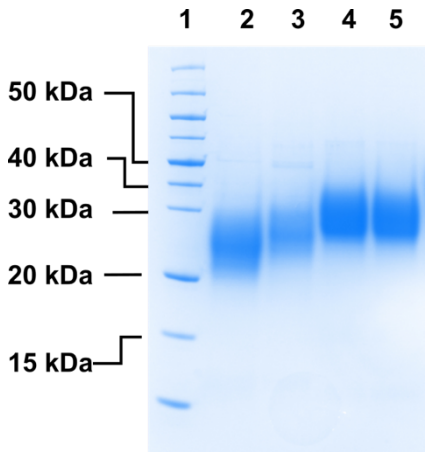


FIGURE 4.7 Expression of hybrid evasins and Evasin-1. SDS-PAGE stained with colloidal Coomassie blue showing 1. Molecular weight marker 2. Purified Evasin-1. 3. Purified P672(1_44):Evasin-1(29_94). 4. Purified P672(1_66):Evasin-1(47_94). 5. Purified P672(1-92):Evasin-1(94_94).

4.3.5 CHARACTERISATION OF HYBRID EVASIN BINDING

Evasin-1 and the hybrid evasins designed and expressed above were screened for chemokine binding at 300nM followed by K_d determination experiments for those that displayed a binding signal (fig. 4.8). Evasin-1 bound CCL3, CCL3L1, CCL4, CCL4L1, CCL14 and CCL18 as described previously[152] and crucially there was no binding to CCL8. Gratifyingly, the hybrid proteins were able to bind CCL8 and also CCL18.

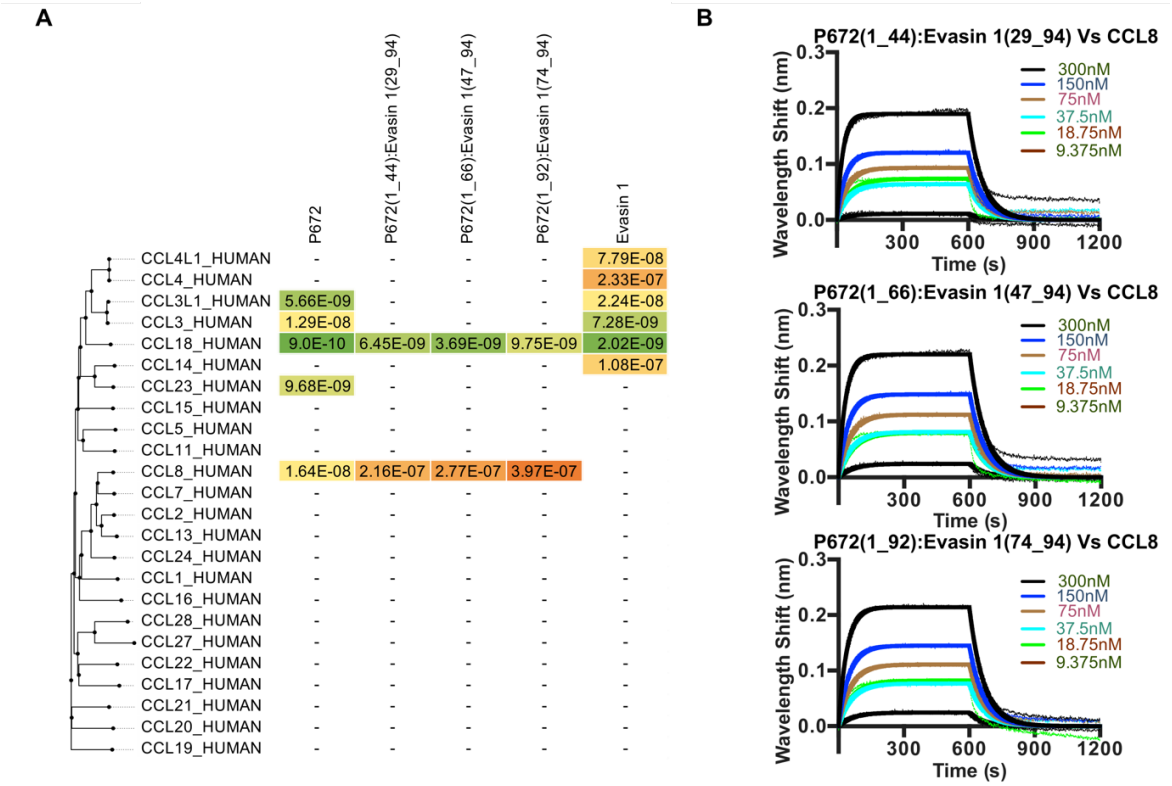


Figure 4.8 BLI binding characterisation of hybrid evasins **A.** Binding affinities (K_d, M) of immobilized P672, P672_Evasin-1 hybrids, and Evasin-1 to human CC-chemokines using biolayer interferometry. High-affinity binding is indicated in shades of *green*, medium affinity in *yellow*, and low affinity in shades of *orange*. Chemokines are arranged by sequence similarity–based phylogeny. A dash (—) indicates that binding was not detected at 300 nm chemokine concentration. **B**. BLI sensograms for the indicated hybrid binding to different concentrations of CCL8 as indicated. Plot displays wavelength shift (y axis, nm) verses time (x axis, second). Dotted lines indicate collected data, solid lines indicate modelled data.

4.3.6 HYBRID EVASIN INHIBITION OF CCL8 MIGRATION

The BLI studies suggested that these hybrids were able to bind CCL8. To determine if this was carried forward into function, as proof-of-principle, the smallest hybrid, P672(1-44):Evasin-1(29-94), was tested functionally against CCL8 and it was found to block CCL8 migration with an IC_{50} of 48nM. As wild type Evasin-1 did not bind CCL8 this result, and those described in section 4.2.5, indicate that the 44 N-terminal residues of P672, which represents 42% of the P672 protein, contain a CCL8 binding domain that is transportable to another evasin.

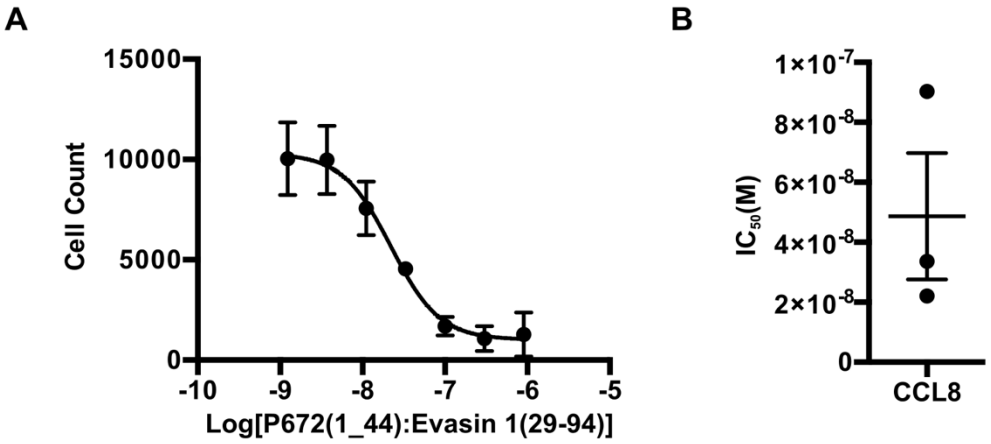


Figure 4.9 Inhibition of CCL8 function by a hybrid evasin. **A.** Representative IC_{50} curve for CCL8 migration in response to different doses of P672(1-44):Evasin-1(29-94). An EC_{80} (5.75nM) of CCL8 was used. Experiment was performed in technical triplicate and the data was fitted to a four-parameter fit in Graph Pad Prism 6. **B.** IC50 values for P672(1-44):Evasin-1(29-94) inhibition of CCL8. Mean is the average of three independent experiment carried out in triplicate analysed as in fig. 4.9A. Error displayed here is as standard error of the mean.

4.4 Discussion

Evasins are an emerging class of biologic that have been shown to be efficacious in animal models of inflammatory disorders[157,158]. Chemokines are a family of chemotactic cytokines that recruit innate and adaptive immune cells to sites of inflammation and evasin activity is due to their ability to bind to and neutralise the activity of multiple chemokines[152]. Previous efforts to understand evasin mechanism of action have used crystallographic studies and *in silico* modelling[159,160]. This work utilised non-denaturing mass spectrometry for elucidating the complex stoichiometry between the evasin P672 and the chemokine CCL8. This revealed that in a similar fashion to the published Evasin-1/CCL3 crystal structure, it forms a 1:1 complex with CCL8. This allowed for the use of the available structure to perform *in silico* modelling to generate a homology model for the complex of P672 with CCL8. This model revealed that it is likely P672 is binding to

the N-terminus of CCL8 and uses a linear segment to form a chemokine binding domain to recognise CCL8.

Studies on the chemokine CCL2 revealed that N-terminal residues are used for receptor binding and activation[49,214] and as CCL8 is a part of the same family it is likely that it uses the same mechanism to bind to and activate its target receptors. As the homology model indicated that P672 binds the N-terminus of CCL8, the inhibitory effect of P672 could therefore be due to it blocking the interaction of CCL8 with its target receptors. Using a fluorescent chemokine/receptor binding blocking assay it was shown here that P672 was able to prevent CCL8-647 from binding to cognate receptors on human monocytic THP-1 cells. Evasin-1 is able to block the binding of ^{125}I-CCL3 to CCR1 and CCR5 and ^{125}I-CCL4 to CCR5[152], suggesting that the mechanism for evasin activity is through the inhibition of chemokine/receptor binding. Other chemokine binding proteins, such as those found in viruses, also block the chemokine/receptor interaction however there are some viral chemokine binding proteins, such as M-T7, that inhibit chemokine binding to glycosylated amino glycans (GAGS) on the surface of endothelial cells[215]. This prevents the formation of the necessary chemokine gradients at the site of inflammation and thus stops the recruitment of immune cells to these loci.

Antibodies are the archetypal biologic and several decades of work has elucidated the structure and the mechanism of action of these proteins. These studies lead to the identification of domains in these proteins that are primarily responsible for antibody/antigen binding[216]. The homology model constructed here suggested the presence of a CCL8 binding domain in P672. To test this hypothesis this domain was transplanted into the Evasin-1 sequence, as this evasin does not bind CCL8, to yield a P672/Evasin-1 hybrid protein. The first 44 amino acids of

P672, which represents 44% of the P672 protein, was the smallest segment that was transplanted into Evasin-1 and was able to confer CCL8 binding. This hybrid evasin was also able to block CCL8 migration *in vitro* as assessed with a Boyden chamber assay. This result confirms that some of the CCL8 binding residues reside at the N-terminus of P672 and that there are chemokine binding domains in evasins which can confer chemokine binding properties to other evasins. This is a rather pertinent point as the identification of domains in antibodies, such as the complementary determining region (CDR) which is responsible for antigen binding, has led to the development of peptides and other modalities which can mimic antibody function[217]. Having small, chemically synthesisable peptides present a much more attractive therapeutic entity than biologics which can suffer from the requirement for parenteral delivery, poor tissue distribution and manufacturing difficulties[218,219]. This is particularly important for challenging targets such as chemokines as their small size precludes the identification of any obvious binding hot spots for peptides and the necessity that any anti-chemokine therapeutic would need to bind multiple chemokines to successfully neutralise this system[127].

Previous studies on evasins highlighted residues at the N and C termini that were important for CCL3 binding by Evasin-1 and solely N-terminal residues for CCL3, CCL5 and CCL8 binding by Evasin-4[160]. This work primarily relied on single or double alanine point mutants and the subsequent loss of binding affinity to determine the importance of residues for chemokine binding. In this work, a chemokine binding domain was identified by the ability of a sequence of amino acids to confer chemokine binding to generate a hybrid evasin, rather than to observe the loss of binding. However, there was a decrease in affinity for CCL8 for the hybrid compared to the wild type protein, suggesting that other residues are needed for

optimal binding or perhaps the folding of this hybrid is not optimal for CCL8 binding. There was loss of binding to CCL3, CCL3L1 or CCL23 when compared to the full-length C-terminally his-tagged P672. This may also be due to other residues being required to bind these chemokines or in this hybrid evasin the folding is not optimal for binding these chemokines. Interestingly, the ability to bind CCL18 was retained. This is a chemokine that Evasin-1 was also able to bind so it is unclear whether the transplantation of the P672 residues were responsible for this binding or whether the hybrid evasin retained the binding residues which Evasin-1 utilises to target CCL18. However, CCL18 shares only a 40% identity with CCL8 and is quite distinct from CCL8 on the amino acid level so whilst it is surprising that the hybrid can recognise such distinct chemokines, it is likely that P672 recognises CCL18 in a different fashion to CCL8.

4.5 CONCLUSIONS

In this work a homology model was constructed for the P672/CCL8 complex. This model suggested that P672 binds the N-terminus of CCL8 and it utilises a continuous segment at the N-terminus of P672 to bind this chemokine. P672 is able to prevent the interaction of CCL8-647 with chemokine receptors on human monocytic THP-1 cells, suggesting that the inhibitory effect of this evasin is due to it blocking the chemokine/receptor interaction. The continuous segment at the N-terminus of P672 that appeared to interact with CCL8 in the homology model was transplanted into Evasin-1, which does not bind CCL8, to give a hybrid evasin. This hybrid evasin was able to bind and neutralise CCL8 suggesting that these N-terminal residues represent a CCL8 binding domain that can be transferred to another evasin to confer CCL8 binding. This work has shown that P672 possesses

a transplantable domain that can confer chemokine binding properties to other evasins.

5 EVASIN DERIVED MULTIPLE CHEMOKINE BINDING PEPTIDES

5.1 INTRODUCTION

Peptide therapeutics present an exciting modality that is gaining traction within the pharmaceutical industry as an alternative to traditional small molecule drugs. This is exemplified by six new peptide-based therapeutics being approved in 2012, a year which saw the greatest number of new molecular entities approved, and that the market share for this class of drug is expected to reach US$46.6 billion by 2024[220,221]. Peptides are able to inhibit protein targets that have been deemed "undruggable" by small molecules, such a protein-protein interactions (PPIs) as they typically involve a large surface area of interaction that provide no obvious small molecule binding sites. Peptides have a slightly larger size compared to small molecules meaning they can occupy the flat, featureless interface that is typically associated with this type of interaction. However, peptides are still smaller than biologics, such as antibodies, so still have the potential to be delivered orally[222]. Peptides may present unique scaffolds to allow for the engineering of drugs with unique mechanism of action. For example, there have been peptides reported that have double or even triple agonist activity against therapeutically relevant receptors for type 2 diabetes[223,224]. This suggests that peptides are able to be engineered to be able to inhibit multiple targets. However, a key challenge involved with peptide therapeutics is the identification of initial hit compounds for lead development. Peptide display technologies, such as mRNA[225] and phage display[226], allow for the rapid screening of huge libraries against an immobilized protein target. Another approach has been to design peptides based on structural information of a known PPI[227].

Crystal structures for several chemokine ligands, and more recently, some chemokine receptors have been solved [228-230]. Chemokines are key mediators of the inflammatory response and several studies have indicated that these may be validated therapeutic targets for a diverse range of inflammatory disorders[89,188,231]. Chemokine ligands interact with their target receptors *via* a two-site interaction model, involving the N-terminus of the receptor interacting with the N-terminal loop region of the ligand and the transmembrane pocket on the receptor interacting with the N-terminus of the ligand, meaning this interaction occurs with a wide surface area[63]. Despite this large surface area of interaction, there are examples of small molecules reported in the literature that can bind to and inhibit the chemokine ligands[232-234]. There have also been several antibodies directed toward the chemokine ligands that have been evaluated in pre-clinical and clinical trials of inflammatory disease[116,120,122]. However, there still remain no therapeutics that target these ligands for inflammatory disorders. This may be due to the chemokine system forming a complex network with a series of "one-to-many" interaction between the ligands and the receptors[235]. As a single chemokine ligand can bind multiple receptors and *vice versa*, the inhibition of a single chemokine may be unable to overcome this network robustness and therefore prevent this approach from being effective. However, due to their key role in the regulation of immune cell trafficking, several pathogens have convergently evolved chemokine binding proteins (CKBPs) to successfully neutralise the chemokine response[66,152,168]. Despite arising in distinct lineages all of these proteins share a common mechanism for targeting chemokines, namely the targeted inhibition of multiple chemokine ligands by a single agent. This shared "one-to-many" binding mechanism that has arisen evolutionally suggests this is a possible way to overcome the robustness of

the chemokine network. Thus, the large area of interaction between the chemokine ligand and its receptor, and the requirement for an agent to possess the “one-to-many” mechanism of action, indicates that peptides present a possible modality that could successfully target this system.

Previous efforts to identify multiple chemokine binding peptides have involved the screening of a random peptide library displayed on the surface of phage against multiple chemokine targets or the identification of chemokine receptor derived peptides through sequence alignment[236,237]. There have been some chemokine binding peptides that have been identified through structural studies and *in silico* design[238,239], but these do not possess the “one-to-many” binding mechanism that has arisen in nature.

Hydrogen-deuterium exchange mass spectrometry (HDX-MS) is a technique that can provide structural information on a protein complex and allow for the characterisation of binding sites between two proteins when they form a complex, and the conformational changes that occur on binding[240]. This technique relies on the slow exchange of the protons present in the amide backbone of the protein with those in the surrounding solvent. However, when the solvent used is deuterated this slow exchange can be monitored using mass spectrometric analysis of protease digested peptide fragments of the protein due to deuterium uptake resulting in an increase in the mass of the digested peptide. By analysing the relative difference in deuterium uptake of a protein alone and in complex it is possible to obtain conformational dynamics and binding interfaces. The rate of exchange depends on the accessibility of the proton to the solvent; if an amide proton sits at the interface of a protein-protein complex then the deuterium uptake will be reduced compared to those readily accessible to the surrounding solvent. Conversely, if

there is a conformational change in the protein upon binding and residues which were once buried in the protein are now exposed to the solvent there will be a corresponding increase in deuterium uptake. Looking at the relative increase or decrease in deuterium uptake one can infer conformational shifts and binding interfaces.

5.2 AIMS

In the previous chapters the novel evasin P672 was identified and characterised and was shown to possess a chemokine binding domain that can confer chemokine binding to other evasins. Crucially, this protein possesses the "one-to-many" chemokine binding mechanism that is essential for neutralising the chemokine network. The aims of this chapter were to:

(i) Study the P672/CCL8 complex using HDX-MS to identify the potential protein-protein interface

(ii) validate this result through the use of site directed mutagenesis and domain swap experiments

(iii) to use the knowledge garnered from these experiments to inform the design of multiple chemokine binding peptides.

5.3 RESULTS

5.3.1 HYDROGEN-DEUTERIUM EXCHANGE MASS SPECTROMETRY OF P672/CCL8 COMPLEX

In the previous chapter it was demonstrated using non-denaturing mass spectrometry (non-denaturing MS) that P672 and CCL8 form a 1:1 complex. Using homology modelling and domain swap experiments it was shown that the first 44

amino acids of P672 represents a CCL8 binding domain that can confer CCL8 binding to other evasins. Here, hydrogen-deuterium exchange mass spectrometry at the peptide level was performed to characterise this interaction further (this experiment was carried out by Dr Lucia Geis-Asteggiante). Satisfactory sequence mapping was achieved, with the identification of 38 peptides for P672 covering its complete sequence and 45 peptides for CCL8 representing 96.9% of its sequence (fig. 5.1). The vast majority of the peptide peptides obtained showed adequate overlap, except for CCL8 P2-N14 and A40 C52 regions for which only one peptide was identified.

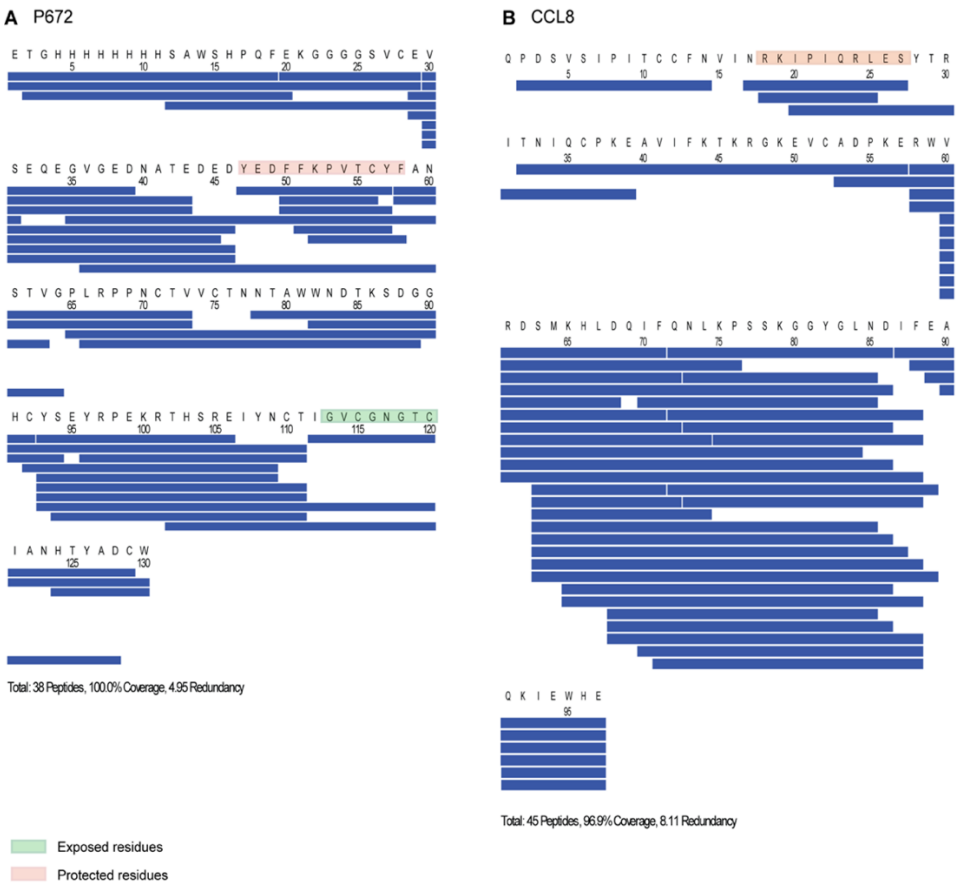


Figure 5.1 Sequence coverage of HDX-MS peptides for **A.** P672 and **B.** CCL8. Peptic peptides that passed identification criteria were used for H/D exchange measurements and are indicated in blue. Residues with reduced relative deuterium uptake upon binding are highlighted in orange and residues with increased relative deuterium uptake are highlighted in green. A total of 38 peptic peptides were identified for P672 yielding 100% sequence coverage and 45 peptides were identified for CCL8 yielding 96.9% coverage.

Deuterium uptake was measured for each peptide after 5s, 30s, 5min and 60 min incubation time points for both unbound and bound species. The percentage of H/D exchange was estimated by comparing the deuterium uptake after complex formation between P672 and CCL8 and the deuterium uptake of each protein in isolation; this was overlaid onto the P672/CCL8 homology model (fig. 5.2). H/D exchange percentages ≥ 5% with *p*-value ≤ 0.05 were considered significant. H/D exchange mapping revealed that for most residues in P672 there was no significant change in deuterium uptake apart from residues Y21-F32 toward the N-terminus of P672, which showed a significant decrease in relative deuterium uptake when compared to unbound P672, and this was maintained for residues F25-C30 and F32 even after 60 min incubation in D_2O. Residues G113-C120 had an increase in deuterium uptake, indicating higher exposure to solvent water after complex formation. For CCL8 there was also no change in the deuterium uptake for most residues, apart from residues R18-S27 in the N-terminal loop region of CCL8 which were protected from deuterium uptake. Taken together, this suggests that the protected residues Y21-F32 in P672 and R18-S27 in CCL8 are at the complex interface as they are shielded from the solvent. This provides some validation for the homology model presented in the previous chapter as when these residues are coloured they appear to be close to each other in space. Moreover, consistent with this domain being able to transfer CCL8 binding, residues 21-32 in P672 are in the first 44 residues that were transplanted into Evasin-1 in the last chapter.

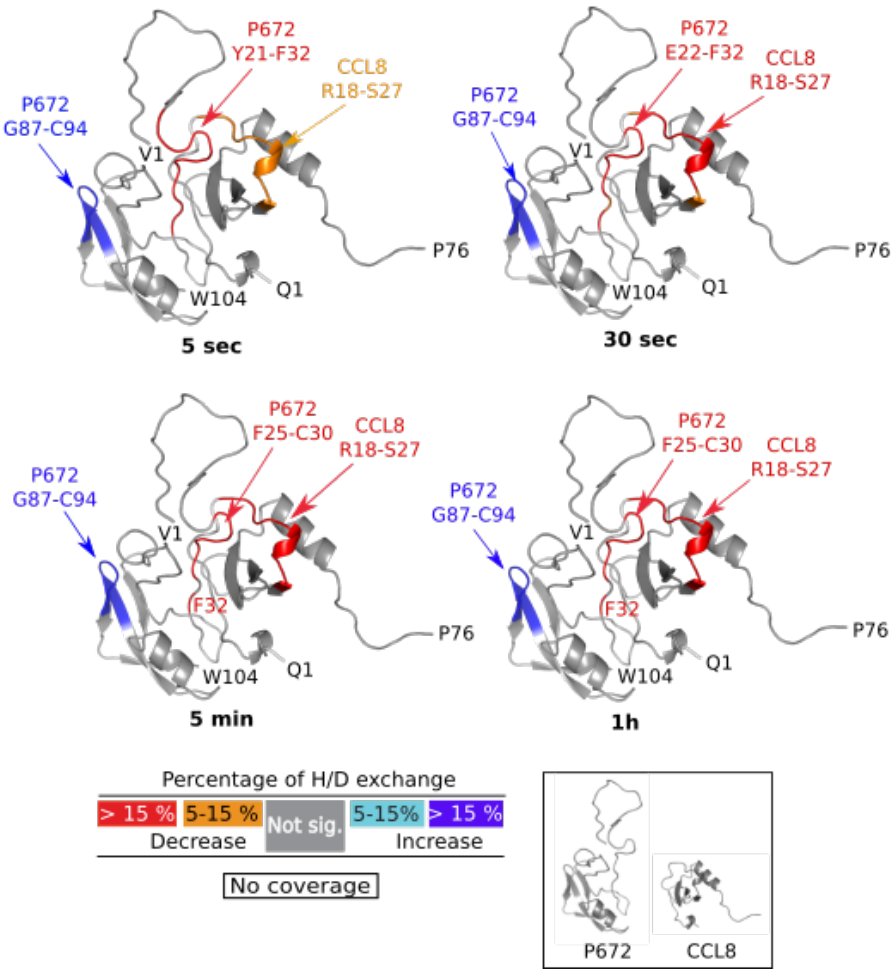


Figure 5.2 Percentage of hydrogen/deuterium exchange measured at four incubation time points (5s, 30s, 5 min, 60min) for the P672/CCL8 complex. Regions with increased HDX rates (exposed residues) are shown in blue (>15%) and cyan (5-15%) and regions with decreased HDX rates (protected residues) are shown in red (>15%) and orange (5-15%). Regions with no significant exchange are indicated in grey. Five residues of CCL8 (Q_1, P_2, V_{15}-N_{17}) were not covered and are indicated in white. All analyses were performed in triplicates. Data from Dr Lucia Geis-Asteggiante.

5.3.2 Exploration of HDX-MS result

To explore the HDX-MS result the region that was protected from deuterium uptake was transplanted into the analogous region in Evasin-1 (fig. 5.3A) to give an Evasin-1 and P672 hybrid protein (Evasin-1/P672). This protein was expressed in HEK293 cells and was found to be glycosylated, as it ran as a smear at a higher

molecular weight than expected (fig. 5.3B). The recombinant protein was tested for CCL8 binding using BLI (fig. 5.3C) and it was found to bind CCL8 with a K_d of 4.87E-07M (table 1) where as P672 wild type (P672_WT) had a much higher affinity of 8.88E-09M. This protein was also tested for binding to CCL3, a chemokine that is only distantly related to CCL8, and no binding was detected even though P672_WT and Evasin-1 are able to bind this chemokine (table 2). It was found to functionally inhibit CCL8 driven THP-1 migration (fig. 5.3D) with an IC_{50} of 14.7E-08M as determined by a Boyden chamber assay. These findings suggest that the region Y21-F32 identified in the HDX-MS experiment is responsible for CCL8 binding and inhibition in P672.

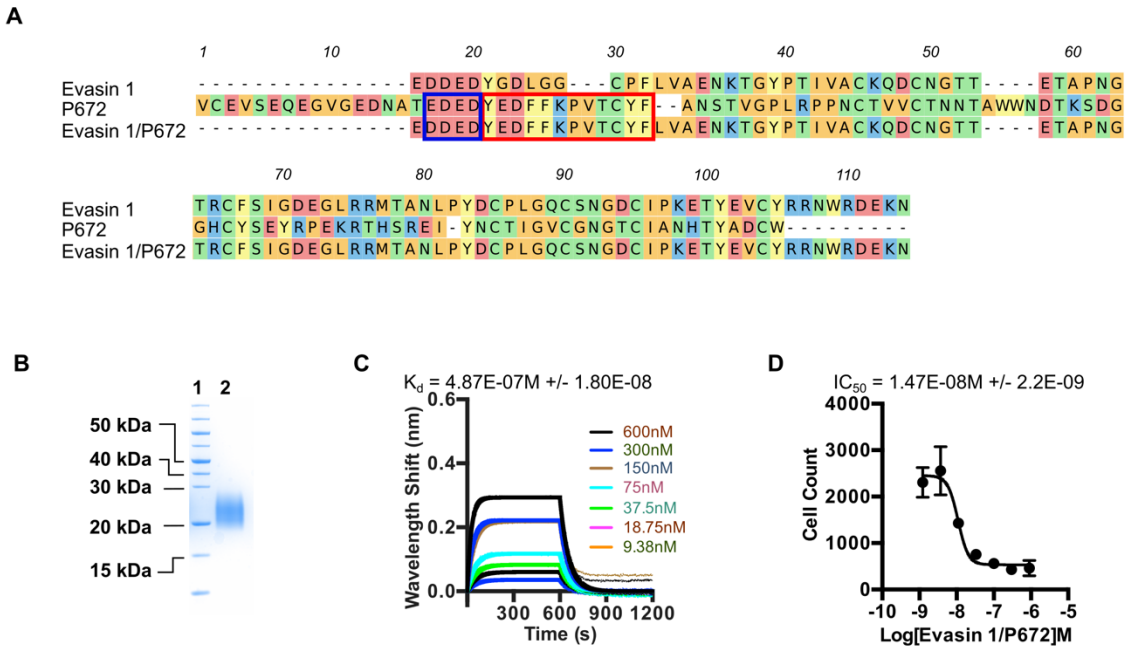


Figure 5.3 Small domain (Evasin-1/P672) transplantation experiment to explore the HDX-MS result. **A.** Alignment of Evasin-1, P672 and evasin1/P672 hybrid protein using MUSCLE algorithm. Amino acids are color-coded according to physicochemical properties: yellow, aromatic (F, W, and Y); red, acidic (D and E); blue, basic (R, H, and K); orange, nonpolar aliphatic (A, G, I, L, M, P, and V); green, polar neutral (C, N, Q, and T). Amino acids that were protected from deuterium uptake in P672 are indicated with a black box. The conserved acidic N-terminal amino acids are shown in a blue box. **B.** SDS-PAGE stained with colloidal Coomassie blue showing 1. Molecular weight marker 2. Purified Evasin-1/P672 **C**. BLI sensogram for Evasin-1/P672 hybrid binding to CCL8. Plot displays wavelength shift (y axis, nm) verses time (x axis, second). Dotted lines indicate collected data, solid lines indicate modelled data. **D.** Representative IC_{50} curve for inhibition of CCL8 driven migration in a THP-1 assay. Experiment was performed in technical triplicate and the data was fitted to a four-parameter fit in Graph Pad Prism 6. Displayed IC_{50} is the average of three independent experiments carried out in triplicate with mean as SEM.

Next, to further explore the PPI regions identified in HDX-MS, alanine mutants of two residues from the region in P672 which was protected from deuterium uptake were prepared. Residues Y31 (P672_Y31) and F32 (P672_F32) were initially chosen as, typically, PPI interfaces are composed of hydrophobic residues, such as phenylalanine, and tyrosine is often a common residue that is found at complex interfaces[241]. Moreover, F32 remained protected from deuterium

uptake even after 60 minutes so is more than likely to be at the PPI interface here. P672_Y31A and P672_F32A were tested for CCL8 (table 2) and CCL3 (table 3) binding. These mutants were tested for CCL8 binding to probe the HDX-MS result and to investigate whether P672 uses the same residues to target a different chemokine such as CCL3.

Evasin	k_{on}(1/Ms)	k_{on} Error	k_{dis}(1/s)	k_{dis} Error	K_D (M)	K_D Error	RT (mins)
P672_WT	*5.76E+04*	*6.71E+02*	*5.11E-04*	*7.15E-06*	*8.88E-09*	*1.62E-10*	*2.20E+01*
Evasin-1	*ND*	*ND*	*ND*	*ND*	*ND*	*ND*	*ND*
Evasin-1/P672	*3.61E+04*	*1.30E+03*	*1.76E-02*	*1.56E-04*	*4.87E-07*	*1.80E-08*	*7.00E-01*
P672_Y31A	*6.01E+04*	*7.59E+02*	*1.05E-03*	*8.28E-06*	*1.75E-08*	*2.60E-10*	*1.10E+01*
P672_F32A	*5.80E+04*	*6.22E+02*	*1.32E-03*	*7.63E-06*	*2.27E-08*	*2.77E-10*	*8.00E+00*
P672_Y31A;F32A	*1.74E+05*	*8.77E+03*	*2.70E-02*	*4.24E-04*	*1.55E-07*	*8.16E-09*	*4.00E-01*

Table 2 Binding parameters for wild type P672, alanine mutants and Evasin-1/P672 hybrid protein to CCL8 as determined using BLI. RT = retention time of complex, calculated using the equation for dissociative half-life RT= ln2/k_{off}. ND = No binding detected at 300nM.

Evasin	k_{on}(1/Ms)	k_{on} Error	k_{dis}(1/s)	k_{dis} Error	K_D (M)	K_D Error	RT (mins)
P672_WT	*3.58E+05*	*2.67E+03*	*3.41E-04*	*3.73E-06*	*9.54E-10*	*1.26E-11*	*3.40E+01*
Evasin-1	*7.68E+04*	*3.80E+02*	*5.60E-04*	*2.83E-06*	*7.28E-09*	*5.15E-11*	*2.10E+01*
Evasin-1/P672	*ND*	*ND*	*ND*	*ND*	*ND*	*ND*	*ND*
P672_Y31A	*4.82E+05*	*1.61E+04*	*4.71E-03*	*4.10E-05*	*9.78E-09*	*3.37E-10*	*2.00E+00*
P672_F32A	*ND*	*ND*	*ND*	*ND*	*ND*	*ND*	*ND*
P672_Y31A;F32A	*ND*	*ND*	*ND*	*ND*	*ND*	*ND*	*0.00E+00*

Table 3 Binding parameters for wild type P672, alanine mutants and Evasin-1/P672 hybrid protein to CCL3 as determined using BLI. RT = retention time of complex calculated using the equation for dissociative half-life RT= ln2/k_{off}.. ND = No binding detected at 300nM.

It was found that for CCL8 binding there was an approximate doubling in the K_d value from 8.88E-09M for P672_WT to 1.75E-08M for P672_Y31A and was

almost three times greater for P672_F32A where the affinity became 2.27E-08M. This indicates a decrease in affinity for CCL8. Interestingly, there was approximately an order of magnitude decrease in affinity for CCL3 for the P672_Y32A mutant and there was no binding at any of the concentrations tested against CCL3 for the P672_F32A mutation (fig. 5.3). To further confirm the importance of these residues, the double alanine mutant (P672_Y32A;F32A) was tested for CCL8 and CCL3 binding. This resulted in decreasing the affinity to 1.6E-07M for P672_Y31A;F32A against CCL8 and a total loss of binding to CCL3 (fig. 5.4).

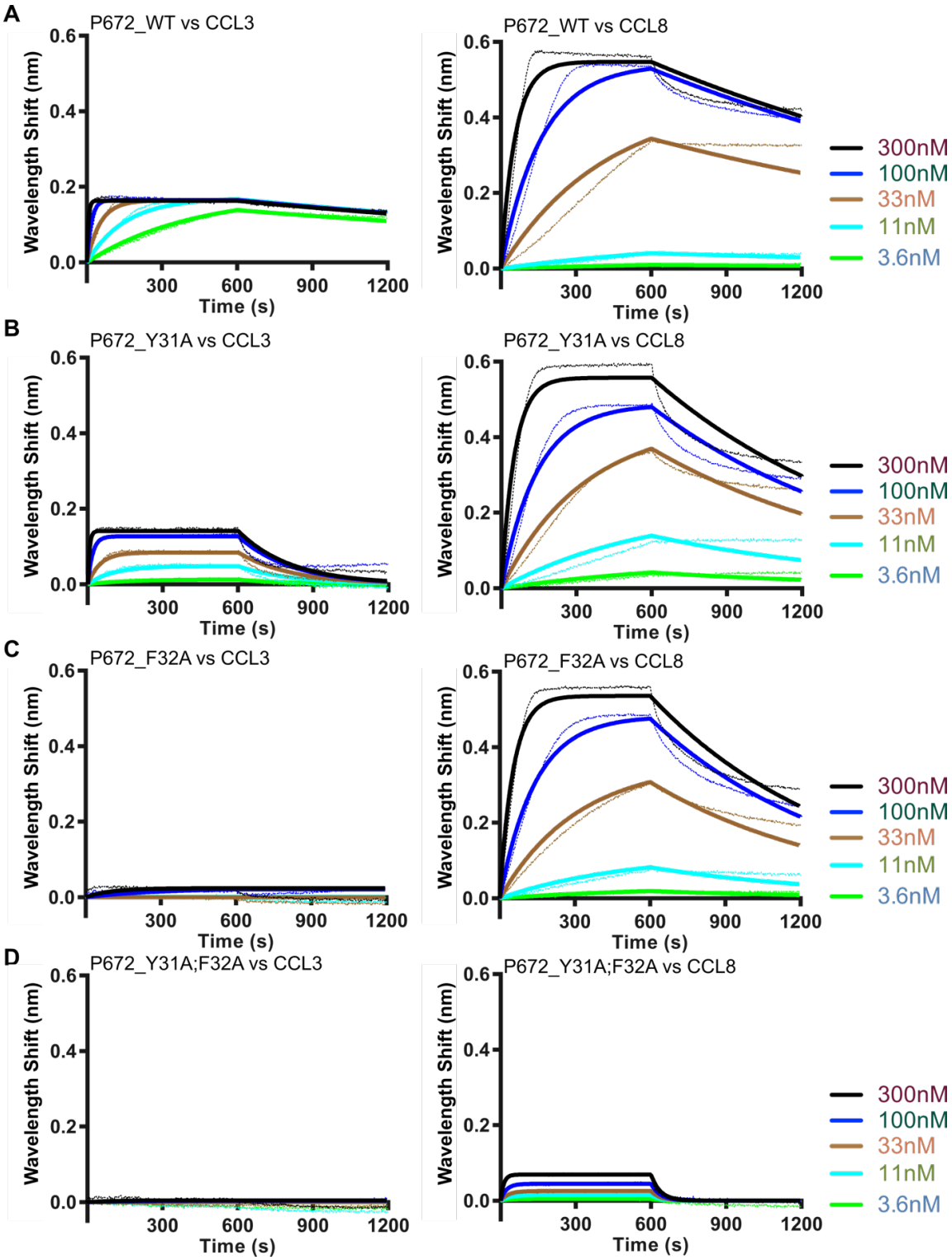


Figure 5.4 BLI traces for alanine mutants of P672. **A.** BLI sensograms for P672_WT binding to CCL3 (left panel) and CCL8 (right panel). **B.** BLI sensograms for P672_Y31A binding to CCL3 (left panel) and CCL8 (right panel). **C.** BLI sensograms for P672_F32A binding to CCL3 (left panel) and CCL8 (right panel). **D.** BLI sensograms for P672_Y31A;F32A binding to CCL3 (left panel) and CCL8 (right panel). In each sensogram, Plot displays wavelength shift (y axis, nm) verses time (x axis, second). Dotted lines indicate collected data, solid lines indicate modelled data.

The BLI result seemed to suggest that a single mutation at F32A abolished the binding of P672 to CCL3 whilst maintaining an affinity toward CCL8 that was only slightly decreased when compared to wild type. Next, functional assays were carried out to determine if the F32A mutation retained its chemokine selectivity in cells. Chemokine driven THP-1 migration was measured the presence of 100nM P672_F32A or 100nM P672_WT (fig. 5.5A). P672_WT was able to inhibit the cell migration by CCL3 to background levels whereas P672_F32A was unable to significantly lower the cell migration in response to CCL3. However, P672_F32A was able to inhibit CCL8 THP-1 migration with an IC_{50} value close to that of P672_WT (fig. 5.5B, C). Although the IC_{50} was slightly higher than the wild type (as would be expected based on the BLI result), it was not significant.

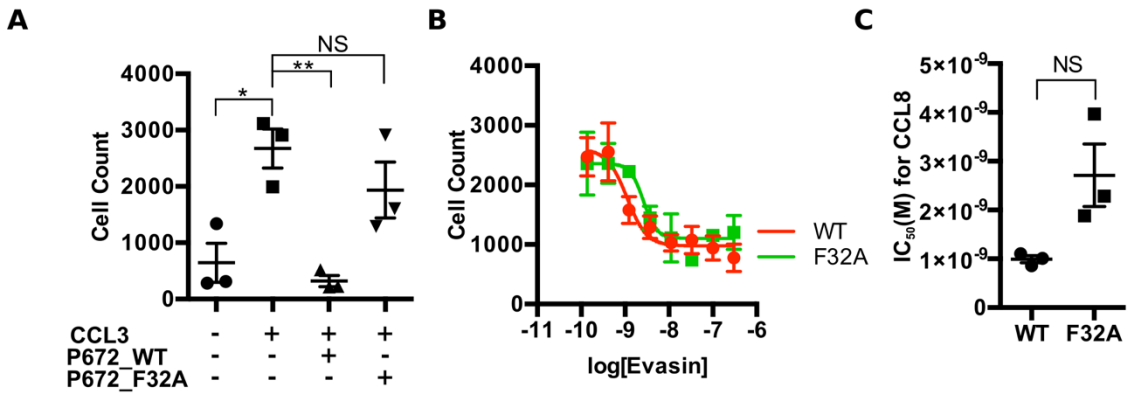


Figure 5.5 Activity of P672_F32A in a Boyden chamber assay using THP-1 cells. **A.** Cell migration in response to CCL3 (3.5nM) incubated with either P672_WT (100nM) and P672_F32A (100nM). Mean with SEM shown. Experiment carried out in triplicate where each data point represents the average of a single experiment carried out in triplicate. Statistical significance was determined with a one-way ANOVA with Sidak's correction for multiple comparisons in Graph Pad Prism 6. * = p<0.5, **= p<0.05, NS= not significant. **B.** Representative IC_{50} curve for P672_WT (red) and P672_F32A (green). Experiment carried out in triplicate with mean and SEM shown. Curve was fitted using a four-parameter fit in Graph Pad Prism 6. **C.** IC_{50} values for P672_WT or P672_F32A against CCL8. Each IC50 determination experiment was carried out in technical triplicate and analysed using a four-parameter fit in Graph Pad Prism 6. Mean with SEM shown. Statistical significance was determined using the Student's t-test in Graph Pad Prism 6. NS= not significant.

5.3.3 DESIGN OF P672_PEP

The HDX-MS result seemed to indicate that it is a contiguous sequence of amino acids in P672 that is interacting with CCL8. Validation of this observation is indicated by the domain swap experiment detailed above where transplantation of these residues into Evasin-1 conferred CCL8 binding and neutralisation to a hybrid evasin. However, it is unclear whether this sequence of amino acids alone is enough to bind CCL8 or whether this sequence in the context of a larger protein is required for CCL8 binding. This motivated the design and testing of an evasin peptide fragment composed of the residues E17-F32 of P672 (P672_PEP; EDEDYEDFFKPVTAYF; fig 5.6A) to determine if this linear chain of amino acids alone was enough to bind CCL8. This peptide contained the four acidic residues toward the N-terminus that were outside of the heavily protected region in P672 in the HDX-MS result as in the domain swap experiment the Evasin-1 sequence imparted acidic residues to this protein sequence (fig. 5.3A). Moreover, alignment of all the evasin sequences (fig. 3.2) shows that this cluster of acidic residues is conserved across of CC binding evasins, suggesting a role for this negatively charged region. For these reasons the “EDED” motif was included in the designed peptide. The linear segment identified to be at the complex interface in P672 contained a cysteine residue that is probably involved in a disulphide bond in the full-length protein. As this would not be present in a linear peptide, this residue was mutated to alanine to prevent any inter-peptide disulphide bonds from forming.

5.3.4 CHARACTERISATION OF P672_PEP CHEMOKINE BINDING

To test for chemokine binding a fluorescently labelled analogue of this peptide was also synthesised (P672_PEP-FITC) and tested for chemokine binding

using a fluorescence polarisation (FP) assay. A dose dependent increase in the anisotropy of the emitted light was observed when CCL8 was titrated into a fixed concentration of P672_PEP-FITC (fig. 5.6B). This indicates that there is a binding interaction between P672_PEP-FITC and CCL8. Next, the peptide was screened for chemokine binding against all the P672 binding chemokines (see chapter 1) at a fixed concentration (1μM). P672_PEP-FITC bound CCL7 and CCL18 (fig. 5.6B) but not to CCL1, CCL2, CCL3, CCL3L1, CCL11, CCL13, CCL14, CCL15, CCL16, CCL17 or CCL23 (fig. 5.7A). CXCL1 served as a negative control in these experiments as P672 is known not to interact with this chemokine. As expected, P672_PEP-FITC did not bind to CXCL1.

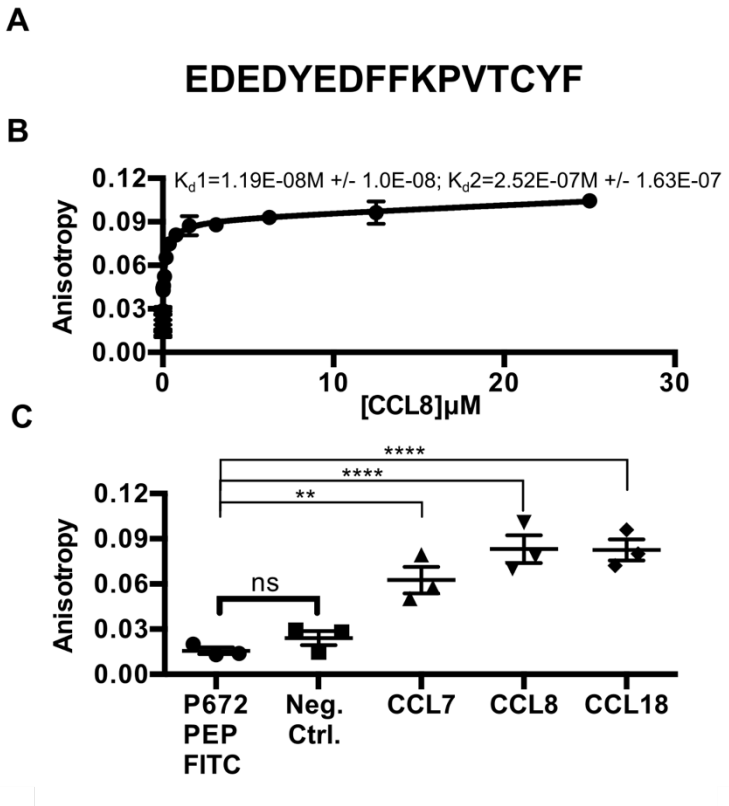


Figure 5.6 Fluorescence polarisation characterisation of P672_PEP-FITC. **A.** One letter amino acid sequence of P672_PEP. **B.** Fluorescence polarisation assay showing different concentrations of CCL8 binding to P672_PEP-FITC (50nM). The x-axis shows CCL8 concentration, and Y-axis the resulting fluorescence anisotropy. The curve was fitted to the two site-total and non-specific binding model in GraphPad Prism 6. Data are shown as mean and SEM of three independent experiments, with each independent experiment performed as three technical replicates. The affinity constants, K_d1 and K_d2, were calculated in GraphPad Prism from the curve fit with the standard error reported. **C.** Fluorescence polarisation assay showing binding of chemokines to P672_PEP-FITC. The measured fluorescence anisotropy (y-axis) of P672_PEP-FITC (50nM) following binding to a fixed dose (1µM)) of CCL7, CCL8, CCL18 and CXCL1 (negative control). Three independent data points are displayed for each chemokine, where each experiment was carried out in technical duplicate, with the mean and SEM are shown. Statistical significance was determined using one-way ANOVA with Sidak's correction for multiple comparisons using Graph Pad Prism 6. **= $p<0.005$, ****=$P<0.00005$, ns= not significant.

Interestingly, when the binding to CCL8 is represented on a log scale (5.7 B) it becomes apparent that there appears to be two binding events occurring. The data fits well to a two-site model where the goodness of fit for a two site and one site binding model in Graph Pad Prism 6 are $R^2 = 0.97$ and $R^2 = 0.96$ respectively, suggesting two binding events may be occurring. Next, competition experiments with unlabelled peptide (P672_PEP) was carried out against P672_PEP-FITC

binding with CCL7, CCL8 and CCL18. When the chemokine was incubated with an excess of P672_PEP and 50nM P672_PEP-FITC there was a concentration dependent decrease in the anisotropy compared to when the chemokine was incubated only with P672_PEP-FITC (fig. 5.7 C, D and E) . This indicates that the unlabelled peptide is competing off the labelled peptide. A peptide with the sequence scrambled (P672_PEP-SCRAM; EFTEVYEFDFKYDAPD) was used as a negative control and this had no effect on the anisotropy at the top concentration tested. P672_PEP-SCRAM has the amino acid composition, MW and PI as P672_PEP and as this had no effect it indicates that it is a specific interaction between P672_PEP and the chemokines tested. The sequence of P672_PEP-SCRAM was designed with the use of an online text scrambler to remove any possible bias from human intervention (http://www.togglecase.com/scramble_text).

To further probe the two-step binding observed in the FP assay the non-denaturing spectrum of the P672_PEP/CCL8 complex was acquired (by Dr Lucia Geis-Asteggiante). In the previous chapter it was shown that CCL8 forms a homodimer under non-denaturing MS conditions that could be disrupted to form a 1:1 heterodimer with P672. Initially, it was shown here that P672_PEP could disrupt the P672/CCL8 heterodimer, clearly forming a 1:1 complex with CCL8 (fig. 5.8 A). A peak corresponding to the mass of a 2:1 P672_PEP/CCL8 complex was not observed here, possibly due to the presence of multiple glycosylation states of P672 and sodium adducts. However, when P672_PEP was incubated with only CCL8 the 2:1 and 1:1 P672_PEP/CCL8 complex is clearly visible (fig. 5.8 B) and when either the 1:1 or 2:1 complex is isolated and then fragmented using HCD this dissociates clearly into the CCL8 and P672_PEP (fig. 5.8 C and 5.8 D). This result shows that

P672_PEP can displace P672 from CCL8 to form a complex with CCL8 and the stoichiometry of this interaction can be 1:1 or 2:1.

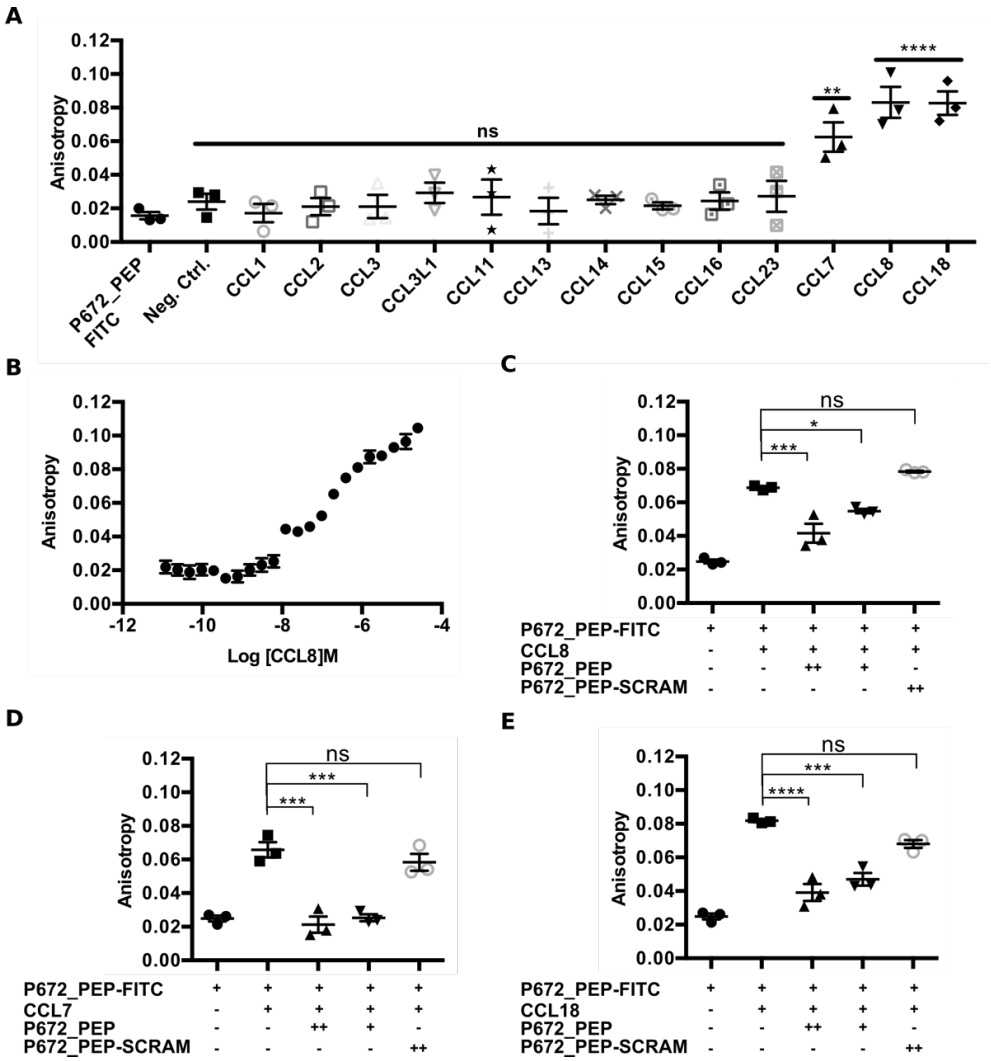


Figure 5.7 Fluorescence polarisation characterisation of P672_PEP and P672_PEP-FITC. **A.** Fluorescence polarisation assay showing binding of chemokines to P672_PEP-FITC. The measured fluorescence anisotropy (y-axis) of P672_PEP-FITC (50nM) following binding to a fixed dose (1μM) of the indicated chemokine, CXCL1 served as the negative control. Experiment carried out in triplicate with each experiment performed in duplicate. Mean of three independent experiments and SEM are shown. Statistical significance was determined using one-way ANOVA with Sidak's correction for multiple comparisons using Graph Pad Prism 6. **= p<0.005, ****=P<0.00005, ns= not significant. **B.** Fluorescence polarisation assay showing different concentrations of CCL8 binding to P672_PEP-FITC (50nM). The x-axis shows CCL8 concentration in log_{10}M, and Y-axis the resulting fluorescence anisotropy. **C.** Competition experiment of P672_PEP and P672_PEP-FITC with CCL8. **D.** Competition experiment of P672_PEP and P672_PEP-FITC with CCL7. **E.** Competition experiment of P672_PEP and P672_PEP-FITC with CCL18. For C, D and E three independent data points are displayed where each experiment was carried out in technical triplicate. The mean and SEM are shown. Statistical significance was determined using one-way ANOVA with Sidak's correction for multiple comparisons using Graph Pad Prism 6. *= p<0.05, ***=P<0.0005, ****=P<0.00005, ns= not significant.

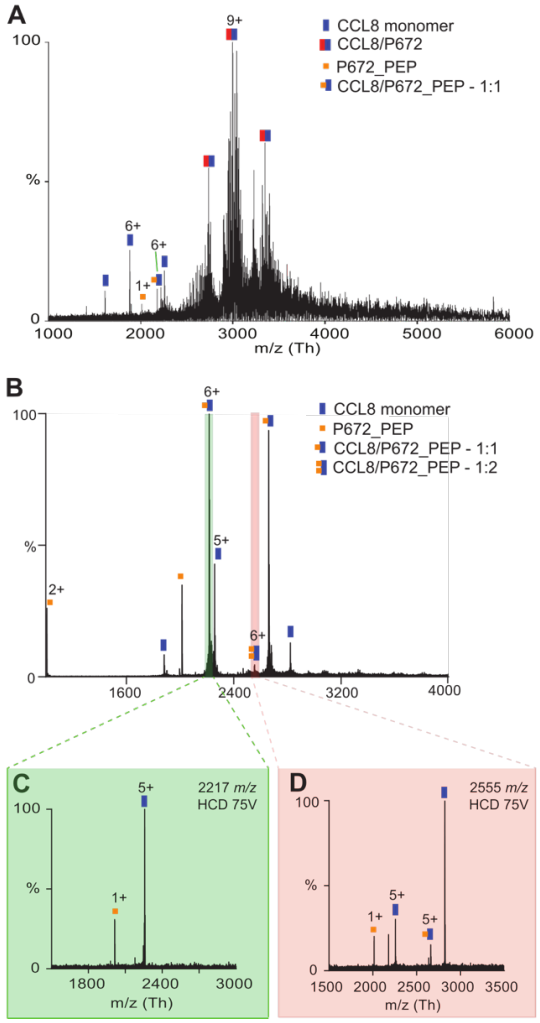


Figure 5.8 Characterisation of P672_PEP binding to CCL8 by non-denaturing mass spectrometry. **A.** In-solution dissociation of P672/CCL8 heterodimer in the presence of P672_PEP. **B.** In-solution dissociation of CCL8 dimer and further binding of CCL8 to one and two P672_PEP. Confirmation of CCL8/P672_PEP complexes by HCD gas-phase dissociation of isolated precursor ions: **C.** 2217 m/z corresponding to CCL8/P672_PEP (1:1) and **D.** 2555 m/z corresponding to CCL8/P672_PEP (1:2). Buffers contained up to 0.5% DMSO. All analyses were performed in triplicate. This work was completed by Dr Lucia Geis-Asteggiante.

5.3.5 Cell based characterisation of P672_PEP

To determine if P672_PEP could inhibit CCL8 binding to its target receptors a fluorescent-ligand/receptor blocking assay was used. This involved incubation of THP-1 cells with fluorescent CCL8 (CCL8-647) and the binding of this chemokine to its cognate receptors was measured by fluorescent assisted cell sorting (FACS). CCL8-647 was able to produce an increase in the median fluorescence intensity

(MFI) of the cells (fig. 5.9). When CCL8-647 was incubated with P672_PEP-SCRAM (60μM) prior to incubating it with the cells there was no change in the MFI but when P672_PEP (60μM) was incubated with CCL8-647 there was a decrease in MFI, indicating the peptide was blocking CCL8-647 binding to the target receptors on THP-1 cells (fig. 5.9). There was a dose dependent increase in the MFI as decreasing amounts of P672_PEP was incubated with CCL8-647, giving an IC_{50} value of 4.9E-06M.

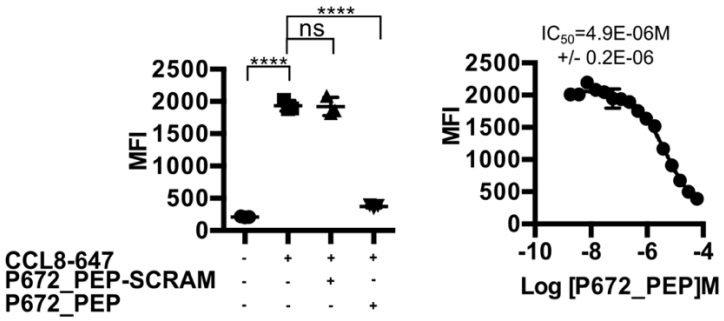


Figure 5.9 Fluorescent ligand blocking assay with P672_PEP. *Left panel* – Control experiments for the assay. CCL8-647 (2.5nM) was incubated with P672_SCRAM (neg. ctrl) or P672_PEP (both at 60μM) and after incubation with THP-1 cells the median fluorescence intensity (MFI) was determined using FACS. Three data points are presented where each data point is the average MFI of one experiment carried out in triplicate. Mean with SEM shown. Statistical significance was calculated using a one-way ANOVA with Sidak's correction for multiple comparisons. ****=P<0.00005, ns= not significant. *Right Panel*- Representative IC_{50} curve for inhibition of CCL8-647 binding to THP-1 cells. Experiment was carried out in triplicate and the mean and SEM are shown. Curve was fit using a four-parameter fit in Graph Pad Prism 6. IC_{50} shown is the average of three independent experiments carried out in triplicate with the SEM shown.

This result indicates that P672_PEP could inhibit the binding of CCL8-647 to its target receptors on THP-1 cells. This would suggest that P672_PEP can prevent CCL8 driven migration as it would prevent the chemokine from binding to and activating its target receptors. To determine if the peptide could functionally inhibit CCL7 and CCL8 a Boyden chamber assay was used to monitor the migration of THP-1 cells in response to these chemokines. CCL7 induced THP-1 migration and this was not affected by preincubation of the chemokine with P672_PEP-SCRAM

(200μM) (fig. 5.10A). However, preincubation of the chemokine with P672_PEP (200μM, 100μM, 50μM) was able to lower CCL7 driven THP-1 migration in a dose dependent fashion. However, 200μM did not lower migration to background levels so it was not possible to fit an IC_{50} curve to this data. CCL8 induced THP-1 migration and this was also not affected by preincubation of this chemokine with P672_PEP-SCRAM (60μM) (fig. 5.10B). However, preincubation of CCL8 with P672_PEP (60μM) was able to lower CCL8 driven THP-1 migration to background levels, allowing for an IC_{50} of 3.39E-07M to be determined for this peptide against CCL8 (fig. 5.10B). These data indicate that P672_PEP is active in a cell-based assay as it is able to inhibit CCL7 and CCL8 driven THP-1 migration.

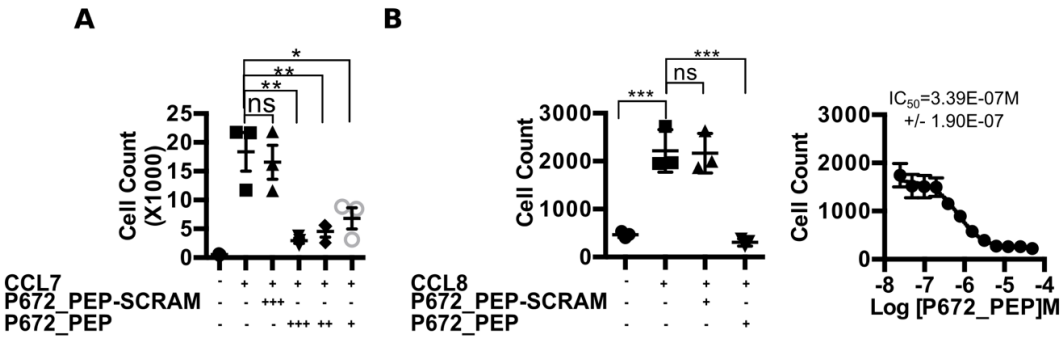


FIGURE 5.10 Cell based characterisation of P672_PEP. **A.** Effect of P672_PEP on CCL7 driven THP-1 migration. CCL7 (7.55nM) was incubated with P672_PEP or P672_PEP-scram (+++ = 200μM, ++ = 100μM, + = 50μM) and the migration of THP-1 cells in response to this chemokine monitored using a Boyden chamber assay. Experiment was carried out in biological triplicate where each data point is the average of a single experiment carried out in technical triplicate. Data was analysed using a one-way ANOVA with Sidak's correction for multiple comparisons. *= $p<0.05$, **=$P<0.005$, ns= not significant. **B.** Effect of P672_PEP on CCL8 migration. *Left Panel* – Control experiments for CCL8 migration. CCL8 (5.75nM) was incubated with P672_PEP or P672_SCRAM (+ = 60μM) and the migration of THP-1 cells in response to this chemokine monitored using a Boyden chamber assay. Experiment was carried out in biological triplicate where each data point is the average of a single experiment carried out in technical triplicate. Data was analysed using a one-way ANOVA with Sidak's correction for multiple comparisons. ***=$P<0.0005$, ns= not significant. *Right panel* – Representative IC_{50} curve for P672_PEP on CCL8 migration. Experiment was carried out in technical triplicate and the curve fit using a four-parameter fit in Graph Pad Prism 6. IC_{50} value is the average of three independent experiments carried out in triplicate with SEM shown

5.4 DISCUSSION

Nature has provided a wealth of biologically active compounds that have inspired the development of countless therapeutics[242]. What is particularly important is not only knowing what the natural product binds to but also how it interacts with its target. Understanding these facets of natural product efficacy leads to a detailed understanding of the mechanism of action of a natural compound, which can in turn encourage the development of entities that have novel mechanisms of action that have been inspired by these insights. In this work, hydrogen-deuterium exchange mass spectrometry (HDX-MS) was used to characterise the P672/CCL8 complex. The knowledge garnered here was then used to aid in the design of multiple chemokine binding peptides. HDX-MS presents a powerful tool for the characterisation of protein-protein interactions as it requires much less sample than other techniques, such as protein crystallography and NMR, that are routinely used to gain structural information on protein complexes. Nonetheless, previous efforts to characterise evasin chemokine interactions have involved crystallisation of the Evasin-1/CCL3 complex and homology modelling of the Evasin-4/CCL3 complex[159,160]. This revealed that Evasin-1 and Evasin-4 use different binding modalities to bind their target chemokines with Evasin-1 using residues at its N and C termini and Evasin-4 primarily uses residues only at its N-terminus. In the previous chapter the domain swap experiment carried out suggested that P672 used a similar binding mechanism as Evasin-4 as the N-terminal 44 residues in P672 represent a CCL8 binding domain. Gratifyingly, the HDX-MS result presented here provides some validation for the work in the previous chapter as the area most heavily protected from deuterium uptake in P672 was Y21-F32, a sequence which formed part of the transplanted domain in chapter 4. Moreover, transplantation of

only these residues in the Evasin-1 sequence yielded a hybrid evasin that represents only 7% of the P672 sequence which was still able to bind and neutralise CCL8. This provides further evidence that this region is involved in binding and neutralising this chemokine. Interestingly, protection from deuterium uptake was maintained for residues F23-C30 and F32 even after one hour, suggesting that P672 latches onto CCL8 and does not release it. Further experiments used to validate the HDX-MS result involved mutation of two of the residues in this protected region to alanine and then testing these for binding to CCL8. P672_Y31A and P672_F32A both had reduced affinities for CCL8 compared to P672_WT, suggesting that these residues are at the complex interface. The decrease in affinity for CCL8 was primarily due to changes in the dissociation rate constant as the association rate constant remained largely unchanged for the mutant proteins when compared to P672_WT. For P672_WT the dissociation rate constant was 5.11E-04 s^{-1} whereas for the P672_Y31A and P672_F32A this increased by over a factor of ten becoming 1.05E-03 s^{-1} and 1.32E-03 s^{-1} respectively. This equates to the retention time of the P672/CCL8 complex decreasing from 22 minutes for P672_WT to 11 minutes for P672_Y31A and 8 minutes for P672_F32A. This increase in dissociation rate constant suggests that these residues are primarily involved in stabilising the complex rather than being involved with initial complex formation. The importance of these residues in binding CCL8 was further confirmed by the double alanine mutant having a greatly reduced affinity for CCL8, suggesting that the effect of these residues on stabilising the complex is more than additive as the dissociation constant was over 15 times greater when compared to the wild type.

Whilst there was a decrease in affinity for CCL8 by the single point mutants, they still retained a relatively high affinity for this chemokine. These mutants were

also tested for their effect on CCL3 binding, a chemokine that is only distantly related to CCL8. The P672_Y31A mutant had an affinity for CCL3 that was approximately ten times greater than that of wild type, indicating that this residue is possibly interacting with CCL3. Although P672_F32A was shown to bind CCL8 with an affinity that was approximately three times less than that of wild type, it had appeared to lose all binding to CCL3 in the BLI experiments. This suggests that this residue contributes more to CCL3 binding than CCL8 binding and that CCL3 and CCL8 binding had been uncoupled from one another for this mutant. This was evaluated further in a cell migration assay which revealed that P672_F32A was unable to inhibit CCL3 migration at 100nM whereas it was able to block CCL8 migration in a comparable fashion to wild type. This may provide an interesting tool compound that can block CCL8 but not CCL3, which could be useful for delineating the role of specific chemokines in disease states involving the expression of multiple chemokines.

The results described above provide partial validation for the HDX-MS result. It may be possible that other residues apart from Y31 and F32 in the protected region stabilise the interaction with CCL8 or CCL3. However, systematic analysis of PPI interfaces has indicated that tyrosine is present in over 10% of the interfaces analysed and hydrophobic residues, such as phenylalanine, also tend to be over represented at complex interfaces[241]. This over representation may be because the aromatic ring in tyrosine and phenylalanine imparts hydrophobicity and the hydroxyl group in tyrosine has the ability to form hydrogen bonds, which may also explain why this residue tends to be present more at complex interfaces than phenylalanine. The formation of hydrophobic interactions is a particularly potent driving force for protein-protein complex formation as the expulsion of water surrounding the

hydrophobic residues leads to a favourable entropy change upon the two proteins coming together. Thus, the loss of binding affinity observed may be due to the loss of hydrophobicity that occurs when these residues are mutated to alanine. Moreover, the aromatic ring in tyrosine and phenylalanine can also form cation-pi interactions with neighbouring positively charged residues to stabilise the complex. The R18-S27 region of CCL8 contains two arginine residues and one lysine residue that would have a positive charge at physiological pH. It is possible that there is the formation of cation-pi interactions between these basic residues and Y31 and F32 in P672, thereby explaining the effect of the alanine mutants on binding affinities. It is also possible that the hydroxyl group of Y31 is forming a hydrogen bond with these basic residues that is disrupted when this is mutated to alanine, thereby explaining the effect of this mutation. This region in CCL8 also contains several hydrophobic residues, such as leucine, isoleucine and proline, and these may be contributing to the hydrophobic effect outlined above. CCL3 also has an arginine residue at the equivalent position to arginine 18 in CCL8. If the formation of a cation-pi interaction between F32 in P672 and R18 in CCL3 is driving this interaction, then this would explain the loss of binding to CCL3 at all concentrations tested for the F32A mutant. As the loss of binding for P672_F32A was not so pronounced for CCL8, it is likely that there are other residues that are contributing to stabilising P672/CCL8 complex.

Further probing of the HDX-MS result, through the transplantation of the protected residues identified in the HDX-MS experiment into Evasin-1 conferred CCL8 binding and neutralisation to a hybrid evasin, thus providing further validation for this experiment. Notably, the Evasin-1/P672 hybrid evasin did not bind CCL3, a chemokine both P672 and Evasin-1 bind. What this suggests is that possibly in the

hybrid evasin the folding is not optimal for CCL3 binding or in the context of this hybrid evasin these residues alone are not sufficient to bind CCL3. Nonetheless, taken together these results provide suitable validation of the HDX-MS experiment.

The HDX-MS result and the subsequent validation experiments provide some insight into how evasins recognise chemokines and whether there is any conserved mechanism for chemokine recognition across evasins. P672_F32A is a mutant of P672_WT that appeared unable to bind or inhibit CCL3 and when the conserved residue in Evasin-1, F14A, was tested for CCL3 binding it also displayed a reduced affinity for CCL3 and a more than 200x increase in the IC_{50} for this chemokine[159,160]. This phenylalanine is conserved across all evasins identified to date apart from two (fig. 3.2) so the utilisation of a phenylalanine at this position may be common mechanism for targeting CCL3. The P672_Y31A mutant displayed a lower affinity for CCL8 and CCL3 and the double mutant Y28Q/N60D of Evasin-4 was also shown to have a lower affinity for this chemokine. This is of note as Y28 in Evasin-4 is conserved with Y31 in P672[160]. However, the single Evasin-4 alanine mutant of Y28 was not tested so it cannot be said definitively that the conserved tyrosine between these two proteins is used by both of them to bind their target chemokines, but it may play a role. It is interesting to note that this tyrosine is conserved only between Evasin-4 and P672 (fig. 3.2) so this may suggest that they share a common residue to bind their target chemokines that is not shared with other evasins. Despite using a conserved phenylalanine with Evasin-1, P672 is more Evasin-4 like in its binding mechanism. Evasin-4 has been shown to primarily use residues at the N-terminus[160] and the results above suggest that P672 also uses residues primarily at the N-terminus to bind CCL8 and CCL3. This comparison

was highlighted in the last chapter and the data presented here supports this observation.

Chemokine ligand/receptor binding has been studied in detail and the N-terminus of the ligand is involved in receptor activation whilst the N-loop region is involved receptor binding[49,50,52]. The HDX-MS result suggested that P672 interacts with residues R18-S27 of CCL8. These residues are in the N-terminal loop region of CCL8 suggesting that P672 targets the receptor binding domain of CCL8, thereby preventing the interaction of the ligand with its target receptors. This result supports the observation in the previous chapter that P672 is able to prevent the binding of CCL8-647 to chemokine receptors on THP-1 cells (fig. 4.5). Moreover, targeting of the N-terminal loop region appears to be a common attribute that is shared amongst other chemokine binding proteins with P672. For example, the viral chemokine binding protein VV-35kDa targets the K19 and R24 of CCL2[243] and the viral chemokine binding protein vCCI also targets R18 and R24 of CCL2[244]. In addition to this, Evasin-4 was shown to interact with the N-terminal region of CCL5[160]. This common mechanism suggests that these proteins have all convergently evolved a way to target the residues found in this region, and perhaps the N-loop region could be a “hot-spot” to target for designed chemokine inhibitors.

Alignment of all the chemokines that P672 has been shown to interact with (fig. 5.10) shows that several chemokines have a similar homology in this region with CCL8, such as CCL7 and CCL2, whereas there are some chemokines where there is little homology, such as CCL18 and CCL15. All of these chemokines do have at least one basic residue in this region, so it is possible that P672 targets these basic residues. However, one would predict that P672 should bind CCL4 or CCL17 based on this argument, for example, as these chemokines also have basic

residues in this region. However, the BLI cross binding screen indicated that P672 did not interact with these chemokines. What this possibly highlights is the difficulty in predicting what chemokines an evasin will bind to purely based on a 2D sequence. It is possible that the subtle differences in the folding of each chemokine produce the exact binding epitope that P672 is able to recognise.

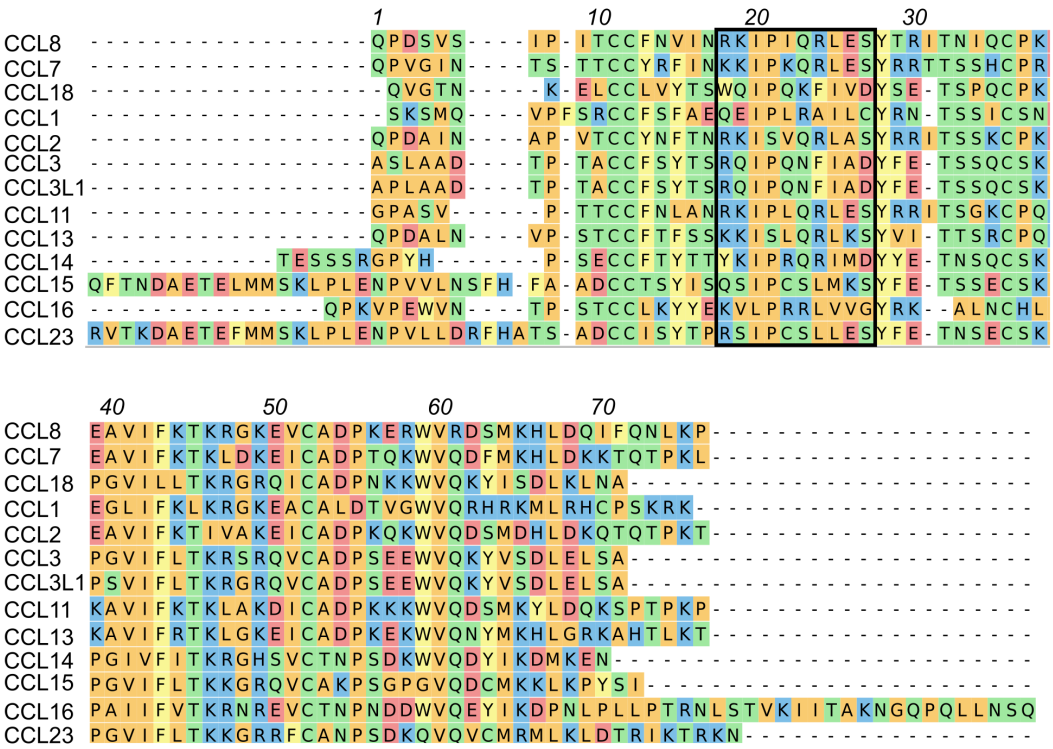


Figure 5.11 Alignment of P672 binding chemokines. Chemokines were aligned using the MUSCLE algorithm. The black box represents the region in CCL8 that was protected from deuterium uptake in the HDX-MS experiment. Amino acid residues are color-coded according to physicochemical properties: yellow, aromatic (F, W, and Y); red, acidic (D and E); blue, basic (R, H, and K); orange, nonpolar aliphatic (A, G, I, L, M, P, and V); green, polar neutral (C, N, Q, and T).

Rationally designed peptides from structural studies of protein complexes have been shown to be able to modulate the activity of a variety of therapeutically relevant targets including receptors, cytokines and transcription factors[245-247]. Additionally, peptides have also been rationally designed to have novel

mechanisms of action, such as tri-agonist activity against receptors that are relevant for metabolic disorders[248]. The structure-based design of chemokine inhibitory peptides based on the chemokine receptor/ligand interaction has proved difficult, possibly due to the challenging nature of performing structural studies with membrane proteins. Consequently, the design of peptides that target the chemokine system has focused on sequence analysis of the chemokine ligands or receptors. For example, a peptide that binds to chemokine receptors and inhibits the binding of multiple chemokines to their target receptors was designed based on the sequence homology of mouse and human CCL2[249]. Sequence alignment of the binding domains of chemokine receptors was also utilised to deliver peptides that can weakly bind and inhibit the action of multiple chemokine ligands[237]. Moreover, epitope mapping of a CCR3 inhibitory antibody using phage display identified peptides that could inhibit the action of the CCR3 ligands CCL11, CCL5, CCL7, CCL8 and CCL24[250]. In this study, the mapping of residues at the interface of a chemokine/evasin complex using HDX-MS allowed for the design of a peptide, P672_PEP, that was able to bind and neutralise CCL8. This shows that through the characterisation of the binding interface of a protein complex using HDX-MS it is possible to design small peptides that maintain a similar function to the larger protein structure. This illustrates that it is possible to integrate HDX-MS into the peptide discovery process. This result also provides strong evidence that it is this region of P672 that is responsible for binding to CCL8 and the peptide binding to CCL8 provides further validation of the HDX-MS result.

The “one-to-many” mechanism that has evolved in nature to neutralise the chemokine network was, serendipitously, observed for P672_PEP as it could also bind CCL7 and CCL18 as well as CCL8. Moreover, this is compelling evidence for

P672 utilising one region to target multiple chemokines and this may inform on the mechanism that P672 adopts for “one-to-many” binding. It is possible that this region may have a “static” complimentary shape for multiple binding partners or this region may have a high degree of structural plasticity thereby allowing for multiple conformations to be adopted to recognise several chemokines[251,252]. CCL7 is a closely related chemokine to CCL8 and shares several conserved residues in the region that P672 was shown to bind in CCL8 (fig. 5.10). It is therefore likely that P672 is adopting one of these mechanisms for CCL7 and CCL8 recognition. However, CCL18 is a part of the MIP family of chemokines and shares little homology to the protected region in CCL8 but was shown to interact with P672_PEP. Another mechanism that has been described for multiple binding partner recognition is to use the same residues to target different regions on multiple binding partners[253]. It may be that this peptide, and P672, bind to CCL18 in a different manner compared to CCL8 yet rely on the same residues. However, to confirm absolutely how P672 is recognising multiple chemokines, structures of multiple P672/chemokine complexes need to be determined.

The testing and design of P672_PEP was motivated by the HDX-MS and domain swap experiment as it was a linear sequence of amino acids that appeared to interact with CCL8 in the HDX-MS analysis, and transplantation of these amino acids into Evasin-1 conferred CCL8 binding and neutralisation. However, the binding of CCL7 and CCL18 by P672_PEP could not have been predicted based on these results. It may have been possible to predict CCL7 binding based on sequence homology to the region in CCL8 that was protected from deuterium uptake upon complex formation. However, this argument would predict that P672_PEP should also bind other members of the MCP family of chemokines, such

as CCL2 or CCL13, as these chemokines also share a high level of homology in this region. However, there was no binding observed to these chemokines at the concentration tested in the FP assay. What may explain the lack of binding to the other P672 target chemokines by P672_PEP at the concentration tested is that this linear peptide retains enough structure to drive favourable binding interactions with CCL7, CCL8 and CCL18, but not to the other chemokines. It is possible that when this sequence of amino acids is taken out of the protein "backbone" of P672 it lacks interactions with other P672 residues that help stabilise the interaction with the other chemokines, hence the lack of binding. It is also possible that P672 uses regions outside this protected area to bind these chemokines, or the affinity for the interaction between P672_PEP and these chemokines is so low, hence why there was no interaction detected in the fluorescence polarisation experiment.

In the previous chapter it was demonstrated using non-denaturing MS that P672 forms a 1:1 heterodimer with CCL8 (fig. 4.1). When performing the fluorescence polarisation binding assay with P672_PEP-FITC and CCL8 the data appeared to be bi-phasic and fit well to a 2:1 binding model. Moreover, the non-denaturing MS of the P672_PEP/CCL8 complex did indeed show that this peptide is binding with a 2:1 P672_PEP: CCL8 stoichiometry. This suggests that the peptide is able to bind at an additional site in P672. However, further work is required to elucidate the exact binding mechanism of the peptide. It is possible to speculate that the R18-S27 P672 binding region of CCL8 identified in the HDX-MS experiment is actually two binding sites, but only one can be occupied at a time by P672. However, as the peptide is much smaller than P672 it is able to bind to both of these sites in CCL8 at the same time, giving rise to the 2:1 stoichiometry that is observed.

Notably, the IC_{50} for the inhibition of CCL8-647 binding to THP-1 cells by P672_PEP is much higher than expected based on the K_d values determined using the fluorescence polarisation assay with P672_PEP-FITC and does not correlate well with the IC_{50} value obtained for the inhibition of CCL8 driven of THP-1 cell chemotaxis by P672_PEP. The lack of correlation between the K_d values and IC_{50} for CCL8-647 binding may be due to P672_PEP-FITC possessing a slightly different affinity to the P672_PEP, therefore resulting in a much higher IC_{50}. A lack of correlation was observed for the K_d and IC_{50} value for CCL8 driven THP-1 cell migration by P672 in the first chapter. This may be observed here as, again, CCL8 is signalling through CCR1 CCR2 and CCR5 on the THP-1 cells and these receptors are known to act synergistically to activate cell migration[207]. P672_PEP may be able to prevent the synergistic effects at a cellular level that occur following binding of CCL8 to its receptors, thereby explain the lack of correlation observed. Moreover, the internalisation and recycling of receptors by the THP-1 cells[179] after CCL8-647 binding may lead to the median fluorescence intensity of the cells not truly representing the number of CCL8-647 molecules bound to the cell. This would mean that more peptide would be needed than expected to totally prevent CCL8-647 binding, thereby explaining the higher IC_{50} value obtained in this experiment.

Hydrogen-deuterium exchange mass spectrometry is a powerful tool for characterising protein-protein interactions due to the low level of sample required and ease of sample preparation[254]. This work has shown that it is possible to characterise an evasin/chemokine interaction using this technique. Moreover, it was shown that it is possible to use the information garnered from these experiments to aid in the design of chemokine binding peptides that possess the “one-to-many” mechanism that has evolved in pathogenic chemokine binding proteins. What this

work shows is that it is possible to integrate HDX-MS into the peptide discovery process to deliver peptides with novel binding properties.

5.5 CONCLUSIONS

In this chapter it has been shown that hydrogen-deuterium exchange mass spectrometry (HDX-MS) can be used to characterise an evasin/chemokine interaction. The result of the HDX-MS studies were validated using a domain swap experiment and site directed mutagenesis of residues predicted to be at the complex interface. The P672_F32A mutant appeared to retain the ability to bind and neutralise CCL8 in a similar fashion to wild type but lost the ability to bind and neutralise CCL3, indicating that CCL3 and CCL8 binding had been uncoupled from one another. From the understanding of the P672/CCL8 interaction gained from the HDX-MS and subsequent validation experiments, a peptide composed of residues 17-32 of P672 was designed and was shown to bind CCL8. This peptide was also shown to bind CCL7 and CCL18. This indicates that these residues in full length P672 are interacting with these chemokines. Moreover, this peptide was able to block CCL8-647 binding to THP-1 cells and was able to inhibit the cell migration of these cells in response to CCL7 and CCL8, showing that this peptide was able to neutralise chemokines in a “one-to-many” fashion. This work has delivered an evasin derived peptide that is able to bind to and neutralise multiple chemokines, suggesting that P672 has discrete regions that are responsible for chemokine recognition. In a broader sense this work has suggested that it is possible to use HDX-MS characterise a PPI interface to aid in the discovery of peptides that go some way to mimicking the function of the larger protein from which they are derived, allowing for peptides with novel mechanisms of action to be discovered.

6 CONCLUSIONS AND FUTURE WORK

6.1 SUMMARY

Evasins are proteins found in tick saliva that are responsible for neutralising chemokine action, thereby allowing the tick to remain on the host for several days to weeks without eliciting an immune response[1]. This may be possible as chemokines are regulators of white blood cell trafficking[185] and inhibition of their activity will prevent an area from becoming inflamed, giving the tick time to draw a decent blood meal. Evasins were initially discovered using an expression cloning approach based on a salivary gland transcriptome library from a single tick species *Rhipicephalus sanguineus* and subsequent experiments identified putative evasins in transcriptome libraries from other species of tick[1,152,162,163]. However, none of these were characterised until a library of putative evasins from several tick species were expressed on the surface of yeast and screened against fluorescent chemokines[164]. This identified ten other evasins that were functionally characterised using biolayer interferometry and cell migration experiments. In addition to this, eight more evasins were identified through the analysis of tick transcriptome libraries and were shown to be active against several chemokines[165].

The work presented here builds upon using a yeast surface display approach to identify functional evasins[164]. This library was screened against CCL8 and this identified the novel evasin P672 (fig. 3.1, 3.2). P672 was shown to bind CCL8 along with a number of other CC class chemokines, with the exact binding profile being determined by the location of a purification tag (fig. 3.5). P672 was also shown to be able to inhibit chemokine driven cell migration in THP-1 cells (fig. 3.7). Crucially, P672 binds multiple chemokines. Chemokines signal through a network with a

series of “one-to-many” interactions driving the chemokine response. This robust network may protect the chemokine system from being inhibited through the use of agents which target only a single a chemokine, such as monovalent antibodies. This may explain the failure of several compounds and antibodies in the clinic that target single chemokines for inflammatory disorders. Moreover, multiple chemokine binding proteins have convergently evolved in viruses and parasitic worms, suggesting that the targeted inhibition of multiple chemokines is nature’s mechanism for overcoming the chemokine response. This feature may be pertinent to the design of anti-chemokine therapeutics. As monovalent therapies targeting chemokines have failed in the clinic, perhaps investigating agents, such as evasins, that can target multiple chemokines may present a route to a new treatment for inflammatory disorders where chemokines are implicated.

Characterisation of the P672/CCL8 complex using non-denaturing and homology modelling aided in the identification of a chemokine binding domain in P672. Non-denaturing mass spectrometry showed that P672 and CCL8 form a 1:1 heterodimer (fig. 4.2). This allowed for the construction of a homology model of P672 in complex with CCL8 based on the Evasin-1/CCL3 complex. (fig. 4.3) The P672/CCL8 model suggested that it was a contiguous segment at the N-terminus of P672 that was forming contacts with CCL8. The corresponding residues in Evasin-1, an evasin which does not bind CCL8, were swapped with the first 44 N-terminal residues of P672 to give a hybrid protein that contained the putative CCL8 binding domain from P672 at the N-terminus and Evasin-1 at the C-terminus (fig. 4.6). This hybrid protein was found to bind CCL8 and CCL18, and to also functionally inhibit CCL8 (fig. 4.8, 4.9). This revealed that P672 possess a distinct CCL8 binding domain that can confer binding to other evasins.

The P672/CCL8 complex was further characterised using hydrogen deuterium exchange mass spectrometry (HDX-MS). This suggested only a contiguous 12 amino acid segment at the N-terminus of P672 was in contact with the N-terminal loop region of CCL8 (fig. 5.1, 5.2). This region in CCL8 is responsible for receptor binding so P672 most likely binds to this region and prevents CCL8 from binding its target receptors, thereby annulling CCL8 signalling. Moreover, transplanting only these residues into Evasin-1 yielded a hybrid protein that was able to bind and neutralise CCL8, providing some validation for the HDX-MS result (fig. 5.3). Further exploration of the HDX-MS result was achieved through evaluating alanine mutants of residues predicted to be at the complex interface for their effect on CCL8 binding. P672_Y31A and P672_F32A were shown to have a reduced affinity for CCL8, as did a P672_Y31A; F32A double mutant. P672_Y31A was also found to have a reduced affinity for CCL3 and P672_F32A appeared to lose all binding to CCL3 at the concentrations tested (tables 2 and 3). Moreover, P672_F32A was able to block CCL8 migration with a slightly higher IC50 than P672 but was totally unable to block CCL3 at 100nM, whereas wild type P672 was able to completely block migration induced by this chemokine at this concentration (fig. 5.5). These results indicate that for P672_F32A CCL3 and CCL8 binding and function had been uncoupled from one another. These validation experiments motivated the synthesis of a linear peptide composed of resides 17-32 in P672 as these residues were shown to be protected from deuterium uptake and were also conserved in the Evasin-1/P672 hybrid that was able to bind CCL8. This peptide was shown to bind CCL8 as well as CCL7 and CCL18, indicating that it had partially retained the “one-to-many” binding mechanism that is associated with evasins (fig. 5.6). Interestingly, this peptide was found to bind CCL8 with a 2:1 stoichiometry (fig.

5.8), which is in contrast to the 1:1 stoichiometry that was determined for the P672/CCL8 complex (fig. 4.2). Importantly, P672_PEP was found to block CCL7 and CCL8 driven THP-1 migration in a dose dependent fashion (5.10). This revealed that it is possible to characterise the P672/CCL8 complex interface using HDX-MS and this can inform on the design of multiple chemokine binding peptides, thereby integrating HDX-MS into the peptide discovery process.

6.2 Conclusions

This work has shown that it is possible to screen a library of yeast expressing putative evasins on their cell surface against the chemokine CCL8 to identify a functional evasin termed P672. The work described in Chapter 3 revealed that P672 was able to bind and neutralise multiple CC class chemokines with its selectivity modulated by the location of a purification tag. Moreover, the work detailed in Chapter 4 showed that P672 possessed a CCL8 binding domain that could be transferred to another evasin to impart chemokine binding. In Chapter 5, hydrogen-deuterium exchange mass spectrometry was used to characterise the P672/CCL8 interaction. The results from this experiment enabled the design of a multiple chemokine binding peptide, P672_PEP, that was able to bind CCL7, CCL8 and CCL18. This work has shown that through the detailed understanding of a protein-protein interaction it is possible to design a peptide that can, to some extent, mimic the function of the parental protein. This could have implications for the identification and design of therapeutic peptides in the future.

6.3 FUTURE WORK

P672 is a new evasin that was identified from a screen of a library of yeast expressing putative evasins on the cell surface against CCL8. This library contained over 350 putative evasins, of which approximately 15 have been characterised in detail to date. This leaves over 300 putative evasins in this library which are to be characterised. This library could be screened against other chemokines to identify chemokine binders or the putative evasin sequences could be expressed individually and characterised outright. This would reveal the evasin “interactome” which may inform on the evolution of evasins and may identify evasins with novel chemokine selectivity.

Characterisation of the P672/CCL8 complex interface showed that P672 possess a CCL8 binding domain and this subsequently allowed for the generation of hybrid evasins and multiple chemokine binding peptides, as described in Chapters 4 and 5. Characterisation of P672 in complex with other chemokines may reveal that there are other domains in P672 that are responsible for chemokine binding which could possibly allow for the identification of other chemokine binding domains to subsequently allow for the development of more multiple chemokine binding peptides. To achieve this, HDX-MS could be used to characterise P672 in complex with other chemokines to identify residues at the complex interface.

P672_PEP identified in Chapter 5 was shown to bind CCL8 with a 2:1 stoichiometry (fig. 5.8). This is in contrast to P672 which was shown in Chapter 4 to bind CCL8 with a 1:1 stoichiometry (fig. 4.2). Further work is required to determine exactly how P672_PEP is binding CCL8 and whether it is binding to CCL8 at the

same site as P672. Experiments to elucidate this binding mechanism could include HDX-MS, protein crystallography or NMR of the protein/peptide complex.

P672_PEP partially retained the “one-to-many” binding mechanism present in P672, as shown by a fluorescence polarisation assay in Chapter 5 (fig. 5.6). As a consequence of this P672_PEP may be active *in vivo* in inflammatory models of disease. However, linear peptides are rapidly degraded *in vivo* so before this can happen it needs to be optimised for metabolic stability. Approaches to improve the metabolic stability of a peptide can include cyclisation, unnatural amino acid incorporation and methylation of the nitrogen in the peptide backbone. Before these modifications can be made, the amino acid positions in P672_PEP that can tolerate being modified need to be determined. This can be elucidated through the screening and testing of alanine point mutants of the peptide. It would also be interesting to know if shorter variants of the peptide are still able to bind and neutralise CCL7, CCL8 and CCL18. Conversely, it was also be informative to determine if slightly longer variants of the peptide gained further chemokine binding functionality or a higher affinity for its target chemokines. Once the optimal peptide length and possible modification sites have been determined, peptide binding and metabolic stability can be readily optimised. Once this optimisation is complete, this peptide can then be evaluated using *in vivo* models of inflammatory disease.

Proteins and peptides can be used as therapeutics; however, the main-stay of the pharmaceutical industry is small molecules. Conversion of P672_PEP into a peptidomimetic would deliver a small molecule with a mechanism of action inspired by nature, namely the ability to bind to and neutralise multiple chemokines. This could be achieved through rational design by obtaining a crystal or NMR structure of the peptide bound to CCL8 and then using this to guide the design of small

molecules the neutralise CCL8 function. Another approach may be to screen a library of small molecules to identify a molecule capable of displacing P672_PEP-FITC from CCL8 using a fluorescence polarisation displacement assay. This could lead to the identification of a molecule that can occupy the same chemical space as P672_PEP and if this were true this molecule would retain the ability to bind multiple chemokines. This would deliver a small molecule that mimics evasin function which, in turn, would be mimicking nature's approach to neutralise the chemokine network.

7 MATERIALS AND METHODS

7.1 MATERIALS

7.1.1 CHEMICALS, OLIGONUCLEOTIDES AND ENZYMES

Chemicals were purchased from Sigma or Scientific Laboratory Supplies. Restriction enzymes were purchased from New England Biolabs or Thermofisher and chemokines were purchased from Peprotech. Alexa-647 labelled chemokines were purchased from Almac. Custom oligonucleotides were purchased from Sigma or Thermofisher.

7.1.2 PEPTIDE SYNTHESIS

Peptides were purchased from GL Biochem (Shanghai) and were synthesised using standard Fmoc solid phase synthesis to give peptides with a C-terminal amide. They were all deemed to be >90% pure by HPLC analysis and verified by LC-MS by GL Biochem. Peptides were dissolved in DMSO and the concentration determined using NMR with TSP as an internal standard[255].

7.1.3 CELL LINES

HEK293F and THP-1 cells were used in this work. HEK293F cells were propagated as suspension cultures maintained at $0.3x10^6$ cells/ml in FreeStyle™293F media. The THP-1 cell line was propagated as a suspension culture maintained at $0.3x10^6$ cells/mL in RPMI-1640 + 10% heat inactivated FCS + 4mM L-glutamine. THP-1 cells were maintained in a 37°C, 5% CO_2 humidified chamber; HEK293F cells were maintained in a 37°C, 8% CO_2 humidified chamber

with 130RPM shaking of the culture flask. Cells were frequently mycoplasma tested using the MycoAlert test kit (Lonza).

7.1.4 Plasmid and PCR product preparation kits

Qiagen miniprep and endofree maxi prep kits were used for the isolation of plasmid DNA according to the manufacturer's instructions. PCR products were either gel purified or PCR purified using the Qiagen gel extraction kit or Qiagen PCR purification kit following the manufacturer's instructions.

7.2 Methods

7.2.1 PCR

Polymerase chain reactions were performed using Phusion polymerase (Thermofisher) using the manufacturer's instructions. PCR primers were all designed to have an annealing temperature of 60°C. An initial denaturing step at 98°C for 30 seconds was performed followed by 30 cycles of 98°C denaturation (10 seconds), 60°C annealing (30 seconds) and 72°C extension (typically 30 seconds). A final extension step was performed for five minutes followed by a 4°C hold. The extension step was increased or decreased depending on the size of the PCR product.

7.2.2 Transformation

DH5-α (Invitrogen) *E. coli* were used for plasmid propagation. Chemically competent DH5-α *E. coli* were thawed on ice and incubated with 50ng of the plasmid

to be transformed for 30 minutes on ice. These cells were then heat shocked for 45 seconds at 42°C and then placed on ice for one minute. 1mL LB media was then added to the cells and they were incubated for one hour at 37°C with vigorous shaking. The cells were then spun down, the media removed, resuspended in 50µL fresh LB media, plated on agar plates with the appropriate antibiotic and incubated overnight at 37°C.

7.2.3 Agarose gel electrophoresis

DNA fragments were typically analysed with a 1% agarose gel. 150mL TAE buffer (Tris-acetate-EDTA buffer. 40mM Tris, 20mM acetic acid, 1mM EDTA, pH 8.3) was combined with 1g agarose and heated until the powder had dissolved. The gel was set, DNA loaded, DNA bands separated with a potential difference of 130V for 45 minutes and visualised under UV light.

7.2.4 SDS-PAGE Electrophoresis

SDS-PAGE was performed using 12% Bolt Bis-Tris Plus Gels (Thermofisher) using the manufacturer's instructions. Protein gels were ran using MES running buffer (Thermofisher) for 23 minutes at 200V. Gels were then washed with water, stained with colloidal Coomassie blue for four hours and then washed in water overnight.

7.2.5 Expression vector construction

N and C terminally tagged P672 mammalian expression vectors were constructed in the pHLSec expression plasmid[195] using PCR and in-fusion cloning (clontech) following the manufacturer's instructions. The purification tags were

either an N-terminal His8-StrepII protein purification tag (HHHHHHHHSAWSHPQFEKGGGGS) or a C-terminal StrepII-His8 protein purification tag (TGGGGGSGGGGSGGASAWSHPQFEKLEHHHHHHHH). Following signal peptide cleavage, an additional ETG sequence was expected at the N terminus of each protein. P672-Evasin-1 hybrids and Evasin-1 expression plasmids were made by PCR and infusion cloning into pHLSec.

The CCL8 expression plasmid was constructed by PCR amplification of a SUMO-CCL8 cassette and ligation-independent cloning[256] into the vector pNIC-BIO3 (a gift from Dr Nicola Burgess-Brown) to create a HIS6-SUMO-CCL8 expression vector with a GSKGGYGLNDIFEAQKIEWHE C-terminal tag.

7.2.6 SITE DIRECTED MUTAGENESIS

P672 alanine mutant expression vectors were constructed using the overlap extension using the polymerase chain reaction method[257]. Briefly, two PCR reactions were performed where the products would have complimentary 3' and 5' overhangs. Within these complimentary regions the alanine mutation would be introduced (alanine codon ggc). The two fragments were then purified using the Qiagen PCR purification kit, joined together using PCR and the resulting PCR products purified as before and ligated into pHLSec using the in-fusion method as above. All plasmids containing mutations had their sequence confirmed through Sanger sequencing (Source Bioscience, UK).

7.2.7 YEAST SURFACE DISPLAY

Yeast surface display screening was performed as described previously[164]. Briefly, EBY100 yeast transformed with putative evasin library plasmids were

induced with galactose to drive expression of the surface-displayed protein, labelled with biotinylated CCL8 (Almac) and streptavidin–Alexa Fluor 647, and then sorted using FACS; cells non-specifically binding streptavidin-AF647 were excluded using a sorting gate. Sorted cells were regrown, and a second round of sorting was performed following which cells were plated at low dilution to recover individual clones. Individual yeast clones were retested by FACS to confirm CCL8 binding. Inserts from plasmids isolated from the individual clones were then PCR-amplified and sequenced to identify the cloned evasin.

7.2.8 SEQUENCE ANALYSIS

MUSCLE in Megalign Pro (DNAStar, version 12.3.1, DNAStar Inc.) was used to construct the CKBP and chemokine sequence alignments and generate sequence similarity–based phylogenetic trees. Glycosylation sites were predicted using NetNGlyc1.0 (http://www.cbs.dtu.dk/services/NetNGlyc/) and NetOGlyc4.0 (http://www.cbs.dtu.dk/services/NetOGlyc/). The molecular weight and pI of proteins were calculated at ExPASy (http://web.expasy.org/compute_pi/).

7.2.9 PROTEIN EXPRESSION IN MAMMALIAN CELLS

HEK293F cells were placed a density of $0.7x10^6$ cells/mL in 80mL of Freestyle™ 293 expression medium (ThermoFisher) and left overnight. The following day the cells were diluted to $1x10^6$ cells/mL and transiently transfected using polyethylineimine and cultured at 37°C, 8% CO_2, with 130RPM shaking for 5 days. Proteins were purified from filtered supernatants by gravity flow through Nickel charged IMAC Sepharose 6 Fast Flow resin (GE Healthcare), equilibrated with binding buffer (20 mM $NaPO_4$, 500 mM NaCl, pH 7.4), washed after binding with

wash buffer (20 mM $NaPO_4$, 1 M NaCl, 20 mM imidazole, pH 7.4) and eluted in elution buffer (20 mM $NaPO_4$, 500 mM NaCl, 500 mM imidazole, pH 7.4). Elutions were concentrated using an Amicon Ultra-15 Centrifugal Filter Unit with Ultracel-3 membrane (Millipore), and purified by size exclusion chromatography on an AKTA Start system using HiLoad 16/600 Superdex 75 (GE Healthcare), in SEC buffer (phosphate buffer saline (Sigma), with 150mM NaCl). Fractions showing absorption at 280 nm were analysed by electrophoresis on a 12% SDS-PAGE gel and stained with colloidal Coomassie. Fractions containing the protein were combined, concentrated, snap frozen and stored at -80°C.

7.2.10 PROTEIN EXPRESSION IN *E.COLI*

Human CCL8 (residues Gln-24 to Pro-99) was expressed in *Escherichia coli* RosettaGami™ 2 (DE3) cells (Novagen). Cells were grown at 37°C overnight in LB medium containing chloramphenicol (25 µg/ml), tetracycline (10 µg/ml), and kanamycin (50 µg/ml). This culture was then diluted 1 in 30 into Terrific Broth containing kanamycin (50 µg/ml) and grown at 37°C until an A600 of 0.8 was reached, at which point isopropyl 1-thio-β-D-galactopyranoside was added to a final concentration of 1 mM and the culture was incubated overnight at 18°C. Cells were pelleted by centrifugation (4000 × g), and the resulting pellet was frozen and stored at −80°C. A 10-g pellet was suspended in sonication buffer (20 mM NaH_2PO_4, 500 mM NaCl, and 1 mM phenylmethylsulfonyl fluoride, pH 7.4) and sonicated on ice to lyse the cells. The soluble and insoluble fractions were separated by centrifugation (31,000 × g, 45 minutes), and the soluble fraction was filtered and loaded by gravity flow through nickel-charged IMAC Sepharose 6 Fast Flow resin (GE Healthcare), equilibrated with binding buffer (20 mM NaH_2PO_4, 500 mM NaCl, pH 7.4), washed

after binding with wash buffer (20 mM NaH_2PO_4, 1 M NaCl, 20 mM imidazole, pH 7.4), and eluted in a 4-ml elution buffer (20 mM NaH_2PO_4, 500 mM NaCl, 500 mM imidazole, pH 7.4) dropwise into a 20-ml cation exchange buffer (20 mM NaH_2PO_4, 100 mM NaCl, pH 7.4). SUMO protease (Ubl-specific protease from *Saccharomyces cerevisiae*, a gift from Dr. Ritika Sethi) was added (final concentration, 50 µg/ml) to the diluted elution and left overnight at 30°C. The cleaved protein mixture was loaded onto a HiTrap Capto S 1-ml cation exchange column (GE Healthcare) pre-equilibrated in cation exchange buffer (20 mM NaH_2PO_4, 100 mM NaCl, pH 7.4) using an AKTA start. The column was then washed with 5% elution buffer (20 mM NaH_2PO_4, 1 M NaCl, pH 7.4) and the protein eluted with a step elution of 50% elution buffer in 1-ml fractions. The cleaved chemokine was purified to homogeneity using size exclusion chromatography (Sephadex 16/600, GE Healthcare) pre-equilibrated in a final buffer consisting of 20 mM HEPES, 500 mM NaCl, pH 7.4.

7.2.11 DEGLYCOSYLATED PROTEIN PRODUCTION

The glycosylated protein precursor was prepared as described above except that upon transfection of the cells kifunensine was added to a final concentration of 7.5 µg/ml. Purified glycosylated protein was concentrated, and the solution was diluted 1:1 with 40 mM HEPES, 300 mM NaCl, and 1 mM TCEP. PNGaseF (New England Biolabs) and Endo F1 (a gift from C. Siebold, Division of Structural Biology (STRUBI), University of Oxford) was added to 2 mg of glycosylated P672 at a ratio of 1:1000 and incubated overnight at 37 °C. Degylcosylated protein was then separated from glycosylase enzymes by size exclusion chromatography into 20 mM HEPES, 150 mM NaCl, and 0.5 mM TCEP. Fractions showing absorption at 280

nm were analysed by electrophoresis on a 12% SDS-PAGE, which was stained with colloidal Coomassie.

7.2.12 MS/MS SAMPLE PREPARATION

P672 was deglycosylated using PNGaseF and Endo-F1. The deglycosylated P672 was reduced with dithiothreitol, alkylated using iodoacetamide and digested with trypsin or neutrophil elastase. Peptide aliquots from tryptic digests (n=3) were analysed by LC-MS/MS using an Easy-nLC 1000 coupled to an Orbitrap-LTQ-XL (Thermo Fisher Scientific). Peptides were desalted and concentrated by a C18 PepMap 100 trap (300um x 5mm, 5um particle size, 100 Å) and separated by a C18 Acclaim PepMap RSLC column (75 um x 250 mm, 2um particle size, 100Å) using a linear gradient from 0 to 80% acetonitrile:H2O with 0.1% formic acid during 25 min at a flow rate of 300 nL/min. For samples run in the orbitrap-LTQ-XL, precursor ions were acquired at a mass resolution of 60,000 (m/z 400) and product ions were acquired in the ion trap. The 5 most intense precursor ions of charge ≥2 were selected for fragmentation by collision induced dissociation (35V) and dynamic exclusion settings allowed a precursor to be selected up to 3 times in a period of 30s prior to be excluded for 60s. A peptide aliquot (n=1) from an elastase digest was analysed using a Q Exactive mass spectrometer coupled with a Dionex Ultimate 3000 UPLC. Samples were desalted online (PepMap C18, 300µm x5mm, 5 µm particle size) for 1 minute at a flow rate of 20 µl/min and separated on a nEASY column (PepMap C18, 75 µm x 500mm, 2 µm particle size) over 60 Minutes using a gradient of 2%-35% acetonitrile in 5% DMSO/0.1% Formic acid at a flow rate of 250nL/min. Survey scans were acquired at a resolution of 70,000 @ 200m/z, and the 15 most abundant precursors of charge between 2 and 7 were selected for HCD

fragmentation (35V) and dynamic exclusion parameters were set in order to select a precursor ion once prior to be excluded for 60s.

7.2.13 MS/MS DATA ANALYSIS

Data files were analysed using Proteome Discoverer 2.2 (Thermo Fisher Scientific) with the search engine SEQUEST HT against a custom-made sequence database including RHIPU-P672 protein sequence and a list of typical contaminant proteins (246 entries). Precursor and product ion tolerances were set to 20 ppm and 0.6 Da and up to 2 missed cleavages were allowed. Carbamidomethylation was required as a static modification, and deamidation of asparagine present in N-X-S/T motif, oxidation of methionine, and HexNAc in Asn residues were considered as variable modifications. The presence of 2 unique peptides with false discovery rate FDR ≤ 1% and PTM site probability threshold ≥ 75 were required for identification and modification site location. Manual inspection of precursor and product ion spectra was performed in order to confirm the sequence fragmentation patterns observed.

7.2.14 NON-DENATURING MASS SPECTROMETRY STUDIES

Studies on P672, CCL8 and P672/CCL8 complex - All samples were analyzed under non-denaturing conditions using a modified Q Exactive mass spectrometer (ThermoFisher Scientific) for high-mass range measurements. CCL8 was buffer-exchanged into 200 mM ammonium acetate solution (pH 6.5), and deglycosylated P672 was buffer-exchanged into 50 mM ammonium bicarbonate buffer (pH 6.5). The proteins were initially analyzed separately using a capillary voltage of 1.2 KV and a source temperature of 100 °C. In the case of deglycosylated P672, 50 V of source-induced dissociation (SID) was added to improve desolvation.

The CCL8 protein sequence was characterized from its monomers by increasing the source temperature to 200 °C and adding 30 V of SID. The two major precursor ions of CCL8 monomer, *m*/*z* 2257 and *m*/*z* 2821, were selected with an isolation window of 5 *m*/*z* and fragmented using several acceleration voltages (80, 100, 150, and/or 180 V) of HCD. All precursor and fragment ions were acquired using a mass resolution of 60,000 with an average of 3 microscans and a signal-to-noise threshold of 3. The Xtract algorithm from Xcalibur 3.0 software (Thermo Fisher Scientific) was used to determine the decharged masses of the observed ions, which were then inserted into ProSight Lite (http://prosightlite.northwestern.edu) for identification of putative post-translational modifications within a precursor and product ion tolerance of 10 ppm. Aliquots of CCL8 and deglycosylated P672 were mixed in a 1:1 ratio to reach a final concentration of 2.5 µM and incubated for 1 h at 4 °C. The mixture was analyzed using the following parameters: capillary voltage of 1.2 KV, source temperature of 130 °C, and 60 V of SID. The most intense charge state was isolated with a 100 *m*/*z* isolation window and dissociated using 100 V of HCD. In this case, precursor and dissociated products were acquired using a mass resolution of 17,500 and 60,000, respectively. Moreover, 2:1 and 3:1 ratios were also evaluated. All measurements were done in triplicate.

Studies on P672, CCL8 and P672_PEP - Protein-protein interaction studies were carried out under non-denaturing conditions using a modified Q-Exactive mass spectrometer (Thermo Fisher Scientific) for high-mass range measurements as previously reported[258]. Briefly, CCL8 was buffered exchanged into 200 mM ammonium acetate solution (pH = 6.5) and deglycosylated P672 was buffer exchanged into 50 mM ammonium bicarbonate buffer (pH = 6.5). Aliquots of CCL8 and deglycosylated P672 were mixed in a 1:1 ratio to reach a final concentration of

5 µM and incubated for 1 h at 4°C31. The P672_PEP obtained in dimethyl sulfoxide (DMSO) was added to the CCL8/P672 complex at levels of 5, 10 and 15µM to reach 1:1, 1:2 and 1:3 CCL8/P672 : P672_PEP ratios. Similarly, this procedure was repeated for CCL8 dimer adding unlabelled P672_PEP and fluorescein labelled P672_PEP-FITC peptide to reach a 1:1 ratio. Note that in all cases no more than 0.5% DMSO was present in the final mixture. In order to evaluate the effect of DMSO in CCL8 dimer and CCL8/P672 complex stability, control samples using 0.5% DMSO were analysed.

Samples were analysed using the following parameters: capillary voltage of 1.2 KV, source temperature of 50°C and 60 V of source induced dissociation (SID). Dissociation studies were carried out by selecting the most intense charge state with a 25 m/z isolation window and dissociating the complexes using 35 or/and 55 V of higher-energy collisional dissociation (HCD). For CCL8/P672 complexes, precursor ions and dissociated products were acquired using a mass resolution of 17500 and 60000, respectively. For CCL8/P672_PEP and CCL8/ P672_PEP-FITC, both precursor ions and dissociated products were acquired using a mass resolution of 60000. All measurements were done in triplicates.

7.2.15 HYDROGEN-DEUTERIUM EXCHANGE MASS SPECTROMETRY

HDX-MS was performed using the continuous labelling methodology[254,259]. Working solutions of recombinant CCL8 and P672 were prepared at a concentration of 35 µM in 50 mM ammonium bicarbonate buffer pH=6.5. For estimation of HDX in the heterodimer state, solutions of CCL8 and P672 were mixed in a (1:1) ratio to reach a final concentration of 17.5 µM and incubated at 4°C for 1h. For estimation of HDX in the unbound state, working solution were diluted to 17.5 µM with 50 mM

ammonium bicarbonate pH=6.5. Aliquots of 4.3 µL of heterodimer or unbound proteins were mixed with 48.2 µL of D_2O containing 50 mM ammonium bicarbonate buffer adjusted to pH=6.5 with DCl (final content of D_2O of 91.8%) and incubated for 5s, 30s, 300s and 60 min. HDX was quenched by adding 22.5 µL of 10% formic acid to reach a final volume of 75 µL and pH=2.5, corresponding to a final concentration of 1 µM. Samples were then rapidly flash frozen in liquid nitrogen and stored at -80°C for up to 5 days before analysis.

Samples were analysed using an Aqcuity M class ultra-high performance liquid chromatographer (uHPLC) and a nanoAcquity uHPLC HDX manager coupled to a Synapt G2-Si time-of-flight mass spectrometer (Waters). The system was controlled using the MassLynx 4.1 software. Samples were loaded at a flow rate of 200 µL/min of 100% solvent A (0.1% formic acid) into an Enzymate pepsin column (2.1 mm x 30 mm, 5 µm particle size) where the proteins were quickly digested at 20°C and then desalted for 2 min in a BEH C18 trap column (300 µm x 30 mm, 1.7 µm particle size) at 0°C. Peptides were then eluted under a 12 minutes linear gradient from 4 to 85% of solvent B (acetonitrile with 0.1% formic acid) at 40 µL/min into a BEH C18 analytical column (2.1 mm x 50 mm, 1.7 µm particle size) at 0°C. Mass spectra were acquired in the 50 to 2000 *m/z* range. For peptide mapping purposes, non-deuterated samples were analysed and precursor ions fragmented utilising the MS^E approach with trap collision energies of 15 to 35 V. Source parameters included: cone voltage 30V, capillary voltage 2.8 KV, source temperature 80°C, desolvation temperature 150°C, gas cone flow rate 80 L/h and desolvation gas 250 L/h.

Peptide identifications and protein sequence coverage were determined using the ProteinLynx Global Server 3.0.2. The acquired data was searched against

a custom database containing the protein sequence of interest. Search parameters set to reflect the use of a non-specific digestion enzyme and to include the variable modifications: N-terminus pyroglutamic acid from glutamine and deamidation or HexNAc (N-acetylhexosamine) of asparagine present in a N-X-S/T motif. At least 3 ion fragment matches per peptide were required for peptide identification. Identified peptides were filtered based on peptide presence in 4 out of 5 replicates analysed, a retention time relative standard deviation of ≤ 5%, a precursor ion mass tolerance of 10 ppm and peptide maximum length of 30 residues. Deuterated samples were analysed in scan mode only and retention time, charge state and possible peak overlap were manually checked for all peptides identified. Deuterium uptakes were estimated using Dynamix 3.0 and compared using a t-student test. Differential deuterium uptakes were considered statistically significant when deuterium changes were equal or higher than 5% with a *p*-value ≤ 0.05.

7.2.16 BIOLYAER INTERFEROMETRY SCREENING

Biolayer interferometry was performed using an OctetRed® system at 30°C using the dip and read Ni-NTA biosensors (ForteBio). The assay buffer used was 10 mM Na_2HPO_4, 1.8 mM KH_2PO_4, 2.7 mM KCl, 500 mM NaCl, 0.1% Bovine serum albumin (BSA), 0.002% Tween-20, pH 7.4. Assay buffer was used to establish the response baseline (180 seconds). The temperature condition was recommended by the manufacturer and buffers optimized to minimize non-specific binding of chemokines to the sensor. Purified His-tagged evasin was immobilized on the Ni-NTA sensor using 1 μM evasin in assay buffer (500 seconds). After washing the sensor with assay buffer (60 seconds), the sensor was then subjected to 300 nM chemokine in assay buffer (600 seconds) to record

the association phase. The cross-binding screen was performed as a single experiment against all human chemokines with the exception of CCL25, CCL26, and CXCL16, where the chemokine non-specifically bound to the sensor, and CXCL17, CXCL4L1, and XCL2, which were not available from Peprotech. Assay buffer was then reapplied (600 seconds) to measure the dissociation. The sensor was then exposed to 10 mM glycine, pH 1.7 for five seconds and assay buffer for five seconds three times to strip the sensors of nickel and protein. The sensor was regenerated by placing the sensor into 10 mM $NiCl_2$ for 60 seconds and then reused. Reference experiments were performed by placing a sensor with evasin alone loaded into buffer to account for baseline drift which was then subtracted. Data was processed in ForteBio Data Analysis 9 software.

7.2.17 BIOLAYER INTERFEROMETRY AFFINITY DETERMINATION

Affinity determination experiments were carried out essentially as above. Each experiment was performed at least twice, with a range of chemokine dilutions typically from 300 nM to 0.4 nM. Briefly, the Ni-NTA sensors were loaded with His-tagged evasin and after washing the sensor with assay buffer for 60 seconds, the sensors were then subjected to a serial dilution of chemokine in assay buffer for 600 seconds to record the association phase. Assay buffer was then reapplied to measure the dissociation for 600 seconds. To account for non-specific binding to the sensor, a non-interacting reference protein of sequence DGGQRNAICRLPPDEGICRASIPRFYFNPAEGKCSFFIYGGCEGNENNFETIEE CEKTCGEPERPSDFEGADFETGCAPKPQRGFCKGFLDHWFFNVTSGECEAFL YSGCGGNDNNYESKEECEIACKLTGGASAWSHPQFEKLEHHHHHHHH was loaded on to the sensor and any binding observed subtracted. This protein was

shown to display no binding to any of the chemokines tested and was expressed following the same protocol used for evasin production in HEK293F cells. Data was processed in ForteBio Data Analysis 9 software. Association (k_{on}), dissociation (k_{off}), and affinity (K_d) constants were determined by using the 1:1 binding-model, and global fitting, followed by 'R_{max} unlinked by sensor' to allow independent fitting of R_{max} (maximal signal response upon saturating binding of the partner to the immobilized protein). Data with poor curve fits ($R^2 < 0.9$) were excluded.

7.2.18 FLUORESCENT LIGAND/RECEPTOR BLOCKING ASSAYS

In fluorescent chemokine binding assay buffer (RPMI-1640 + L-glu (2mM) + 10% heat treated fetal bovine serum, 0.2% DMSO) varying concentrations (0-100nM) of CCL8-647 (Almac) were prepared and added to 50,000 THP-1 cells in a 96 well V-bottomed plate in a final volume of 50µL. The cells and CCL8-647 were then incubated together for half an hour at 37°C after which time 100µL of cold PBSA was added. The cells were spun down (2000 RPM, 3 minutes) the supernatant flicked off and washed with cold PBSA. This was repeated twice more and then the cells were resuspended in 150µL PBSA and the median fluorescence intensity of 10,000 cells on the RL-1 channel was determined using an ATTUNE flow cytometer. Experiments were performed three time in triplicate.

The blocking of CCL8-647 binding to endogenous chemokine receptors on THP-1 cells was carried out in a similar manner to that of the binding assay. Briefly, CCL8-647 (2.5nM) was incubated with varying doses of peptide (0-60µM) in fluorescent chemokine binding assay buffer for half an hour at 37°C and then

added to 50,000 THP-1 cells. The cells were then incubated for half an hour at 37°C and then washed thrice with cold PBSA. The median fluorescence intensity of 10,000 cells on the RL-1 channel was determined using an ATTUNE flow cytometer and plotted as function of peptide concentration and the data fitted to an inhibitor response curve with 4 parameters using Graph Pad prism 6.

7.2.19 CELL MIGRATION

The dose of chemokine that produced 80% maximal migration (an EC_{80} dose) was determined in three technical and three biological replicates essentially as described[73] using a 96 well transwell migration plate (5 μM pore size, Corning). Chemokines (0–100 nM (Peprotech) in 150 μl migration media (RPMI-1640 + L-glu (2mM) + 0.5% heat treated fetal bovine serum, all from Sigma) were placed in the bottom chamber. Cells (THP-1, 300,000 cells, in 50 μl migration media) were placed in the top chamber, and incubated at 37°C, 5% CO_2 for 4 hours. The migration plate was shaken at 850 r.p.m. for 10 minutes, and media from bottom plate transferred to a U-bottomed 96 well plate containing 50μL migration media . Cells were counted using an ATTUNE flow cytometer using a FSC versus SSC dot plot, and data analysed in GraphPad Prism fitting an agonist response curve with 4 parameters.

IC_{50} values for each evasin was determined in three technical and three biological replicates essentially as described[260] using the above system. Chemokine (EC_{80} dose) and evasin (typically 0–300 nM doses) were added to the bottom chamber and incubated for 30 min at 37 °C before beginning the cell migration assay as outlined above. Data (3 technical replicates for each

IC_{50}determination) were analysed in GraphPad Prism fitting an inhibitor response curve with 4 parameters.

For migration assays involving peptides 0.2% DMSO was added to the migration media to maintain peptide solubility.

7.2.20 FLUORESCENCE POLARISATION ASSAYS

Fluorescence polarisation assays were performed using the Polarstar Omega (BMG tech) plate reader with the supplied FITC filters and FP optic with 96 half area well plates (corning). The buffer used (FP assay buffer) was 50mM HEPES, 150mM NaCl, 0.1% BSA, 0.002% Tween-20, 0.2% DMSO, pH 7.4.

Direct CCL8/P672_PEP-FITC binding fluorescence polarisation assays - 50nM labelled peptide was incubated with varying concentrations of recombinant CCL8 (0-25μM) in 30μL FP assay buffer for 30 minutes and the resulting polarisation of the fluorophore measured. Measurements were performed in technical triplicate three times. Polarisation was converted to anisotropy using the equation A = (2*P)/(3-P) and plotted as a function of CCL8 concentration with a two-site total binding model curve fitted in Graph Pad Prism 6.

*P672_PEP-FITC/Chemokine cross binding assays using Fluorescence Polarisation- 1*μM Chemokine (Peprotech) was incubated with 50nM FITC conjugated peptide for half an hour in FP assay buffer and the resulting polarisation measured as above. Measurements were performed in technical duplicate three times. The resulting polarisation was converted to anisotropy as above and analysed using a one way ANOVA with Sidak's correction for multiple comparisons in Graph Pad Prism 6.

Displacement of P672_PEP-FITC with P672_PEP fluorescence polarisation assays - CCL7 (900nM final concentration, Peprotech) CCL8 (500nM final concentration, recombinant) or CCL18 (900nM final concentration, Peprotech) was incubated with varying concentration of unlabelled peptide (100 μM, 50μM, 25 μM final concentration) or scrambled peptide (100μM) for 20 minutes in FP assay buffer. Peptide-488 was added to give a final concentration of 50nM in a total volume of 30μL and everything was incubated together for a further 30 minutes. Polarisation was measured and converted to anisotropy as above. Data was analysed using a one-way ANOVA with Sidak's correction for multiple comparisons using Graph Pad Prism 6.

7.2.21 HOMOLOGY MODELLING

Homology modelling was performed using MODELLER[212] within PyMod 2.0[261] with the Evasin-1-CCL3 structure 3FPU[159] as template. The P672 and Evasin-1 sequence were aligned using the muscle algorithm, as were the CCL3 and CCL8 sequences, within the PyMol plug-in. Homolog modelling was then performed using the default settings within MODELLER to produce the P672/CCL8 homology model. Disulfide bonds prediction was performed using the Protein Interaction Calculator[262] and interchain interactions using the Arpeggio server[213].

8 REFERENCES

1 Déruaz, M. *et al.* Ticks produce highly selective chemokine binding proteins with antiinflammatory activity. *J. Exp. Med.* **205**, 9, 2019-2031, (2008).

2 Golia, E. *et al.* Inflammation and cardiovascular disease: from pathogenesis to therapeutic target. *Curr. Atheroscler. Rep.* **16**, 435, (2014).

3 Go, A. S. *et al.* Heart disease and stroke statistics--2014 update: a report from the American Heart Association. *Circulation* **129**, e28-e292, (2014).

4 Gaziano, T. A. Cardiovascular disease in the developing world and its cost-effective management. *Circulation,* **112**, 3547-3553, (2005).

5 Magnani, J. W. & Dec, G. W. Myocarditis: current trends in diagnosis and treatment. *Circulation,* **113**, 876-890, (2006).

6 Fordyce, C. B. *et al.* Cardiovascular drug development: is it dead or just hibernating? *J. Am. Coll. Cardiol.* **65**, 1567-1582, (2015).

7 Berliner, J. A. *et al.* Atherosclerosis: basic mechanisms. Oxidation, inflammation, and genetics. *Circulation,* **91**, 2488-2496, (1995).

8 Sutton, M. G. S. J. & Sharpe, N. Left Ventricular Remodeling After Myocardial Infarction. *Circulation,* **101**, 2981–2988, (2000).

9 Travers, J. G. *et al.* Cardiac Fibrosis: The Fibroblast Awakens. *Circ. Res.* **118**, 1021-1040, (2016).

10 Suthahar, N. *et al.* in *Curr. Heart Fail. Rep.* Vol. 14 235-250 (2017).

11 Segura, A. M. *et al.* Fibrosis and heart failure. *Heart Fail. Rev.* **19**, 173-185, (2014).

12 Fung, G. *et al.* Myocarditis. *Circ. Res.* **118**, 496-514, (2016).

13 Kindermann, I. *et al.* Update on myocarditis. *J. Am. Coll. Cardiol.* **59**, 779-792, (2012).

14 Epelman, S. *et al.* Role of innate and adaptive immune mechanisms in cardiac injury and repair. *Nat. Rev. Immunol.* **15**, 117-129, (2015).

15 Istvan, E. S. & Deisenhofer, J. Structural mechanism for statin inhibition of HMG-CoA reductase. *Science,* **292**, 1160-1164, (2001).

16 Stancu, C. & Sima, A. Statins: mechanism of action and effects. *J. Cell. Mol. Med.* **5**, 378-387, (2001).

17 Greenwood, J. *et al.* Statin therapy and autoimmune disease: from protein prenylation to immunomodulation. *Nat. Rev. Immunol.* **6**, 358-370, (2006).

18 Ridker, P. M. Clinical application of C-reactive protein for cardiovascular disease detection and prevention. *Circulation,* **107**, 363-369, (2003).

19 Ridker, P. M. *et al.* Rosuvastatin to prevent vascular events in men and women with elevated C-reactive protein. *N. Engl. J. Med.* **359**, 2195-2207, (2008).

20 Ridker, P. M. *et al.* Antiinflammatory Therapy with Canakinumab for Atherosclerotic Disease. *N. Engl. J. Med.* **377**, 1119-1131, (2017).

21 Graves, D. T. & Jiang, Y. Chemokines, a family of chemotactic cytokines. *Crit. Rev. Oral Biol. Medicine,* **6**, 109-118, (1995).

22 Fernandez, E. J. & Lolis, E. Structure, function, and inhibition of chemokines. *Annu. Rev. Pharmacol. Toxicol.* **42**, 469-499, (2002).

23 Zlotnik, A. & Yoshie, O. Chemokines: a new classification system and their role in immunity. *Immunity,* **12**, 121-127, (2000).

24 Yoshimura, T. *et al.* Purification of a human monocyte-derived neutrophil chemotactic factor that has peptide sequence similarity to other host defense cytokines. *Proc. Natl. Acad. Sci. U. S. A.* **84**, 9233-9237, (1987).
25 Walz, A. *et al.* Purification and amino acid sequencing of NAF, a novel neutrophil-activating factor produced by monocytes. *Biochem. Biophys. Res. Commun,* **149**, 755-761, (1987).
26 Yoshimura, T. *et al.* Purification and amino acid analysis of two human glioma-derived monocyte chemoattractants. *J. Exp. Med.* **169**, 1449-1459, (1989).
27 Matsushima, K. *et al.* Purification and characterization of a novel monocyte chemotactic and activating factor produced by a human myelomonocytic cell line. *J. Exp. Med.* **169**, 1485-1490, (1989).
28 Holmes, W. E. *et al.* Structure and functional expression of a human interleukin-8 receptor. *Science,* **253**, 1278-1280, (1991).
29 Murphy, P. M. & Tiffany, H. L. Cloning of complementary DNA encoding a functional human interleukin-8 receptor. *Science,* **253**, 1280-1283, (1991).
30 Lodowski, D. T. & Palczewski, K. Chemokine receptors and other G protein-coupled receptors. *Current Opinion in HIV and AIDS,* **4**, 88-95, (2009).
31 Gilman, A. G. G proteins: transducers of receptor-generated signals. *Annu. Rev. Biochem.* **56**, 615-649, (1987).
32 Oldham, W. M. & Hamm, H. E. Heterotrimeric G protein activation by G-protein-coupled receptors. *Nat. Rev. Mol. Cell Biol.* **9**, 60-71, (2008).
33 Murdoch, C. & Finn, A. Chemokine receptors and their role in inflammation and infectious diseases. *Blood,* **95**, 3032-3043, (2000).
34 Baggiolini M, D. B., Moser B. Human chemokines: an update. *Annu Rev Immunol.* **15**, 675-705, (1997).
35 Moser, B. & Loetscher, P. Lymphocyte traffic control by chemokines. *Nat. Immunol.* **2**, 123-128, (2001).
36 Broxmeyer, H. E. Chemokines in hematopoiesis. *Curr. Opin. Hematol.* **15**, 49-58, (2008).
37 Xia, M. *et al.* CCR10 regulates balanced maintenance and function of resident regulatory and effector T cells to promote immune homeostasis in the skin. *J. Allergy Clin. Immunol.* **134**, 634-644.e610, (2014).
38 Martin, C. A. & Dorf, M. E. Differential regulation of interleukin-6, macrophage inflammatory protein-1, and JE/MCP-1 cytokine expression in macrophage cell lines. *Cell. Immunol.* **135**, 245-258, (1991).
39 Rankin, J. A. *et al.* Macrophages cultured in vitro release leukotriene B4 and neutrophil attractant/activation protein (interleukin 8) sequentially in response to stimulation with lipopolysaccharide and zymosan. *J. Clin. Invest.* **86**, 1556-1564, (1990).
40 Clore, G. M. *et al.* Three-dimensional structure of interleukin 8 in solution. *Biochemistry* **29**, 1689-1696, (1990).
41 Lodi, P. J. *et al.* High-resolution solution structure of the beta chemokine hMIP-1 beta by multidimensional NMR. *Science,* **263**, 1762-1767, (1994).
42 Swaminathan, G. J. *et al.* Crystal structures of oligomeric forms of the IP-10/CXCL10 chemokine. *Structure,* **11**, 521-532, (2003).
43 Lubkowski, J. *et al.* The structure of MCP-1 in two crystal forms provides a rare example of variable quaternary interactions. *Nat. Struct. Mol. Biol.* **4**, 64-69, (1997).

44 Handel, T. M. & Domaille, P. J. Heteronuclear (1H, 13C, 15N) NMR assignments and solution structure of the monocyte chemoattractant protein-1 (MCP-1) dimer. *Biochemistry,* **35**, 6569-6584, (1996).
45 Paavola, C. D. *et al.* Monomeric monocyte chemoattractant protein-1 (MCP-1) binds and activates the MCP-1 receptor CCR2B. *J. Biol. Chem.* **273**, 33157-33165, (1998).
46 Rajarathnam, K. *et al.* Neutrophil activation by monomeric interleukin-8. *Science,* **264**, 90-92, (1994).
47 Das, S. T. *et al.* Monomeric and dimeric CXCL8 are both essential for in vivo neutrophil recruitment. *PloS one,* **5**, e11754, (2010).
48 Crown, S. E. *et al.* Heterodimerization of CCR2 chemokines and regulation by glycosaminoglycan binding. *J. Biol. Chem.* **281**, 25438-25446, (2006).
49 Gong, J. H. & Clark-Lewis, I. Antagonists of monocyte chemoattractant protein 1 identified by modification of functionally critical NH2-terminal residues. *J. Exp. Med.* **181**, 631-640, (1995).
50 Proudfoot, A. E. *et al.* Extension of recombinant human RANTES by the retention of the initiating methionine produces a potent antagonist. *J. Biol. Chem.* **271**, 2599-2603, (1996).
51 Jarnagin, K. *et al.* Identification of surface residues of the monocyte chemotactic protein 1 that affect signaling through the receptor CCR2. *Biochemistry,* **38**, 16167-16177, (1999).
52 Hemmerich, S. *et al.* Identification of residues in the monocyte chemotactic protein-1 that contact the MCP-1 receptor, CCR2. *Biochemistry,* **38**, 13013-13025, (1999).
53 Laurence, J. S. *et al.* CC chemokine MIP-1 beta can function as a monomer and depends on Phe13 for receptor binding. *Biochemistry,* **39**, 3401-3409, (2000).
54 Pease, J. E. *et al.* The N-terminal extracellular segments of the chemokine receptors CCR1 and CCR3 are determinants for MIP-1alpha and eotaxin binding, respectively, but a second domain is essential for efficient receptor activation. *J. Biol. Chem.* **273**, 19972-19976, (1998).
55 Ahuja, S. K. *et al.* CXC chemokines bind to unique sets of selectivity determinants that can function independently and are broadly distributed on multiple domains of human interleukin-8 receptor B. Determinants of high affinity binding and receptor activation are distinct. *J. Biol. Chem.* **271**, 225-232, (1996).
56 Monteclaro, F. S. & Charo, I. F. The amino-terminal domain of CCR2 is both necessary and sufficient for high affinity binding of monocyte chemoattractant protein 1. Receptor activation by a pseudo-tethered ligand. *J. Biol. Chem.* **272**, 23186-23190, (1997).
57 Blanpain, C. *et al.* The core domain of chemokines binds CCR5 extracellular domains while their amino terminus interacts with the transmembrane helix bundle. *J. Biol. Chem.* **278**, 5179-5187, (2003).
58 Xanthou, G. *et al.* Molecular characterization of the chemokine receptor CXCR3: evidence for the involvement of distinct extracellular domains in a multi-step model of ligand binding and receptor activation. *Eur. J. Immunol.* **33**, 2927-2936, (2003).
59 Scholten, D. J. *et al.* Pharmacological modulation of chemokine receptor function. *Br. J. Pharmacol.* **165**, 1617-1643, (2012).

60 Zhu, J. Z. *et al.* Tyrosine sulfation influences the chemokine binding selectivity of peptides derived from chemokine receptor CCR3. *Biochemistry,* **50**, 1524-1534, (2011).
61 Millard, C. J. *et al.* Structural basis of receptor sulfotyrosine recognition by a CC chemokine: the N-terminal region of CCR3 bound to CCL11/eotaxin-1. *Structure,* **22**, 1571-1581, (2014).
62 Wescott, M. P. *et al.* Signal transmission through the CXC chemokine receptor 4 (CXCR4) transmembrane helices. *Proc. Natl. Acad. Sci. U. S. A.* **113**, 9928-9933, (2016).
63 Qin, L. *et al.* Structural biology. Crystal structure of the chemokine receptor CXCR4 in complex with a viral chemokine. *Science,* **347**, 1117-1122, (2015).
64 Nagasawa, T. *et al.* Defects of B-cell lymphopoiesis and bone-marrow myelopoiesis in mice lacking the CXC chemokine PBSF/SDF-1. *Nature,* **382**, 635-638, (1996).
65 Zou, Y. R. *et al.* Function of the chemokine receptor CXCR4 in haematopoiesis and in cerebellar development. *Nature*, **393**, 595-599, (1998).
66 Kledal, T. N. *et al.* A broad-spectrum chemokine antagonist encoded by Kaposi's sarcoma-associated herpesvirus. *Science,* **277**, 1656-1659, (1997).
67 Rot, A. Neutrophil attractant/activation protein-1 (interleukin-8) induces in vitro neutrophil migration by haptotactic mechanism. *Eur. J. Immunol.* **23**, 303-306, (1993).
68 Hoogewerf, A. J. *et al.* Glycosaminoglycans mediate cell surface oligomerization of chemokines. *Biochemistry,* **36**, 13570-13578, (1997).
69 Kuschert, G. S. *et al.* Identification of a glycosaminoglycan binding surface on human interleukin-8. *Biochemistry,* **37**, 11193-11201, (1998).
70 Proudfoot, A. E. *et al.* The BBXB motif of RANTES is the principal site for heparin binding and controls receptor selectivity. *J. Biol. Chem.* **276**, 10620-10626, (2001).
71 Deshauer, C. *et al.* Interactions of the Chemokine CCL5/RANTES with Medium-Sized Chondroitin Sulfate Ligands. *Structure,* **23**, 1066-1077, (2015).
72 Shaw, J. P. *et al.* The X-ray structure of RANTES: heparin-derived disaccharides allows the rational design of chemokine inhibitors. *Structure,* **12**, 2081-2093, (2004).
73 Proudfoot, A. E. *et al.* Glycosaminoglycan binding and oligomerization are essential for the in vivo activity of certain chemokines. *Proc. Natl. Acad. Sci. U. S. A.* **100**, 1885-1890, (2003).
74 Ulvmar, M. H. *et al.* Atypical chemokine receptors. *Exp. Cell Res.* **317**, 556-568, (2011).
75 Bachelerie, F. *et al.* New nomenclature for atypical chemokine receptors. *Nat. Immunol.* **15**, 207-208, (2014).
76 Weber, M. *et al.* The chemokine receptor D6 constitutively traffics to and from the cell surface to internalize and degrade chemokines. *Mol. Biol. Cell* **15**, 2492-2508, (2004).
77 Pruenster, M. *et al.* The Duffy antigen receptor for chemokines transports chemokines and supports their promigratory activity. *Nat. Immunol.* **10**, 101-108, (2009).

78 Lee, J. S. *et al.* Duffy antigen facilitates movement of chemokine across the endothelium in vitro and promotes neutrophil transmigration in vitro and in vivo. *J. Immunol.* **170**, 5244-5251, (2003).
79 Castanheira, F. *et al.* The Atypical Chemokine Receptor ACKR2 is Protective Against Sepsis. *Shock,* **49**, 682-689, (2018).
80 Yao, L. *et al.* Roles of the chemokine system in development of obesity, insulin resistance, and cardiovascular disease. *Journal of Immunology Research,* 181450, (2014).
81 Karten, B. *et al.* Macrophage-enhanced formation of cholesteryl ester-core aldehydes during oxidation of low density lipoprotein. *J. Lipid Res.* **40**, 1240-1253, (1999).
82 Li, D. & Mehta, J. L. Antisense to LOX-1 inhibits oxidized LDL-mediated upregulation of monocyte chemoattractant protein-1 and monocyte adhesion to human coronary artery endothelial cells. *Circulation* **101**, 2889-2895, (2000).
83 Yu, X. *et al.* Elevated expression of monocyte chemoattractant protein 1 by vascular smooth muscle cells in hypercholesterolemic primates. *Proc. Natl. Acad. Sci. U. S. A.* **89**, 6953-6957, (1992).
84 Yla-Herttuala, S. *et al.* Expression of monocyte chemoattractant protein 1 in macrophage-rich areas of human and rabbit atherosclerotic lesions. *Proc. Natl. Acad. Sci. U. S. A.* **88**, 5252-5256, (1991).
85 Tacke, F. *et al.* Monocyte subsets differentially employ CCR2, CCR5, and CX3CR1 to accumulate within atherosclerotic plaques. *J. Clin. Invest.* **117**, 185-194, (2007).
86 Veillard, N. R. *et al.* Differential expression patterns of proinflammatory and antiinflammatory mediators during atherogenesis in mice. *Arter. Thromb. Vasc. Biol.* **24**, 2339-2344, (2004).
87 Gonzalez, P. *et al.* Genetic variation at the chemokine receptors CCR5/CCR2 in myocardial infarction. *Genes Immun.* **2**, 191-195, (2001).
88 Boring, L. *et al.* Decreased lesion formation in CCR2-/- mice reveals a role for chemokines in the initiation of atherosclerosis. *Nature,* **394**, 894-897, (1998).
89 Aiello, R. J. *et al.* Monocyte chemoattractant protein-1 accelerates atherosclerosis in apolipoprotein E-deficient mice. *Arter., Thromb. Vasc. Biol.* **19**, 1518-1525, (1999).
90 Wilcox, J. N. *et al.* Local expression of inflammatory cytokines in human atherosclerotic plaques. *Journal of Atherosclerosis and Thrombosis* **1 Suppl 1**, S10-13, (1994).
91 de Jager, S. C. *et al.* Leukocyte-specific CCL3 deficiency inhibits atherosclerotic lesion development by affecting neutrophil accumulation. *Arter. Thromb. Vasc. Biol.* **33**, e75-83, (2013).
92 Terkeltaub, R. *et al.* Oxidized LDL induces monocytic cell expression of interleukin-8, a chemokine with T-lymphocyte chemotactic activity. *Arterioscler. Thromb.* **14**, 47-53, (1994).
93 Boisvert, W. A. *et al.* A leukocyte homologue of the IL-8 receptor CXCR-2 mediates the accumulation of macrophages in atherosclerotic lesions of LDL receptor-deficient mice. *J. Clin. Invest.* **101**, 353-363, (1998).
94 Jennings, R. B. *et al.* Development of cell injury in sustained acute ischemia. *Circulation,* **82**, Ii2-12, (1990).

95 Talman, V. & Ruskoaho, H. Cardiac fibrosis in myocardial infarction-from repair and remodeling to regeneration. *Cell Tissue Res.* **365**, 563-581, (2016).
96 Frangogiannis, N. G. Regulation of the inflammatory response in cardiac repair. *Circ. Res.* **110**, 159-173, (2012).
97 Ono, K. *et al.* Prevention of myocardial reperfusion injury in rats by an antibody against monocyte chemotactic and activating factor/monocyte chemoattractant protein-1. *Lab. Invest.* **79**, 195-203, (1999).
98 Liehn, E. A. *et al.* A new monocyte chemotactic protein-1/chemokine CC motif ligand-2 competitor limiting neointima formation and myocardial ischemia/reperfusion injury in mice. *J. Am. Coll. Cardiol.* **56**, 1847-1857, (2010).
99 Parissis, J. T. *et al.* Serum profiles of C-C chemokines in acute myocardial infarction: possible implication in postinfarction left ventricular remodeling. *J. Interferon Cytokine Res.* **22**, 223-229, (2002).
100 Braunersreuther, V. *et al.* Chemokine CCL5/RANTES inhibition reduces myocardial reperfusion injury in atherosclerotic mice. *J. Mol. Cell. Cardiol.* **48**, 789-798, (2010).
101 Buggey, J. & ElAmm, C. A. Myocarditis and cardiomyopathy. *Curr. Opin. Cardiol.* **33**, 341-346, (2018).
102 Escher, F. *et al.* Development of diastolic heart failure in a 6-year follow-up study in patients after acute myocarditis. *Heart (British Cardiac Society),* **97**, 709-714, (2011).
103 Nogueira, L. G. *et al.* Myocardial chemokine expression and intensity of myocarditis in Chagas cardiomyopathy are controlled by polymorphisms in CXCL9 and CXCL10. *PLoS Negl. Trop. Dis.* **6**, e1867, (2012).
104 Cook, D. N. *et al.* Requirement of MIP-1 alpha for an inflammatory response to viral infection. *Science,* **269**, 1583-1585, (1995).
105 Szekanecz, Z. *et al.* Chemokines and chemokine receptors in arthritis. *Front. Biosci.* **2**, 153-167, (2010).
106 Atreya, R. & Neurath, M. F. Chemokines in inflammatory bowel diseases. *Dig. Dis.* **28**, 386-394, (2010).
107 Nickoloff, B. J. *et al.* The cytokine and chemokine network in psoriasis. *Clin. Dermatol.* **25**, 568-573, (2007).
108 Solari, R. *et al.* "Chemokine receptors as therapeutic targets: Why aren't there more drugs?". *Eur. J. Pharmacol.* **746**, 363-367, (2015).
109 Samson, M. *et al.* Resistance to HIV-1 infection in caucasian individuals bearing mutant alleles of the CCR-5 chemokine receptor gene. *Nature* **382**, 722-725, (1996).
110 Dragic, T. *et al.* HIV-1 entry into CD4+ cells is mediated by the chemokine receptor CC-CKR-5. *Nature* **381**, 667-673, (1996).
111 Van Der Ryst, E. Maraviroc – A CCR5 Antagonist for the Treatment of HIV-1 Infection. *Front. Immunol.* **6**, (2015).
112 Feng, Y. *et al.* HIV-1 entry cofactor: functional cDNA cloning of a seven-transmembrane, G protein-coupled receptor. *Science,* **272**, 872-877, (1996).
113 De Clercq, E. The bicyclam AMD3100 story. *Nat. Rev. Drug Discov.* **2**, 581-587, (2003).
114 Nagasawa, T. CXCL12/SDF-1 and CXCR4. *Front. Immunol.* **6**, (2015).
115 Moser, B. *et al.* Chemokines: multiple levels of leukocyte migration control. *Trends Immunol.* **25**, 75-84, (2004).

116 Nanki, T. *et al.* Inhibition of fractalkine ameliorates murine collagen-induced arthritis. *J. Immunol.* **173**, 7010-7016, (2004).
117 Shahrara, S. *et al.* Inhibition of monocyte chemoattractant protein-1 ameliorates rat adjuvant-induced arthritis. *J. Immunol.* **180**, 3447-3456, (2008).
118 Barnes, D. A. *et al.* Polyclonal antibody directed against human RANTES ameliorates disease in the Lewis rat adjuvant-induced arthritis model. *J. Clin. Invest.* **101**, 2910-2919, (1998).
119 Zhong, C. *et al.* Development and preclinical characterization of a humanized antibody targeting CXCL12. *Clin. Cancer Res.* **19**, 4433-4445, (2013).
120 Haringman, J. J. *et al.* A randomized controlled trial with an anti-CCL2 (anti-monocyte chemotactic protein 1) monoclonal antibody in patients with rheumatoid arthritis. *Arthritis Rheum.* **54**, 2387-2392, (2006).
121 Vergunst, C. E. *et al.* Modulation of CCR2 in rheumatoid arthritis: a double-blind, randomized, placebo-controlled clinical trial. *Arthritis Rheum.* **58**, 1931-1939, (2008).
122 Veillard, N. R. *et al.* Antagonism of RANTES receptors reduces atherosclerotic plaque formation in mice. *Circ. Res.* **94**, 253-261, (2004).
123 Braunersreuther, V. *et al.* A novel RANTES antagonist prevents progression of established atherosclerotic lesions in mice. *Arter. Thromb. Vasc. Biol.***28**, 1090-1096, (2008).
124 van Wanrooij, E. J. *et al.* HIV entry inhibitor TAK-779 attenuates atherogenesis in low-density lipoprotein receptor-deficient mice. *Arter. Thromb. Vasc. Biol.***25**, 2642-2647, (2005).
125 Lutgens, E. *et al.* Gene profiling in atherosclerosis reveals a key role for small inducible cytokines: validation using a novel monocyte chemoattractant protein monoclonal antibody. *Circulation* **111**, 3443-3452, (2005).
126 Gilbert, J. *et al.* Effect of CC chemokine receptor 2 CCR2 blockade on serum C-reactive protein in individuals at atherosclerotic risk and with a single nucleotide polymorphism of the monocyte chemoattractant protein-1 promoter region. *Am. J. Cardiol.* **107**, 906-911, (2011).
127 Horuk, R. Chemokine receptor antagonists: overcoming developmental hurdles. *Nat. Rev. Drug Discov.* **8**, 23-33, (2009).
128 Cheng, S. S. *et al.* Granulocyte-macrophage colony stimulating factor up-regulates CCR1 in human neutrophils. *J. Immunol.* **166**, 1178-1184, (2001).
129 Szekanecz, Z. & Koch, A. E. Successes and failures of chemokine-pathway targeting in rheumatoid arthritis. *Nat. Rev. Rheumatol.* **12**, 5-13, (2015).
130 Proudfoot, A. E. Is CCR2 the right chemokine receptor to target in rheumatoid arthritis? *Arthritis Rheum.* **58**, 1889-1891, (2008).
131 Mantovani, A. The chemokine system: redundancy for robust outputs. *Immunol. Today* **20**, 254-257, (1999).
132 Bardi, G. *et al.* The T cell chemokine receptor CCR7 is internalized on stimulation with ELC, but not with SLC. *Eur. J. Immunol.* **31**, 3291-3297, (2001).
133 Richardson, R. M. *et al.* Role of the cytoplasmic tails of CXCR1 and CXCR2 in mediating leukocyte migration, activation, and regulation. *J. Immunol.* **170**, 2904-2911, (2003).
134 Katschke, K. J., Jr. *et al.* Differential expression of chemokine receptors on peripheral blood, synovial fluid, and synovial tissue monocytes/macrophages in rheumatoid arthritis. *Arthritis Rheum.* **44**, 1022-1032, (2001).

135 Henneken, M. *et al.* Differential expression of chemokine receptors on peripheral blood B cells from patients with rheumatoid arthritis and systemic lupus erythematosus. *Arthritis. Res. Ther.* **7**, R1001-1013, (2005).
136 Brandes, M. *et al.* A systems analysis identifies a feedforward inflammatory circuit leading to lethal influenza infection. *Cell,* **154**, 197-212, (2013).
137 Chou, R. C. *et al.* Lipid-cytokine-chemokine cascade drives neutrophil recruitment in a murine model of inflammatory arthritis. *Immunity,* **33**, 266-278, (2010).
138 Paesen, G. C. *et al.* Tick histamine-binding proteins: isolation, cloning, and three-dimensional structure. *Mol. Cell* **3**, 661-671, (1999).
139 Valenzuela, J. G. *et al.* Purification, cloning, and expression of a novel salivary anticomplement protein from the tick, Ixodes scapularis. *J. Biol. Chem.* **275**, 18717-18723, (2000).
140 Waxman, L. *et al.* Tick anticoagulant peptide (TAP) is a novel inhibitor of blood coagulation factor Xa. *Science,* **248**, 593-596, (1990).
141 Wikel, S. K. Tick modulation of host cytokines. *Exp. Parasitol.* **84**, 304-309, (1996).
142 Konik, P. *et al.* Anti-tumour necrosis factor-alpha activity in Ixodes ricinus saliva. *Parasite Immunol.* **28**, 649-656, (2006).
143 Fuentes, M. E. *et al.* Controlled recruitment of monocytes and macrophages to specific organs through transgenic expression of monocyte chemoattractant protein-1. *J. Immunol.* **155**, 5769-5776, (1995).
144 Kobayashi, Y. Neutrophil infiltration and chemokines. *Crit. Rev. Immunol.* **26**, 307-316, (2006).
145 Baggiolini, M. *et al.* Interleukin-8 and related chemotactic cytokines--CXC and CC chemokines. *Adv. Immunol.* **55**, 97-179, (1994).
146 Ribeiro, J. M. *et al.* Saliva of the tick Ixodes dammini inhibits neutrophil function. *Exp. Parasitol.* **70**, 382-388, (1990).
147 Hajnicka, V. *et al.* Anti-interleukin-8 activity of tick salivary gland extracts. *Parasite Immunol.* **23**, 483-489, (2001).
148 Kocakova, P. *et al.* Effect of fast protein liquid chromatography fractionated salivary gland extracts from different ixodid tick species on interleukin-8 binding to its cell receptors. *Folia parasitologica* **50**, 79-84, (2003).
149 Jose, P. J. *et al.* Eotaxin: a potent eosinophil chemoattractant cytokine detected in a guinea pig model of allergic airways inflammation. *J. Exp. Med.* **179**, 881-887, (1994).
150 Keepers, T. R. *et al.* Monocyte chemoattractant protein 1, macrophage inflammatory protein 1 alpha, and RANTES recruit macrophages to the kidney in a mouse model of hemolytic-uremic syndrome. *Infect. Immun.* **75**, 1229-1236, (2007).
151 Hajnicka, V. *et al.* Manipulation of host cytokine network by ticks: a potential gateway for pathogen transmission. *Parasitology,* **130**, 333-342, (2005).
152 Frauenschuh, A. *et al.* Molecular cloning and characterization of a highly selective chemokine-binding protein from the tick Rhipicephalus sanguineus. *J. Biol. Chem.* **282**, 27250-27258, (2007).
153 Deruaz, M. *et al.* Evasin-4, a tick-derived chemokine-binding protein with broad selectivity can be modified for use in preclinical disease models. *FEBS J.* **280**, 4876-4887, (2013).
154 Bonvin, P. *et al.* Evasins: Therapeutic Potential of a New Family of Chemokine-Binding Proteins from Ticks. *Front. Immunol.,* **7**, (2016).

155 Russo, R. C. *et al.* Therapeutic effects of evasin-1, a chemokine binding protein, in bleomycin-induced pulmonary fibrosis. *Am. J. Respir. Cell Mol. Biol.* **45**, 72-80, (2011).
156 Vieira, A. T. *et al.* Treatment with a novel chemokine-binding protein or eosinophil lineage-ablation protects mice from experimental colitis. *Am. J. Pathol.* **175**, 2382-2391, (2009).
157 Braunersreuther, V. *et al.* Treatment with the CC chemokine-binding protein Evasin-4 improves post-infarction myocardial injury and survival in mice. *Thromb. Haemost.* **110**, 807-825, (2013).
158 Montecucco, F. *et al.* Treatment with Evasin-3 abrogates neutrophil-mediated inflammation in mouse acute pancreatitis. *Eur. J. Clin. Invest.* **44**, 940-950, (2014).
159 Dias, J. M. *et al.* Structural basis of chemokine sequestration by a tick chemokine binding protein: the crystal structure of the complex between Evasin-1 and CCL3. *PloS one* **4**, e8514, (2009).
160 Bonvin, P. *et al.* Identification of the pharmacophore of the CC chemokine-binding proteins Evasin-1 and -4 using phage display. *J. Biol. Chem.* **289**, 31846-31855, (2014).
161 Anatriello, E. *et al.* An insight into the sialotranscriptome of the brown dog tick, Rhipicephalus sanguineus. *BMC genomics,* **11**, 450, (2010).
162 Karim, S. *et al.* A deep insight into the sialotranscriptome of the gulf coast tick, Amblyomma maculatum. *PloS one,* **6**, e28525, (2011).
163 Radulovic, Z. M. *et al.* A 24-48 h fed Amblyomma americanum tick saliva immuno-proteome. *BMC genomics,* **15**, 518, (2014).
164 Singh, K. *et al.* Yeast surface display identifies a family of evasins from ticks with novel polyvalent CC chemokine-binding activities. *Scientific Reports,* **7**, 4267, (2017).
165 Hayward, J. *et al.* Ticks from diverse genera encode chemokine-inhibitory evasin proteins. *J. Biol. Chem.* **292**, 15670-15680, (2017).
166 Smith, C. A. *et al.* Poxvirus genomes encode a secreted, soluble protein that preferentially inhibits beta chemokine activity yet lacks sequence homology to known chemokine receptors. *Virology,* **236**, 316-327, (1997).
167 Counago, R. M. *et al.* Structures of Orf Virus Chemokine Binding Protein in Complex with Host Chemokines Reveal Clues to Broad Binding Specificity. *Structure,* **23**, 1199-1213, (2015).
168 Smith, P. *et al.* Schistosoma mansoni secretes a chemokine binding protein with antiinflammatory activity. *J. Exp. Med.* **202**, 1319-1325, (2005).
169 Veeresham, C. Natural products derived from plants as a source of drugs. *Journal of Advanced Pharmaceutical Tecnology and Research,* **3**, 200-201, (2012).
170 Pathan, H. & Williams, J. Basic opioid pharmacology: an update. *British Journal of Pain,* **6**, 11-16, (2012).
171 Gong, L. *et al.* Celecoxib pathways: pharmacokinetics and pharmacodynamics. *Pharmacogenetics and genomics,* **22**, 310-318, (2012).
172 Markwardt, F. Hirudin as alternative anticoagulant--a historical review. *Semin. Thromb. Hemost.* **28**, 405-414, (2002).
173 Barratt-Due, A. *et al.* Ornithodoros moubata complement inhibitor is an equally effective C5 inhibitor in pigs and humans. *J. Immunol.* **187**, 4913-4919, (2011).

174 Bryan, J. *From snake venom to ACE inhibitor - The discovery and rise of captopril*. Vol. 282 (2009).
175 Koh, C. Y. & Kini, R. M. From snake venom toxins to therapeutics--cardiovascular examples. *Toxicon,* **59**, 497-506, (2012).
176 Proost, P. *et al.* The role of chemokines in inflammation. *Int. J. Clin. Lab. Res.* **26**, 211-223, (1996).
177 Sultana, A. & Lee, J. E. Measuring protein-protein and protein-nucleic Acid interactions by biolayer interferometry. *Current protocols in protein science* **79**, 19.25.11-26, (2015).
178 Harding, S. D. *et al.* The IUPHAR/BPS Guide to PHARMACOLOGY in 2018: updates and expansion to encompass the new guide to IMMUNOPHARMACOLOGY. *Nucleic Acids Res* **46**, D1091-d1106, (2018).
179 Mueller, A. *et al.* Pathways for internalization and recycling of the chemokine receptor CCR5. *Blood* **99**, 785-791, (2002).
180 Cross, A. K. *et al.* Migration responses of human monocytic cell lines to alpha- and beta-chemokines. *Cytokine,* **9**, 521-528, (1997).
181 Hunter, P. The inflammation theory of disease: The growing realization that chronic inflammation is crucial in many diseases opens new avenues for treatment. *EMBO Rep.* **13**, 968-970, (2012).
182 Firestein, G. S. Inhibiting inflammation in rheumatoid arthritis. *N. Engl. J. Med.* **354**, 80-82, (2006).
183 Garin, A. & Proudfoot, A. E. Chemokines as targets for therapy. *Exp. Cell Res.* **317**, 602-612, (2011).
184 Chemokine/chemokine receptor nomenclature. *Cytokine* **21**, 48-49, (2003).
185 Moser, B. & Willimann, K. Chemokines: role in inflammation and immune surveillance. *Ann. Rheum. Dis.* **63**, ii84-ii89, (2004).
186 Gerard, C. & Rollins, B. J. Chemokines and disease. *Nat. Immunol.* **2**, 108-115, (2001).
187 Proudfoot, A. E. I. Chemokine receptors: multifaceted therapeutic targets. *Nat. Rev. Immunol.* **2**, 106-115, (2002).
188 Haringman, J. *et al.* Expression of chemokines and their receptors in synovial tissue of patients with rheumatoid arthritis, osteoarthritis and reactive arthritis. *Arthritis Res Ther* **5**, 1, (2003).
189 Ogata, H. *et al.* The role of monocyte chemoattractant protein-1 (MCP-1) in the pathogenesis of collagen-induced arthritis in rats. *J. Pathol.* **182**, 106-114, (1997).
190 Mahler, D. A. *et al.* Efficacy and safety of a monoclonal antibody recognizing interleukin-8 in COPD: a pilot study. *Chest* **126**, 926-934, (2004).
191 Gong, J. H. *et al.* Post-onset inhibition of murine arthritis using combined chemokine antagonist therapy. *Rheumatology (Oxford, England)* **43**, 39-42, (2004).
192 Li, Z. *et al.* Influence of molecular size on tissue distribution of antibody fragments. *mAbs* **8**, 113-119, (2016).
193 Raman, D. *et al.* Chemokines in health and disease. *Exp. Cell Res.* **317**, 575-589, (2011).
194 Steentoft, C. *et al.* Precision mapping of the human O-GalNAc glycoproteome through SimpleCell technology. *EMBO J.* **32**, 1478-1488, (2013).

195 Aricescu, A. R. *et al.* A time- and cost-efficient system for high-level protein production in mammalian cells. *Acta Crystallogr. D Biol. Crystallogr.* **62**, 1243-1250, (2006).
196 Yen, T. Y. *et al.* Overcoming challenges and opening new opportunities in glycoproteomics. *Biomolecules,* **3**, 270-286, (2013).
197 Jefferis, R. Recombinant antibody therapeutics: the impact of glycosylation on mechanisms of action. *Trends Pharmacol. Sci.* **30**, 356-362, (2009).
198 Proudfoot, A. E. *et al.* Targeting chemokines: Pathogens can, why can't we? *Cytokine,* **74**, 259-267, (2015).
199 Lubman, O. Y. & Fremont, D. H. Parallel Evolution of Chemokine Binding by Structurally Related Herpesvirus Decoy Receptors. *Structure,* **24**, 57-69, (2016).
200 Kurihara, T. *et al.* Defects in macrophage recruitment and host defense in mice lacking the CCR2 chemokine receptor. *J. Exp. Med.* **186**, 1757-1762, (1997).
201 Wei, X. *et al.* Antibody neutralization and escape by HIV-1. *Nature,* **422**, 307-312, (2003).
202 Déruaz, M. *et al.* Ticks produce highly selective chemokine binding proteins with antiinflammatory activity. *J. Exp. Med.* **205**, 2019-2031, (2008).
203 Goel, A. *et al.* Relative position of the hexahistidine tag effects binding properties of a tumor-associated single-chain Fv construct. *Biochim. Biophys. Acta* **1523**, 13-20, (2000).
204 Tiller, K. E. & Tessier, P. M. Advances in Antibody Design. *Annu. Rev. Biomed. Eng.* **17**, 191-216, (2015).
205 Lu, Q. *et al.* Optimized procedures for producing biologically active chemokines. *Protein Expr. Purif.* **65**, 251-260, (2009).
206 Kiss, D. L. *et al.* The functional antagonist Met-RANTES: a modified agonist that induces differential CCR5 trafficking. *Cell. Mol. Biol. Lett.* **14**, 537-547, (2009).
207 Gouwy, M. *et al.* Possible mechanisms involved in chemokine synergy fine tuning the inflammatory response. *Immunol. Lett.* **145**, 10-14, (2012).
208 Saeed, A. F. *et al.* Antibody Engineering for Pursuing a Healthier Future. *Frontiers in Microbiology,* **8**, 495, (2017).
209 Raju, T. N. The Nobel chronicles. 1972: Gerald M Edelman (b 1929) and Rodney R Porter (1917-85). *Lancet,* **354**, 1040, (1999).
210 Alcami, A. & Saraiva, M. in *Pathogen-Derived Immunomodulatory Molecules* (ed Padraic G. Fallon) 167-179 (Springer New York, 2009).
211 Rajagopalan, L. & Rajarathnam, K. Structural Basis of Chemokine Receptor Function—A Model for Binding Affinity and Ligand Selectivity. *Biosci Rep* **26**, 325-339, (2006).
212 Eswar, N. *et al.* Protein structure modeling with MODELLER. *Methods Mol. Biol.* **426**, 145-159, (2008).
213 Jubb, H. C. *et al.* Arpeggio: A Web Server for Calculating and Visualising Interatomic Interactions in Protein Structures. *J. Mol. Biol.* **429**, 365-371, (2017).
214 Beall, C. J. *et al.* Site-directed mutagenesis of monocyte chemoattractant protein-1 identifies two regions of the polypeptide essential for biological activity. *Biochem. J.* **313 (Pt 2)**, 633-640, (1996).

215 Gonzalez-Motos, V. *et al.* Chemokine binding proteins: An immunomodulatory strategy going viral. *Cytokine Growth Factor Rev.* **30**, 71-80, (2016).
216 Sela-Culang, I. *et al.* The structural basis of antibody-antigen recognition. *Front. Immunol.* **4**, 302, (2013).
217 Feng, Y. *et al.* Peptides derived from the complementarity-determining regions of anti-Mac-1 antibodies block intercellular adhesion molecule-1 interaction with Mac-1. *J. Biol. Chem.* **273**, 5625-5630, (1998).
218 Baker, M. P. *et al.* in *Self Nonself* Vol. 1 314-322 (2010).
219 Arkin, M. R. & Wells, J. A. Small-molecule inhibitors of protein-protein interactions: progressing towards the dream. *Nat. Rev. Drug Discov.* **3**, 301-317, (2004).
220 Kaspar, A. A. & Reichert, J. M. Future directions for peptide therapeutics development. *Drug Discov. Today* **18**, 807-817, (2013).
221 Al Musaimi, O. *et al.* 2017 FDA Peptide Harvest. *Pharmaceuticals (Basel, Switzerland)* **11**, (2018).
222 Robinson, J. A. *et al.* The design, structures and therapeutic potential of protein epitope mimetics. *Drug Discov. Today* **13**, 944-951, (2008).
223 Fosgerau, K. *et al.* The novel GLP-1-gastrin dual agonist, ZP3022, increases beta-cell mass and prevents diabetes in db/db mice. *Diabetes Obes. Metab.* **15**, 62-71, (2013).
224 Gault, V. A. *et al.* A novel glucagon-like peptide-1 (GLP-1)/glucagon hybrid peptide with triple-acting agonist activity at glucose-dependent insulinotropic polypeptide, GLP-1, and glucagon receptors and therapeutic potential in high fat-fed mice. *J. Biol. Chem.* **288**, 35581-35591, (2013).
225 Kawamura, A. *et al.* Highly selective inhibition of histone demethylases by de novo macrocyclic peptides. *Nat. Commun.* **8**, 14773, (2017).
226 Mourez, M. & Collier, R. J. Use of phage display and polyvalency to design inhibitors of protein-protein interactions. *Methods Mol. Biol.* **261**, 213-228, (2004).
227 Kneissl, S. *et al.* Photocontrollable peptide-based switches target the anti-apoptotic protein Bcl-xL. *Chembiochem* **9**, 3046-3054, (2008).
228 Miller, M. C. & Mayo, K. H. Chemokines from a Structural Perspective. *Int. J. Mol. Sci.* **18**, (2017).
229 Zheng, Y. *et al.* Structure of CC chemokine receptor 2 with orthosteric and allosteric antagonists. *Nature,* **540**, 458-461, (2016).
230 Tan, Q. *et al.* Structure of the CCR5 chemokine receptor – HIV entry inhibitor Maraviroc complex. *Science,* **341**, (2013).
231 Berres, M. L. *et al.* Antagonism of the chemokine Ccl5 ameliorates experimental liver fibrosis in mice. *J. Clin. Invest.* **120**, 4129-4140, (2010).
232 Hachet-Haas, M. *et al.* Small neutralizing molecules to inhibit actions of the chemokine CXCL12. *J. Biol. Chem.* **283**, 23189-23199, (2008).
233 Smith, E. W. *et al.* Structure-Based Identification of Novel Ligands Targeting Multiple Sites within a Chemokine-G-Protein-Coupled-Receptor Interface. *J. Med. Chem.* **59**, 4342-4351, (2016).
234 Veldkamp, C. T. *et al.* Targeting SDF-1/CXCL12 with a ligand that prevents activation of CXCR4 through structure-based drug design. *J. Am. Chem. Soc.* **132**, 7242-7243, (2010).

235 Colobran, R. *et al.* The chemokine network. I. How the genomic organization of chemokines contains clues for deciphering their functional complexity. *Clin. Exp. Immunol.* **148**, 208-217, (2007).
236 Abraham, M. *et al.* Development of Novel Promiscuous Anti-Chemokine Peptibodies for Treating Autoimmunity and Inflammation. *Front. Immunol.* **8**, (2017).
237 Ezerzer, C. *et al.* Chemokine receptor-derived peptides as multi-target drug leads for the treatment of inflammatory diseases. *Peptides,* **30**, 1296-1305, (2009).
238 Wichapong, K. *et al.* Structure-Based Design of Peptidic Inhibitors of the Interaction between CC Chemokine Ligand 5 (CCL5) and Human Neutrophil Peptides 1 (HNP1). *J. Med. Chem.* **59**, 4289-4301, (2016).
239 Helmer, D. *et al.* Rational design of a peptide capture agent for CXCL8 based on a model of the CXCL8:CXCR1 complex. *RSC Advances,* **5**, 25657-25668, (2015).
240 Yan, X. & Maier, C. S. Hydrogen/deuterium exchange mass spectrometry. *Methods Mol. Biol.* **492**, 255-271, (2009).
241 Moreira, I. S. *et al.* Hot spots--a review of the protein-protein interface determinant amino-acid residues. *Proteins,* **68**, 803-812, (2007).
242 Cragg, G. M. & Newman, D. J. Natural products: a continuing source of novel drug leads. *Biochim. Biophys. Acta* **1830**, 3670-3695, (2013).
243 Seet, B. T. *et al.* Molecular determinants for CC-chemokine recognition by a poxvirus CC-chemokine inhibitor. *Proc. Natl. Acad. Sci. U. S. A.* **98**, 9008-9013, (2001).
244 Beck, C. G. *et al.* The viral CC chemokine-binding protein vCCI inhibits monocyte chemoattractant protein-1 activity by masking its CCR2B-binding site. *J. Biol. Chem.* **276**, 43270-43276, (2001).
245 Park, B. W. *et al.* Rationally designed anti-HER2/neu peptide mimetic disables P185HER2/neu tyrosine kinases in vitro and in vivo. *Nat. Biotechnol.* **18**, 194-198, (2000).
246 Feng, J. *et al.* Rational design of potent mimic peptide derived from monoclonal antibody: antibody mimic design. *Immunol. Lett.* **98**, 311-316, (2005).
247 Timofeeva, O. A. *et al.* Rationally designed inhibitors identify STAT3 N-domain as a promising anticancer drug target. *ACS Chem. Biol.* **2**, 799-809, (2007).
248 Finan, B. *et al.* A rationally designed monomeric peptide triagonist corrects obesity and diabetes in rodents. *Nat. Med.* **21**, 27-36, (2015).
249 Reckless, J. & Grainger, D. J. Identification of oligopeptide sequences which inhibit migration induced by a wide range of chemokines. *Biochem. J.* **340 (Pt 3)**, 803-811, (1999).
250 Houimel, M. & Mazzucchelli, L. Chemokine CCR3 ligands-binding peptides derived from a random phage-epitope library. *Immunol. Lett.* **149**, 19-29, (2013).
251 Arevalo, J. H. *et al.* Molecular basis of crossreactivity and the limits of antibody-antigen complementarity. *Nature,* **365**, 859-863, (1993).
252 James, L. C. *et al.* Antibody multispecificity mediated by conformational diversity. *Science,* **299**, 1362-1367, (2003).

253 Sethi, D. K. *et al.* Differential epitope positioning within the germline antibody paratope enhances promiscuity in the primary immune response. *Immunity,* **24**, 429-438, (2006).
254 Marcsisin, S. R. & Engen, J. R. Hydrogen exchange mass spectrometry: what is it and what can it tell us? *Anal. Bioanal. Chem.* **397**, 967-972, (2010).
255 Larive, C. K. *et al.* Quantitative Analysis of Peptides with NMR Spectroscopy. *Appl. Spectrosc.* **51**, 1531-1536, (1997).
256 Gileadi, O. *et al.* High throughput production of recombinant human proteins for crystallography. *Methods Mol. Biol.* **426**, 221-246, (2008).
257 Ho, S. N. *et al.* Site-directed mutagenesis by overlap extension using the polymerase chain reaction. *Gene,* **77**, 51-59, (1989).
258 Gault, J. *et al.* High-resolution mass spectrometry of small molecules bound to membrane proteins. *Nat. Methods,* **13**, 333-336, (2016).
259 Ahn, J. *et al.* Pepsin immobilized on high-strength hybrid particles for continuous flow online digestion at 10,000 psi. *Anal. Chem.* **84**, 7256-7262, (2012).
260 Proudfoot, A. E. I. *et al.* Glycosaminoglycan binding and oligomerization are essential for the in vivo activity of certain chemokines. *Proc. Natl. Acad. Sci. U. S. A.* **100**, 1885-1890, (2003).
261 Janson, G. *et al.* PyMod 2.0: improvements in protein sequence-structure analysis and homology modeling within PyMOL. *Bioinformatics,* **33**, 444-446, (2017).
262 Tina, K. G. *et al.* PIC: Protein Interactions Calculator. *Nucleic Acids Res.* **35**, W473-476, (2007).